Solutions Manual for Continuum Electromechanics

11

Streaming Interactions

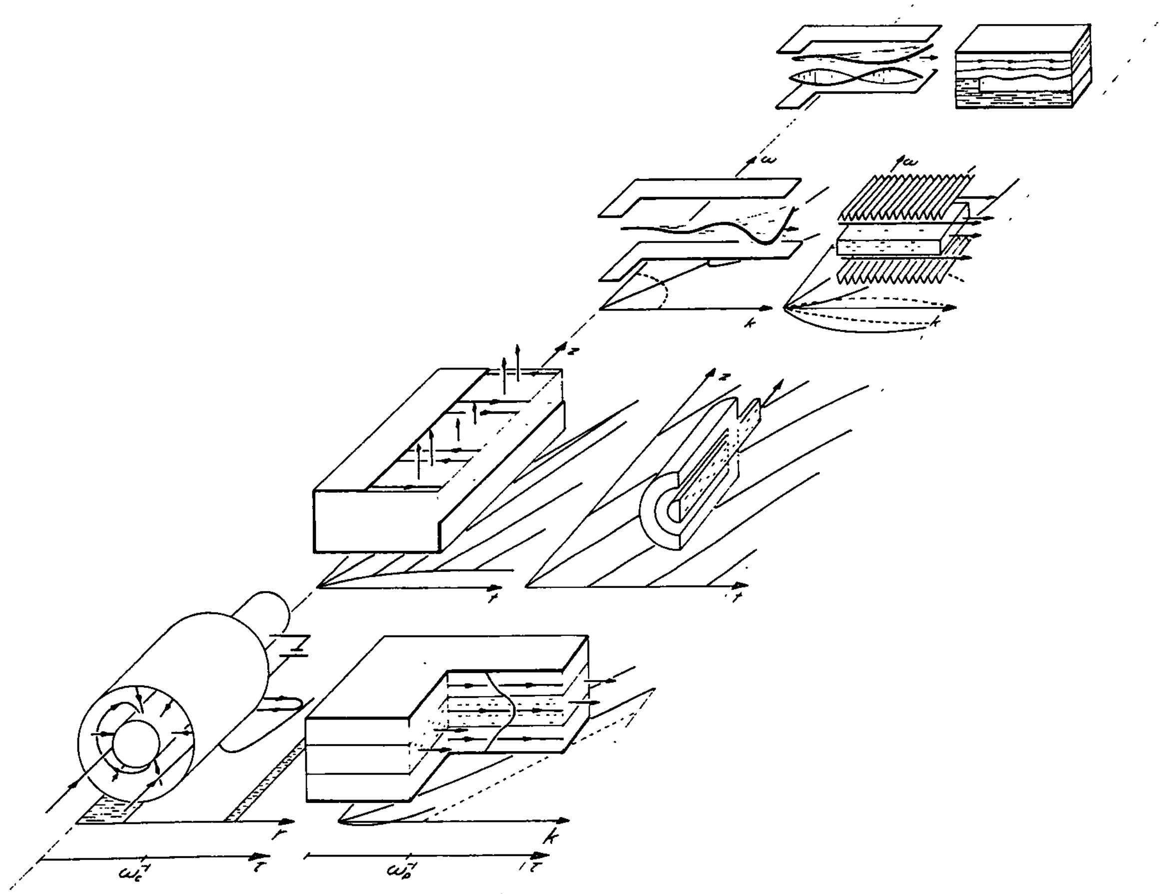

Prob. 11.2.1 With the understanding that the time derivative on the left is the rate of change of $\bar{v}$ for a given particle (for an observer moving with the particle velocity $\bar{v}$) the equation of motion is

$$m\frac{\partial\bar{v}}{\partial t} = q\left(\bar{E} + \bar{v}\times\mu_o\bar{H}\right) \tag{1}$$

Substitution of $\bar{E} = -\nabla\Phi$ and dot multiplication of this expression with $\bar{v}$ gives

$$\bar{v}\cdot\left[m\frac{\partial\bar{v}}{\partial t} = -q\nabla\Phi + q\bar{v}\times\mu_o\bar{H}\right] \tag{2}$$

Because $\bar{v}\times\mu_o\bar{H}$ is perpendicular to $\bar{v}$,

$$\frac{\partial}{\partial t}\left(\frac{1}{2}m\,\bar{v}\cdot\bar{v}\right) = -q\,\bar{v}\cdot\nabla\Phi \tag{3}$$

By definition, the rate of change of Φ with respect to time is

$$\frac{D\Phi}{Dt} = \frac{\partial\Phi}{\partial t} + \bar{v}\cdot\nabla\Phi = \bar{v}\cdot\nabla\Phi \tag{4}$$

where here it is understood that $\partial\Phi/\partial t$ means the partial is taken holding the Eulerian coordinates (x,y,z) fixed. Thus, this partial derivative is zero. It follows that because the del operator used in expressing Eq. 3 is also written in Eulerian coordinates, that the right-hand side of Eq. 4 can be taken as the rate of change of a spatially varying Φ with respect to time as observed by a particle. So, now with the understanding that the partial is taken holding the identity of a particle fixed (for example, using the initial coordinates of the particle as the independent spatial variables) Eq. 3 becomes the desired energy conservation statement.

$$\frac{\partial}{\partial t}\left[\frac{1}{2}m\,\bar{v}\cdot\bar{v} + q\,\Phi\right] = 0 \tag{5}$$

Prob. 11.3.1 (a) Using (x,y,z) to denote the cartesian coordinates of a given electron between the electrodes shown to the right, the particle equations of motion (Eq. 11.2.2) are simply

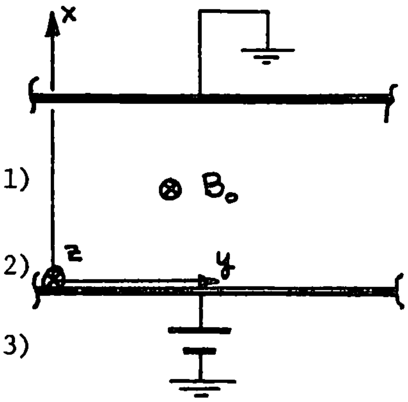

$$m\frac{d^2x}{dt^2} = -\frac{eV}{a} - B_o e\frac{dy}{dt} \qquad (1)$$

$$m\frac{d^2y}{dt^2} = B_o e\frac{dx}{dt} \qquad (2)$$

$$m\frac{d^2z}{dt^2} = 0 \qquad (3)$$

There is no initial velocity in the z direction, so it follows from Eq. 3 that the motion in the z direction can be taken as zero.

(b) To obtain the required expression for x(t), take the time derivative of Eq. (1) and replace the second derivative of y using Eq. (2). Thus,

$$m\frac{d^3x}{dt^3} = -\frac{(B_oe)^2}{m}\frac{dx}{dt} \Rightarrow \frac{d}{dt}\left(\frac{d^2x}{dt^2}+\omega_c^2x\right)=0\ ;\ \omega_c^2 \equiv \left(\frac{B_oe}{m}\right)^2 \qquad (4)$$

When the electron is at x = 0,

$$\frac{dx}{dt}=0\ ;\ \frac{dy}{dt}=0 \Rightarrow (\text{Eq } 2 \text{ at } x=0)\quad m\frac{d^2x}{dt^2} = -\frac{eV}{a} \qquad (5)$$

So that Eq. 4 becomes

$$\frac{d^2x}{dt^2} + \omega_c^2 x = \frac{-eV}{am} \qquad (6)$$

Note that for operation with electrons, $V < 0$.

(c) This expression is most easily solved by adding to the particular solution, $qV/am\omega_c^2$, the combination of $\sin\omega_c x$ and $\cos\omega_c x$ (the homogeneous solutions) required to satisfy the initial conditions. However, to proceed in a manner analogous to that required in the text, Eq. 6 is multiplied by dx/dt and the resulting expression written in the form

$$\frac{d}{dt}\left[\frac{1}{2}\left(\frac{dx}{dt}\right)^2 + \omega_c^2\frac{x^2}{2} + \frac{eV}{am}x\right] = 0 \qquad (7)$$

so that it is evident that the quantity in brackets is conserved. To satisfy the condition of Eq. 5, the constant of integration is zero

Prob. 11.3.1 (cont.)

(the initial total energy is zero) so it follows from Eq. 7 that

$$\frac{dx}{dt} = \pm\sqrt{-\frac{2eV}{am}x - \omega_c^2 x^2} \qquad \pm\sqrt{0 - \left(\omega_c^2 x^2 + \frac{2eV}{am}x\right)} \tag{8}$$

where $eV < 0$.

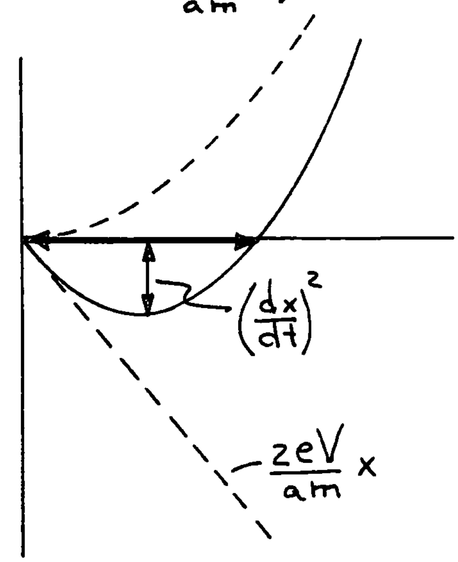

The potential well picture given by this expression is shown at the right. Rearrangement of Eq. 8 puts it in a form that can be integrated. First, it is written as

$$\pm\int_0^x \frac{dx}{\sqrt{-\frac{2eV}{am}x - \omega_c^2 x^2}} = \int_0^t dt \tag{9}$$

Then, integration gives

$$\cos^{-1}\left[\frac{\frac{-eV}{am\omega_c^2} - x}{\frac{-eV}{am\omega_c^2}}\right] = \omega_c t \Rightarrow x = \frac{eV}{am\omega_c^2}(\cos\omega_c t - 1) \tag{10}$$

Of course, this is just the combination of particular and homogeneous solutions to Eq. 6 required to satisfy the initial condition.

The associated motion in the y direction follows by using Eq. 10 to evaluate the right-hand side of Eq. 2. Then, integration gives the velocity

$$\frac{dy}{dt} = \frac{B_o e^2 V}{a m^2 \omega_c^2}(\cos\omega_c t - 1) \tag{11}$$

where the integration constant is evaluated to satisfy Eq. 5. A second integration, this time with the constant of integration evaluated to make y=0 when t=0, gives (note that $\omega_c = -B_o e/m$).

$$y = \frac{Ve}{\omega_c^2 am}(\sin\omega_c t - \omega_c t) \tag{12}$$

Thus, with t as a parameter, Eqs. 10 and 12 give the trajectory of a particle starting out from the origin when t=0. Electrons coming from the cathode at other times or other locations along the y axis have similar trajectories.

Prob. 11.3.1 (cont.)

(d) The construction shown in the figure is useful in picturing particle motions that are the planar analogous of those found in cylindrical geometry in the text.

(e) The trajectory just grazes the anode if the peak amplitude given by Eq. 10 is just equal to the spacing, a. The potential resulting from this equality is then the critical one.

$$V_c = -a^2 m \omega_c^2 / 2e \qquad (13)$$

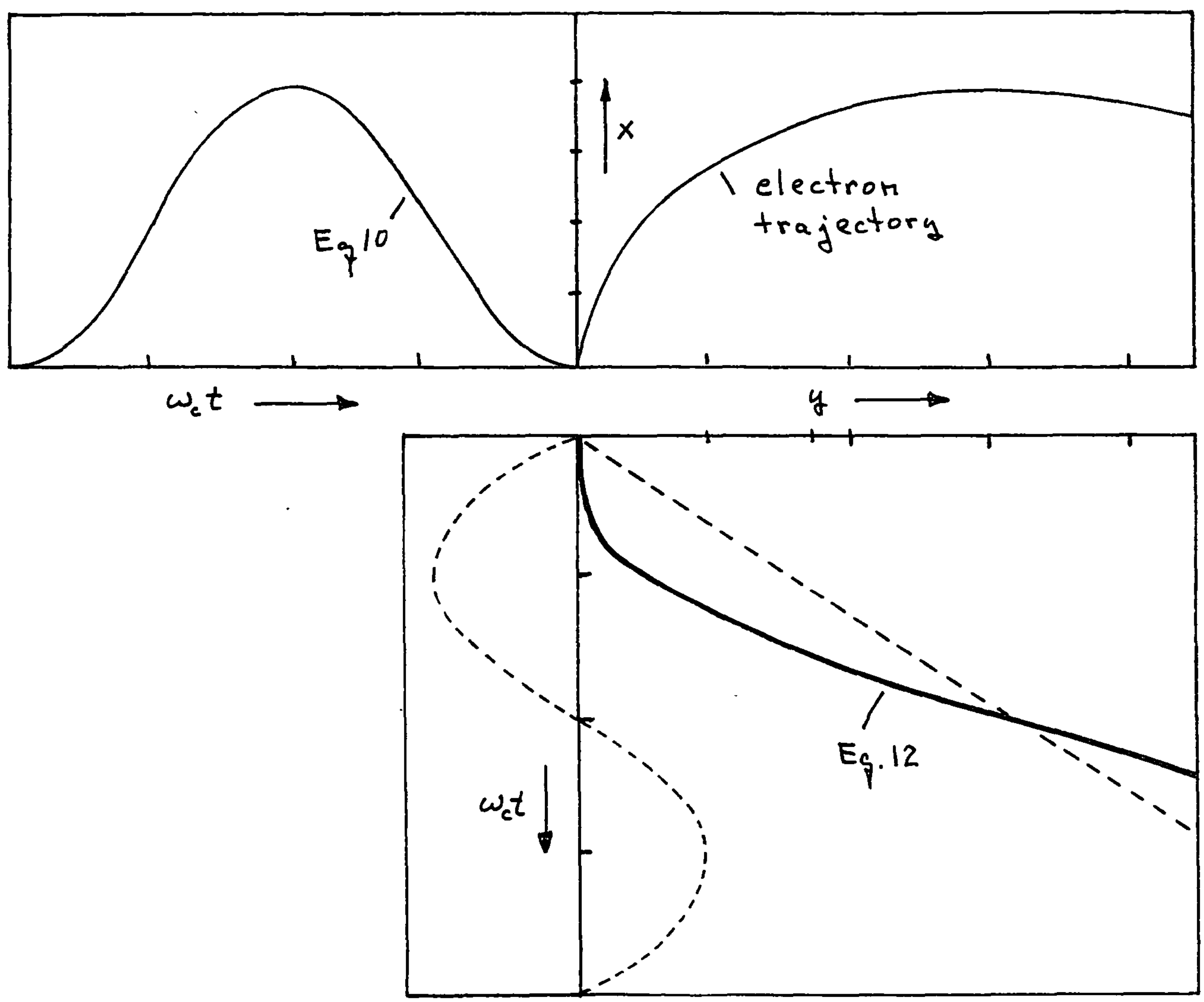

P11.3 (cont.)

c) To find Φ_c,

$$\frac{\Delta}{2} = \int_{-\zeta}^{\Phi_c} \frac{d\Phi}{\sqrt{2\cosh\Phi - 2\cosh\Phi_c}} \qquad (8)$$

must be numerically evaluated. The procedure would be given values for Δ and ζ and would start with a "best guess" value of Φ_c (perhaps $\emptyset$). It would then determine equal interval spacings Φ so that a specified number of points would be used to do the numerical evaluation. A simple numerical integration, such as trapezoidal areas, would then be used to evaluate the integrand of (8). The resulting integration would then be compared to $\Delta/2$ for a re-evaluation of Φ_c. The process would iterate until an appropriate answer of the evaluated integral falls within specified error tolerances of $\Delta/2$.

A potentially sticky situation appears as $\Phi \to \Phi_c$. The integrand is singular at that value of Φ. One way around this is to use small enough interval spacing of Φ so that the $\Phi = \Phi_c$ value can be neglected. Another way is to expand the denominator of the integrand into a Taylor expansion around Φ_c,

$$2\cosh\Phi - 2\cosh\Phi_c \cong 2(\cancel{\cosh\Phi_c} + \sinh\Phi_c\cdot(\Phi-\Phi_c) - \cancel{\cosh\Phi_c})\Big|_{\Phi\to\Phi_c}$$

$$\cong 2\sinh\Phi_c\cdot(\Phi-\Phi_c)\Big|_{\Phi\to\Phi_c} \qquad (9)$$

As the numerical Φ's approach Φ_c, (9) would be plugged into the integral of (8). The integration would still need to stop before $\Phi = \Phi_c$ is reached.

Once Φ_c is determined, $\Phi(x)$ is easily evaluated by numerical integration.

d) given $\Delta = 2$ and $\zeta = 3$, I did the integration using Lotus 123. The worksheet is shown on pgs 5 and 6 while the graph is on page 7. To understand the worksheet,

Col. A = % of way through numerical integration x 100
Col. B = Potential (where end of Col. B is Φ_c)
Col. C = Cosh of potential (I had to make a Cosh func. from exponetials)
Col. D = Value of integrand with given Potential in B
Col. E = Trapezoidal area integration, e.g. $E_2 = (D_1 + D_2)*(B_2 - B_1)/2$
Col. F = Sum of Col. E, i.e. $F1 = \Delta/2$
Col. G = Φ_c
Col. H = X as a function of Φ.

The result: $\Phi_c = -1.38$.

The Plot is on pg. 7.

123 Worksheet used to do calculations for 6.672 P10.8.2

	Potential		Integrand		midplane	Phi of mid.	
1	ς -3	10.06766	0.250715	0	1.009043	-1.38	0
2	-2.9676	9.748310	0.255904	0.008207	$\Delta/2$		0.008207
3	-2.9514	9.592493	0.258556	0.004167		Φ_c	0.012374
4	-2.9352	9.439193	0.261247	0.004210			0.016584
5	-2.919	9.288371	0.263979	0.004254			0.020839
6	-2.9028	9.139986	0.266752	0.004298			0.025138
7	-2.8866	8.994000	0.269567	0.004344			0.029482
8	-2.8704	8.850375	0.272425	0.004390			0.033872
9	-2.8542	8.709072	0.275327	0.004436			0.038309
10	-2.838	8.570055	0.278276	0.004484			0.042793
11	-2.8218	8.433287	0.281270	0.004532			0.047325
12	-2.8056	8.298732	0.284313	0.004581			0.051906
13	-2.7894	8.166356	0.287405	0.004630			0.056537
14	-2.7732	8.036122	0.290548	0.004681			0.061219
15	-2.757	7.907998	0.293742	0.004732			0.065952
16	-2.7408	7.781949	0.296990	0.004784			0.070737
17	-2.7246	7.657942	0.300293	0.004838			0.075575
18	-2.7084	7.535945	0.303652	0.004891			0.080466
19	-2.6922	7.415926	0.307069	0.004946			0.085413
20	-2.676	7.297853	0.310546	0.005002			0.090416
21	-2.6598	7.181696	0.314084	0.005059			0.095476
22	-2.6436	7.067423	0.317686	0.005117			0.100593
23	-2.6274	6.955005	0.321353	0.005176			0.105769
24	-2.6112	6.844412	0.325087	0.005236			0.111005
25	-2.595	6.735616	0.328891	0.005297			0.116303
26	-2.5788	6.628588	0.332766	0.005359			0.121662
27	-2.5626	6.523299	0.336715	0.005422			0.127085
28	-2.5464	6.419722	0.340740	0.005487			0.132572
29	-2.5302	6.317830	0.344844	0.005553			0.138125
30	-2.514	6.217596	0.349029	0.005620			0.143746
31	-2.4978	6.118993	0.353299	0.005688			0.149435
32	-2.4816	6.021997	0.357656	0.005758			0.155193
33	-2.4654	5.926581	0.362103	0.005830			0.161023
34	-2.4492	5.832721	0.366643	0.005902			0.166926
35	-2.433	5.740391	0.371280	0.005977			0.172903
36	-2.4168	5.649568	0.376018	0.006053			0.178957
37	-2.4006	5.560227	0.380859	0.006130			0.185087
38	-2.3844	5.472346	0.385809	0.006210			0.191297
39	-2.3682	5.385901	0.390871	0.006291			0.197588
40	-2.352	5.300870	0.396050	0.006374			0.203962
41	-2.3358	5.217229	0.401351	0.006458			0.210421
42	-2.3196	5.134958	0.406778	0.006545			0.216967
43	-2.3034	5.054035	0.412337	0.006634			0.223602
44	-2.2872	4.974438	0.418033	0.006726			0.230328
45	-2.271	4.896146	0.423872	0.006819			0.237148
46	-2.2548	4.819140	0.429862	0.006915			0.244063
47	-2.2386	4.743398	0.436007	0.007013			0.251076
48	-2.2224	4.668901	0.442316	0.007114			0.258191
49	-2.2062	4.595630	0.448797	0.007218			0.265409
50	-2.19	4.523564	0.455456	0.007324			0.272733
51	-2.1738	4.452686	0.462304	0.007433			0.280167

52	-2.1576	4.382977	0.469350	0.007546	0.287714
53	-2.1414	4.314417	0.476603	0.007662	0.295376
54	-2.1252	4.246990	0.484075	0.007781	0.303157
55	-2.109	4.180678	0.491777	0.007904	0.311062
56	-2.0928	4.115462	0.499722	0.008031	0.319093
57	-2.0766	4.051327	0.507923	0.008161	0.327255
58	-2.0604	3.988255	0.516395	0.008296	0.335552
59	-2.0442	3.926230	0.525154	0.008436	0.343988
60	-2.028	3.865235	0.534217	0.008580	0.352569
61	-2.0118	3.805255	0.543604	0.008730	0.361300
62	-1.9956	3.746273	0.553334	0.008885	0.370185
63	-1.9794	3.688275	0.563429	0.009045	0.379231
64	-1.9632	3.631244	0.573916	0.009212	0.388443
65	-1.947	3.575167	0.584819	0.009385	0.397829
66	-1.9308	3.520028	0.596170	0.009566	0.407395
67	-1.9146	3.465812	0.608001	0.009753	0.417149
68	-1.8984	3.412506	0.620348	0.009949	0.427098
69	-1.8822	3.360096	0.633252	0.010154	0.437252
70	-1.866	3.308568	0.646757	0.010368	0.447621
71	-1.8498	3.257908	0.660914	0.010592	0.458213
72	-1.8336	3.208103	0.675779	0.010827	0.469040
73	-1.8174	3.159140	0.691416	0.011074	0.480114
74	-1.8012	3.111006	0.707897	0.011334	0.491449
75	-1.785	3.063688	0.725305	0.011608	0.503058
76	-1.7688	3.017175	0.743731	0.011899	0.514957
77	-1.7526	2.971453	0.763286	0.012206	0.527164
78	-1.7364	2.926511	0.784092	0.012533	0.539697
79	-1.7202	2.882337	0.806295	0.012882	0.552580
80	-1.704	2.838920	0.830065	0.013254	0.565834
81	-1.6878	2.796248	0.855602	0.013653	0.579488
82	-1.6716	2.754310	0.883145	0.014083	0.593572
83	-1.6554	2.713094	0.912981	0.014548	0.608120
84	-1.6392	2.672591	0.945459	0.015053	0.623174
85	-1.623	2.632789	0.981006	0.015604	0.638778
86	-1.6068	2.593678	1.020155	0.016209	0.654988
87	-1.5906	2.555247	1.063579	0.016878	0.671866
88	-1.5744	2.517487	1.112144	0.017623	0.689489
89	-1.5582	2.480388	1.166981	0.018460	0.707950
90	-1.542	2.443940	1.229610	0.019412	0.727363
91	-1.5258	2.408134	1.302123	0.020507	0.747870
92	-1.5096	2.372959	1.387499	0.021785	0.769656
93	-1.4934	2.338407	1.490157	0.023309	0.792965
94	-1.4772	2.304469	1.616992	0.025167	0.818132
95	-1.461	2.271135	1.779507	0.027511	0.845644
96	-1.4448	2.238398	1.998733	0.030603	0.876248
97	-1.4286	2.206248	2.318587	0.034970	0.911218
98	-1.4124	2.174677	2.852775	0.041888	0.953106
99	-1.3962	2.143677	4.053033	0.055937	1.009043
100	-1.28	2.113240	ERR	0.034481	1.043524

2.113240

Divide by Zero error

Could be Fixed as explained in part (c) of problem.

12/14/88 pg. 7

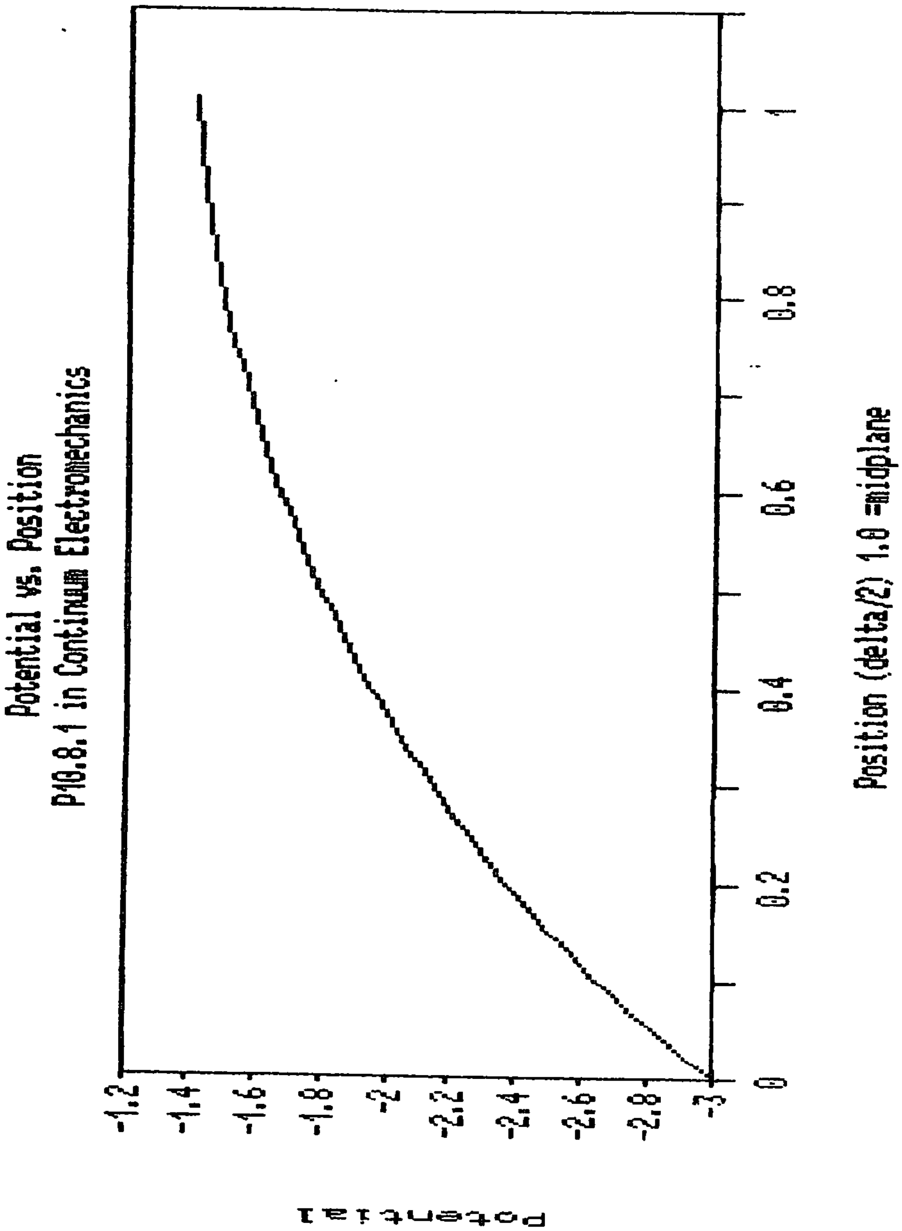

Courtesy of James Brennan. Used with permission.

Prob. 11.4.1 The point in this problem is to appreciate the quasi-one-dimensional model represented by the paraxial ray equation. First, observe that it is not simply a one-dimensional version of the general equations of motion. The exact equations are satisfied identically in a region where E_r, E_z and H_r are zero by the solution r = constant, θ = constant and a uniform motion in the z direction, z=Ut. That the magnetic field, B_z, has a z variation (and hence that there are radial components of $\bar{B}$) is implied by the use of Busch's Theorem (Eq. 11.4.2). The angular velocity implicit in writing the radial force equation reflects the arrival of the electron at the point in question from a region where there is no magnetic flux density. It is the centrifugal force caused by the angular velocity created in the transition from the field free region to the one where B_z is uniform that appears in Eq. 11.4.9, for example.

Prob. 11.4.2 The theorem is a consequence of the property of solutions to Eq. 11.4.9.

$$-\frac{d^2r}{dz^2} = \varkappa^2 r \tag{1}$$

In this expression, $\varkappa = \varkappa(z)$, reflecting the possibility that the B_z varies in an arbitrary way in the z-direction. Integration of Eq. 1 gives

$$-\int_0^z \frac{d}{dz}\left(\frac{dr}{dz}\right)dz = \int_0^z \varkappa^2 r\,dz \Rightarrow \left.\frac{dr}{dz}\right|_0 - \left.\frac{dr}{dz}\right|_z = \int_0^z \varkappa^2 r\,dz > 0 \tag{2}$$

Because the quantity on the right is positive definite, it follows that the derivative at some downstream location is less than that at the entrance.

$$\left.\frac{dr}{dz}\right|_0 > \left.\frac{dr}{dz}\right|_z \tag{3}$$

Prob. 11.4.3 For the magnetic lens, Eq. 11.4.8 reduces to

$$\frac{d^2r}{dz^2} + \frac{e}{8\Phi m}B_z^2 r = 0 \tag{1}$$

Integration through the length of the lens gives

$$\int_{z_-}^{z_+} \frac{d}{dz}\left(\frac{dr}{dz}\right)dz + \int_{z_-}^{z_+} \frac{1}{8\Phi}\frac{e}{m}B_z^2 r\,dz = 0 \tag{2}$$

Prob. 11.4.3 (cont.)

and this expression becomes

$$\left.\frac{dr}{dz}\right|_{z_+} - \left.\frac{dr}{dz}\right|_{z_-} = -\int_{z_-}^{z_+} \frac{e}{8\Phi m} B_z^2 r\,dz = -\frac{er}{8\Phi m}\int_{z_-}^{z_+} B_z^2\,dz \tag{3}$$

On the right it has been assumed that the variation through the "weak" lens of the radial position is negligible. The definition of f that follows from Fig. 11.4.2 is

$$\frac{dr}{dz} = -\frac{r}{f} \tag{4}$$

so that for electrons entering the lens as parallel rays, it follows from Eq. 3 that

$$\frac{r}{f} = \frac{er}{8\Phi m}\int_{z_-}^{z_+} B_z^2\,dz \tag{5}$$

which can be solved for f to obtain the expression given. As a check, observe for the example given in the text where $B_z = B_o$ over the length of the lens,

$$\int_{z_-}^{z_+} B_z^2\,dz = B_o^2\,\ell \tag{6}$$

and it follows from Eq. 5 that

$$f = \frac{8\Phi m}{e\ell B_o^2} \tag{7}$$

This same expression is found from Eq. 11.4.12 in the limit $\ell\gamma \ll 1$.

<u>Prob. 11.4.4</u> For the given potential distribution

$$\Phi = V_o J_o(\gamma r)\, e^{-\gamma z} \tag{1}$$

the coefficients in Eq. 11.4.8 are

$$A = -\frac{\gamma}{2} \;;\; C = \frac{\gamma^2}{4} \tag{2}$$

and the differential equation reduces to one having constant coefficients.

$$\frac{d^2r}{dz^2} - \frac{\gamma}{2}\frac{dr}{dz} + \frac{\gamma^2}{4} r = 0 \tag{3}$$

At $z = z_+$, just to the downstream side of the plane z=0, boundary conditions are

$$r = r_o \;;\; \frac{dr}{dz} = 0 \tag{4}$$

Prob. 11.4.4 (cont.)

Solutions to Eq. 3 are of the form

$$r = De^{P_1 z} + Fe^{P_2 z}\,; \quad P_{\substack{1\\2}} \equiv \frac{\gamma}{4}(1 \pm j\sqrt{3}) \tag{5}$$

and evaluation of the coefficients by using the conditions of Eq. 4 results in the desired electron trajectory.

$$r = r_o e^{\frac{\gamma z}{4}}\left(\cos\frac{\sqrt{3}\gamma}{4}z - \frac{1}{\sqrt{3}}\sin\frac{\sqrt{3}\gamma}{4}z\right) \tag{6}$$

Prob. 11.5.1 In Cartesian coordinates, the transverse force equations are

$$\left(\frac{\partial}{\partial t} + U\frac{\partial}{\partial z}\right)v_x = \frac{e}{m}\frac{\partial\Phi}{\partial x} - \frac{e}{m}B_o v_y \tag{1}$$

$$\left(\frac{\partial}{\partial t} + U\frac{\partial}{\partial z}\right)v_y = \frac{e}{m}\frac{\partial\Phi}{\partial y} + \frac{e}{m}B_o v_x \tag{2}$$

With the same substitution as used in the zero order equations, these relations become

$$\begin{bmatrix} j(\omega - kU) & \frac{e}{m}B_o \\ -\frac{e}{m}B_o & j(\omega - kU) \end{bmatrix}\begin{bmatrix} \hat{v}_x \\ \hat{v}_y \end{bmatrix} = \begin{bmatrix} \frac{e}{m}\frac{d\hat{\Phi}}{dx} \\ -j\frac{e}{m}k_y\hat{\Phi} \end{bmatrix} \tag{3}$$

where the potential distributions on the right are predetermined from the zero order fields. For example, solution of Eqs. 3 gives

$$\hat{v}_x = \frac{j(\omega - kU)\frac{e}{m}\frac{d\hat{\Phi}}{dx} + j\frac{e}{m}\left(\frac{B_o e}{m}\right)k_y\hat{\Phi}}{\left(\frac{e}{m}B_o\right)^2 - (\omega - kU)^2} \tag{4}$$

If the Doppler shifted frequency is much less than the electron cyclotron frequency, $\omega_c = eB_o/m$,

$$\left(\frac{e}{m}B_o\right)^2 >> (\omega - kU)^2$$

Typically, $|d\hat{\Phi}/dx| \sim |k_z\hat{\Phi}|$ and $k_y \sim k_z$ so that Eqs. 4 and 11.5.5 show

Prob. 11.5.1 (cont.)

that

$$\frac{|\hat{v}_x|}{|\hat{v}_z|} = \frac{(\omega - kU)^2}{\omega_c^2} + \frac{(\omega - kU)}{\omega_c} \tag{6}$$

so, if $|\omega - kU| < \omega_c$, then the transverse motions are negligible compared to the longitudinal ones. Most likely $\omega - kU \sim \omega_p$ so the requirement is essentially that the plasma frequency be low compared to the electron cyclotron frequency.

Prob. 11.5.2 (a) Equations 11.5.5 and 11.5.6 remain valid in cylindrical geometry. However, Eq. 11.5.7 is replaced by the circular version of Eq. 11.5.4 combined with Eq. 11.5.6

$$\frac{d^2\hat{\Phi}}{dr^2} + \frac{1}{r}\frac{d\hat{\Phi}}{dr} - \left(\frac{m^2}{r^2} + \gamma^2\right)\hat{\Phi} = 0 \tag{1}$$

Thus, it has the form of Bessel's equation, Eq. 2.16.19, with $k \to \gamma$. The derivation of the transfer relations in Table 2.16.2 remains valid because the displacement vector is found from the potential by taking the radial derivative and that involves γ and not k. (If the derivation involved a derivative with respect to z, there would be two ways in which k entered in the original derivation, and γ could not be unambiguously identified with k everywhere.)

(b) Using (c), (d) and (e) to designate the radii r=a and r=+b and -b respectively, the solid circular beam is described by

$$\hat{D}_r^e = \epsilon_o f_m(0,b,\gamma)\hat{\Phi}^e \tag{2}$$

while the free space annulus has

$$\begin{bmatrix} \hat{D}_r^c \\ \hat{D}_r^d \end{bmatrix} = \epsilon_o \begin{bmatrix} f_m(b,a,k) & g_m(a,b,k) \\ g_m(b,a,k) & f_m(a,b,k) \end{bmatrix} \begin{bmatrix} \hat{\Phi}^c \\ \hat{\Phi}^d \end{bmatrix} \tag{3}$$

Thus, in view of the conditions that $\hat{D}_x^d = \hat{D}_x^e$ and $\hat{\Phi}^d = \hat{\Phi}^e$, Eqs. 2 and 3b show that

$$\hat{\Phi}^e = \frac{g_m(b,a,k)\hat{\Phi}^c}{f_m(0,b,\gamma) - f_m(a,b,k)} \tag{4}$$

Prob. 11.5.2 (cont.)

This expression is then substituted into Eq. 3a to show that

$$\hat{D}_r^c = \frac{\epsilon_o[f_m(0,b,\gamma)f_m(b,a,k) - f_m(b,a,k)f_m(a,b,k) + g_m(a,b,k)g_m(b,a,k)]}{f_m(0,b,\gamma) - f_m(a,b,k)}\hat{\Phi}^c \tag{5}$$

which is the desired driven response.

(c) The dispersion equation follows from Eq. 5, and takes the same form as Eq. 11.5.12

$$f_m(0,b,\gamma) = f_m(a,b,k) \tag{6}$$

For the temporal modes, what is on the right (a function of geometry and the wavenumber) is real. From the properties of the f_m determined in Sec. 2.17, $f_m(a,b,k) > 0$ for $a > b$ and $f_m(0,b,\gamma) < 0$, so it is clear that for γ real, Eq. 6 cannot be satisfied. However, for $\gamma = -j\alpha$ where α is defined as real, Eq. 6 becomes

$$-\alpha\frac{J_m'(\alpha b)}{J_m(\alpha b)} = f_m(a,b,k) \tag{7}$$

This expression can be solved graphically to find an infinite number of solutions, α_n . Given these values, the eigenfrequencies follow from the definition of γ given with Eq. 11.5.7.

$$\omega_n = kU \pm \frac{\omega_p}{\sqrt{1 + \left(\frac{\alpha_n}{k}\right)^2}} \tag{8}$$

Prob. 11.6.1 The system of m first order differential equations takes the form

$$\sum_{j=1}^{m}\left(F_{ij}\frac{\partial x_j}{\partial t} + G_{ij}\frac{\partial x_j}{\partial z}\right) = 0 \tag{1}$$

where i = 1 .... m generates the m equations.

(a) Following the method of "undetermined multipliers, multiply the ith equation by λ_i and add all m equations

$$\begin{aligned}
\lambda_1\sum_{j=1}^{m}\left(F_{1j}\frac{\partial x_j}{\partial t} + G_{1j}\frac{\partial x_j}{\partial z}\right) &= 0\\
&\vdots\\
\lambda_i\sum_{j=1}^{m}\left(F_{ij}\frac{\partial x_j}{\partial t} + G_{ij}\frac{\partial x_j}{\partial z}\right) &= 0\\
&\vdots\\
\lambda_m\sum_{j=1}^{m}\left(F_{mj}\frac{\partial x_j}{\partial t} + G_{mj}\frac{\partial x_j}{\partial z}\right) &= 0
\end{aligned} \tag{2}$$

$$\sum_{j=1}^{m}\sum_{i=1}^{m}\left(\lambda_i F_{ij}\frac{\partial x_j}{\partial t} + \lambda_i G_{ij}\frac{\partial x_j}{\partial z}\right) = 0 \tag{3}$$

Now, for directional derivatives of each x_j to be the same

$$\frac{dz}{dt} = \frac{\sum_{i=1}^{m}\lambda_i G_{ij}}{\sum_{i=1}^{m}\lambda_i F_{ij}} \tag{4}$$

These expressions, j = 1 .... m can be written as m equations in the λ_i's.

Prob. 11.6.1 (cont.)

$$\sum_{i=1}^{m}\left(F_{ij}\frac{dz}{dt} - G_{ij}\right)\lambda_i = 0$$

The first characteristic equations are given by the condition that the determinant of the coefficients of the λ_i's vanish.

$$\mathrm{Det}\left[\sum_{i=1}^{m}\left(F_{ij}\frac{dz}{dt} - G_{ij}\right)\right] = 0$$

(b) Now, to form the coefficient matrix, write Eq. 1 as the first m of the 2 m expressions

$$\begin{bmatrix} F_{11} & G_{11} & F_{12} & G_{12} & \cdots & F_{1m} & G_{1m} \\ F_{21} & G_{21} & F_{22} & G_{21} & \cdots & F_{2m} & G_{2m} \\ \cdot & \cdot & \cdot & \cdot & & \cdot & \cdot \\ \cdot & \cdot & \cdot & \cdot & & \cdot & \cdot \\ \cdot & \cdot & \cdot & \cdot & & \cdot & \cdot \\ F_{m1} & G_{m1} & F_{m2} & G_{m2} & \cdots & F_{mn} & G_{mn} \\ dt & dz & 0 & 0 & & 0 & 0 \\ \cdot & \cdot & & & & & \\ \cdot & \cdot & & & & & \\ \cdot & \cdot & & & & & \\ 0 & 0 & 0 & 0 & \cdots & dt & dz \end{bmatrix} \begin{bmatrix} x_{1,t} \\ x_{1,z} \\ x_{2,t} \\ \cdot \\ \cdot \\ \cdot \\ \cdot \\ \cdot \\ x_{m,t} \\ x_{m,z} \end{bmatrix} = \begin{bmatrix} 0 \\ 0 \\ 0 \\ \cdot \\ \cdot \\ \cdot \\ dx_1 \\ \cdot \\ \cdot \\ \cdot \\ dx_m \end{bmatrix}$$

The second m of these expressions are

$$dx_i = \frac{\partial x_i}{\partial t}dt + \frac{\partial x_i}{\partial z}dz \quad ; \quad i = 1 \cdots m$$

To show that determinant of these coefficients is the same as Eq. 6, operate on Eq. 7 in ways motivated by the special case of obtaining Eq. 11.6.19 from Eq. 11.6.17. Multiply the $(m+1)$'st equation through 2m'th equation (the last m equations) by dt^{-1}. Then, these last m

Prob. 11.6.1 (cont.)

rows (m+1....2m) are first respectively multiplied by F_{11}, F_{12}....F_{1m} and subtracted from the first equation. The process is then repeated using of F_{21}, F_{22}....F_{2m} and the result subtracted from the second equation, and so on to the mth equation. Thus, Eq. 7 becomes

$$\begin{bmatrix} 0 & G_{11}-F_{11}\frac{dz}{dt} & 0 & G_{12}-F_{12}\frac{dz}{dt} & \cdots & 0 & G_{1m}-F_{1m}\frac{dz}{dt} \\ \vdots & & & & & & \\ 0 & G_{m1}-F_{m1}\frac{dz}{dt} & 0 & G_{m2}-F_{m2}\frac{dz}{dt} & \cdots & 0 & G_{mm}-F_{mm}\frac{dz}{dt} \\ 1 & \frac{dz}{dt} & 0 & 0 & \cdots & 0 & 0 \\ \vdots & \vdots & & & & & \\ 0 & 0 & 0 & 0 & \cdots & 1 & \frac{dz}{dt} \end{bmatrix} = 0 \qquad (9)$$

Now, this expression is expanded by "minors" about the 1'ns that appear as the only entries in the odd columns to obtain

$$\begin{bmatrix} G_{11}-F_{11}\frac{dz}{dt} & G_{12}-F_{12}\frac{dz}{dt} & \cdots & G_{1m}-F_{1m}\frac{dz}{dt} \\ \vdots & & & \vdots \\ G_{m1}-F_{m1}\frac{dz}{dt} & G_{m2}-F_{m2}\frac{dz}{dt} & \cdots & G_{mm}-F_{mm}\frac{dz}{dt} \end{bmatrix} \qquad (10)$$

Multiplied by (-1) this is the same as Eq. 6.

Prob. 11.7.1 Eqs. 9.13.11 and 9.13.12, with $V=0$ and $b=0$ are

$$\frac{\partial v}{\partial t} + v\frac{\partial v}{\partial z} + g\frac{\partial \xi}{\partial t} = 0 \tag{1}$$

$$\frac{\partial \xi}{\partial t} + \frac{\partial}{\partial z}(v\xi) = 0 \tag{2}$$

In a uniform channel, the compressible equations of motion are Eqs. 11.6.3 and 11.6.4

$$\frac{\partial v}{\partial t} + v\frac{\partial v}{\partial z} + \frac{a^2}{\rho}\frac{\partial \rho}{\partial z} = 0 \tag{3}$$

$$\frac{\partial \rho}{\partial t} + v\frac{\partial \rho}{\partial z} + \rho\frac{\partial v}{\partial z} = 0 \tag{4}$$

These last expressions are identical to the first two if the identification is made $v \rightarrow v$, $\rho \rightarrow \xi$ and $a^2/\rho \rightarrow g$. Because $a = a(\rho)$ (Eq. 11.6.2) the analogy is not complete unless a^2/ρ is independent of ρ . This requires that (from Eq. 11.6.2)

$$\frac{a^2}{\rho} = \gamma\frac{p_o}{\rho_o}\left(\frac{\rho}{\rho_o}\right)^{\gamma-1}\Big/\rho \tag{5}$$

be independent of ρ , which it is if $\rho^{\gamma-1}/\rho = \rho^{\gamma-2} = 1$, or if $\gamma = 2$.

Prob. 11.7.2 Eqs. 9.13.4 and 9.13.9 with A and f defined by $f = -\frac{1}{2}(\epsilon-\epsilon_0)\frac{V^2}{\pi\xi^2}+\frac{\gamma}{\xi}$ and $A = \pi\xi^2/2$ are

$$\frac{\partial v}{\partial t} + v\frac{\partial v}{\partial z} + \frac{\partial}{\partial z}\left[\frac{1}{2}\frac{(\epsilon-\epsilon_0)}{\rho}\frac{V^2}{\pi^2\xi^2} - \frac{\gamma}{\rho\xi}\right] = 0 \tag{1}$$

$$\frac{\partial}{\partial t}\xi^2 + \frac{\partial}{\partial z}(\xi^2 v) = 0 \tag{2}$$

These form the first two of the following 4 equations.

$$\begin{bmatrix} 1 & v & 0 & \frac{(\epsilon-\epsilon_0)V^2}{\pi^2\rho}\frac{1}{\xi^3} - \frac{\gamma}{\rho\xi^2} \\ 0 & \xi^2 & 2\xi & 2v\xi \\ dt & dz & 0 & 0 \\ 0 & 0 & dt & dz \end{bmatrix}\begin{bmatrix} v_t \\ v_z \\ \xi_t \\ \xi_z \end{bmatrix} = \begin{bmatrix} 0 \\ 0 \\ dv \\ d\xi \end{bmatrix} \tag{3}$$

The last two state that dv and $d\xi$ are computed along the characteristic lines.

The Ist characteristic equations follow from requiring that the determinant of the coefficients vanish.

To reduce this determinant divide the third and fourth columns by dt and $dt/2\xi$ respectively, and subtract from the first and second respectively. Then expand by minors to obtain the new determinant

$$\begin{bmatrix} v - \frac{dz}{dt} & \frac{(\epsilon-\epsilon_0)V^2}{\pi^2\rho\xi^3} - \frac{\gamma}{\rho\xi^2} \\ \xi^2 & 2\xi\left[v - \frac{dz}{dt}\right] \end{bmatrix} = 0 \tag{4}$$

Prob. 11.7.2 (cont.)

Thus, the Ist characteristic equations are

$$\left(\frac{dz}{dt} - v\right)^2 = \frac{1}{2}\xi\left[\frac{(\epsilon-\epsilon_0)V^2}{\pi^2 \rho \xi^3} - \frac{\gamma}{\rho \xi^2}\right] \tag{5}$$

or

$$\frac{dz}{dt} = v \pm a(\xi) \; ; \; a(\xi) \equiv \left[\frac{(\epsilon-\epsilon_0)V^2}{2\pi^2 \rho \xi^2} - \frac{\gamma}{2\rho\xi}\right]^{1/2} \text{ on } C^{\pm} \tag{6}$$

The IInd characteristics are found from the determinant obtained by substituting the column matrix on the right for the column on the left.

$$\begin{bmatrix} 0 & v & 0 & \frac{(\epsilon-\epsilon_0)V^2}{\pi^2\rho}\frac{1}{\xi^3} - \frac{\gamma}{\rho\xi^2} \\ 0 & \xi^2 & 2\xi & 2v\xi \\ dv & dz & 0 & 0 \\ d\xi & 0 & dt & dz \end{bmatrix} = 0 \tag{7}$$

Solution, expanding in minors about dv and $d\xi$, gives

$$dv\left\{v\left(2\xi\frac{dz}{dt} - 2v\xi\right) + \xi^2\left(\frac{2a^2}{\xi}\right)\right\}$$
$$+ d\xi\left\{2\xi\frac{dz}{dt}\left(\frac{2a^2}{\xi}\right)\right\} = 0 \tag{8}$$

With the understanding the $\pm$ signs mean that the relations pertain to $C^{\pm}$, Eq. 6 reduces this expression to the IInd characteristic equations.

$$\frac{2a}{\xi}d\xi \pm dv = 0 \quad \text{on} \quad C^{\pm} \tag{9}$$

Prob. 11.7.3 (a) The equations of motion are 9.13.11 and 9.13.12 with $V = 0$ and $b = 0$.

$$\frac{\partial v}{\partial t} + v\frac{\partial v}{\partial z} + g\frac{\partial \xi}{\partial z} = 0 \tag{1}$$

$$\frac{\partial \xi}{\partial t} + v\frac{\partial \xi}{\partial z} + \xi\frac{\partial v}{\partial z} = 0 \tag{2}$$

These are the first two of the following relations

$$\begin{bmatrix} 1 & v & 0 & g \\ 0 & \xi & 1 & v \\ dt & dz & 0 & 0 \\ 0 & 0 & dt & dz \end{bmatrix} \begin{bmatrix} v_{,t} \\ v_{,z} \\ \xi_{,t} \\ \xi_{,z} \end{bmatrix} \begin{bmatrix} 0 \\ 0 \\ dv \\ d\xi \end{bmatrix} \tag{3}$$

The last two define dv and $d\xi$ as the differentials computed in the characteristic directions.

The determinant of the coefficients gives the Ist characteristics. Using the same reduction as in going from Eq. 11.6.18 to 11.6.19 gives

$$\begin{bmatrix} v - \frac{dz}{dt} & g \\ \xi & v - \frac{dz}{dt} \end{bmatrix} = \left(v - \frac{dz}{dt}\right)^2 - g\xi = 0 \tag{4}$$

or

$$\frac{dz}{dt} = v \pm \sqrt{g\xi} = v \pm \tfrac{1}{2}R(\xi)\,;\; R(\xi) \equiv 2\sqrt{g\xi} \tag{5}$$

Prob. 11.7.3 (cont.)

The second characteristics are this same determinant with the column matrix on the right substituted for the first column on the left.

$$\begin{bmatrix} 0 & v & 0 & g \\ 0 & \xi & 1 & v \\ dv & dz & 0 & 0 \\ d\xi & 0 & dt & dz \end{bmatrix} = dv\left[v(dz - v\,dt) + \xi(g\,dt)\right] + d\xi(g\,dz) \tag{6}$$

In view of Eq. 5, this expression becomes

$$dv \pm \sqrt{\frac{g}{\xi}}\, d\xi = 0 \quad ; \; C^{\pm} \tag{7}$$

Integration gives

$$v \pm R(\xi) = c_{\pm} \quad ; \; C^{\pm} \tag{8}$$

(b) The initial and boundary conditions are as shown to the right. C^+ characteristics are straight lines.

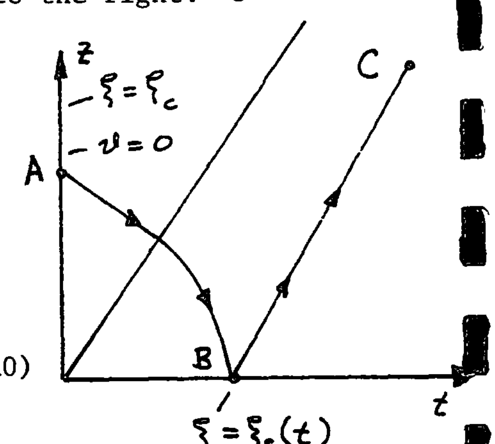

On C^- from $A \to B$ the invariant is

$$-R(\xi_c) = c_- \tag{9}$$

At B, it follows that

$$v_B = c_- + R(\xi_s) = R(\xi_s) - R(\xi_c) \tag{10}$$

and hence from $B \to C$

$$c_+ = v_B + R(\xi_B) = R(\xi_s) - R(\xi_c) + R(\xi_s) = 2R(\xi_s) - R(\xi_c) \tag{11}$$

Also, from $B \to C$

$$c_- = -R(\xi_c) \tag{12}$$

Prob. 11.7.3 (cont.)

Eq. 8 shows that at a point where C^+ and C^- characteristics cross

$$v = \frac{c_+ + c_-}{2} \tag{13}$$

$$R(\xi) = \frac{c_+ - c_-}{2} \tag{14}$$

So, at any point on $B \rightarrow C$, these equations are evaluated using Eqs. 11 and 12 to give

$$v = R(\xi_s) - R(\xi_c) \tag{15}$$

$$R(\xi) = R(\xi_s) \tag{16}$$

Further, the slope of the line is the constant, from Eq. 5,

$$\frac{dz}{dt} = 2\,R(\xi_s) + \frac{1}{2}\left[R(\xi_s) - R(\xi_c)\right]$$
$$= \frac{3}{2} R(\xi_s) - R(\xi_c) \tag{17}$$

Thus, the response on all C^+ characteristics originating on the t axis is determined. For those originating on the z axis, the solution is $v = 0$ and $\xi = \xi_c$.

(c) Initial conditions set the invariants $c_\pm$

$$c_\pm = v \pm 2\sqrt{g\xi} = 1 \pm 2\sqrt{\xi} \tag{18}$$

The numerical values are shown on the respective characteristics in Fig. 11.7.3a to the left of the z axis.

(d) At the intersections of the characteristics, v and ξ follow from Eqs. 13 and 14

Prob. 11.7.3 (cont.)

$$\vartheta = \frac{1}{2}(c_+ + c_-) \tag{19}$$

$$\xi = \left(\frac{c_+ - c_-}{4}\right)^2 \tag{20}$$

The numerical values are displayed above the intersections in the figure as (ϑ, ξ). Note that the characteristic lines in this figure are only schematic.

(e) The slopes of the characteristics at each intersection now follow from Eq. 5.

$$\left(\frac{dz}{dt}\right)_{\pm} = \vartheta \pm \sqrt{\xi} \tag{21}$$

The numerical values are displayed under the characteristic intersections as $\left[\left(\frac{dz}{dt}\right)_+, \left(\frac{dz}{dt}\right)_-\right]$. Based on these slopes, the characteristics are drawn in Fig. P11.7.3b.

(f) Note (ϑ, ξ) are constant along characteristics $C^{\pm}$ leaving the "cone". All other points outside the "cone" have characteristics originating where $\vartheta = 1$ and $\xi = 1$ (constant state) and hence at these points the solution is $\vartheta = 1$ and $\xi = 1$. The velocity is shown as a function of z when $t = 0$, and 4 in Fig. P11.7.3c. As can be seen from either these plots or the characteristics, the wavefronts steepen into shocks.

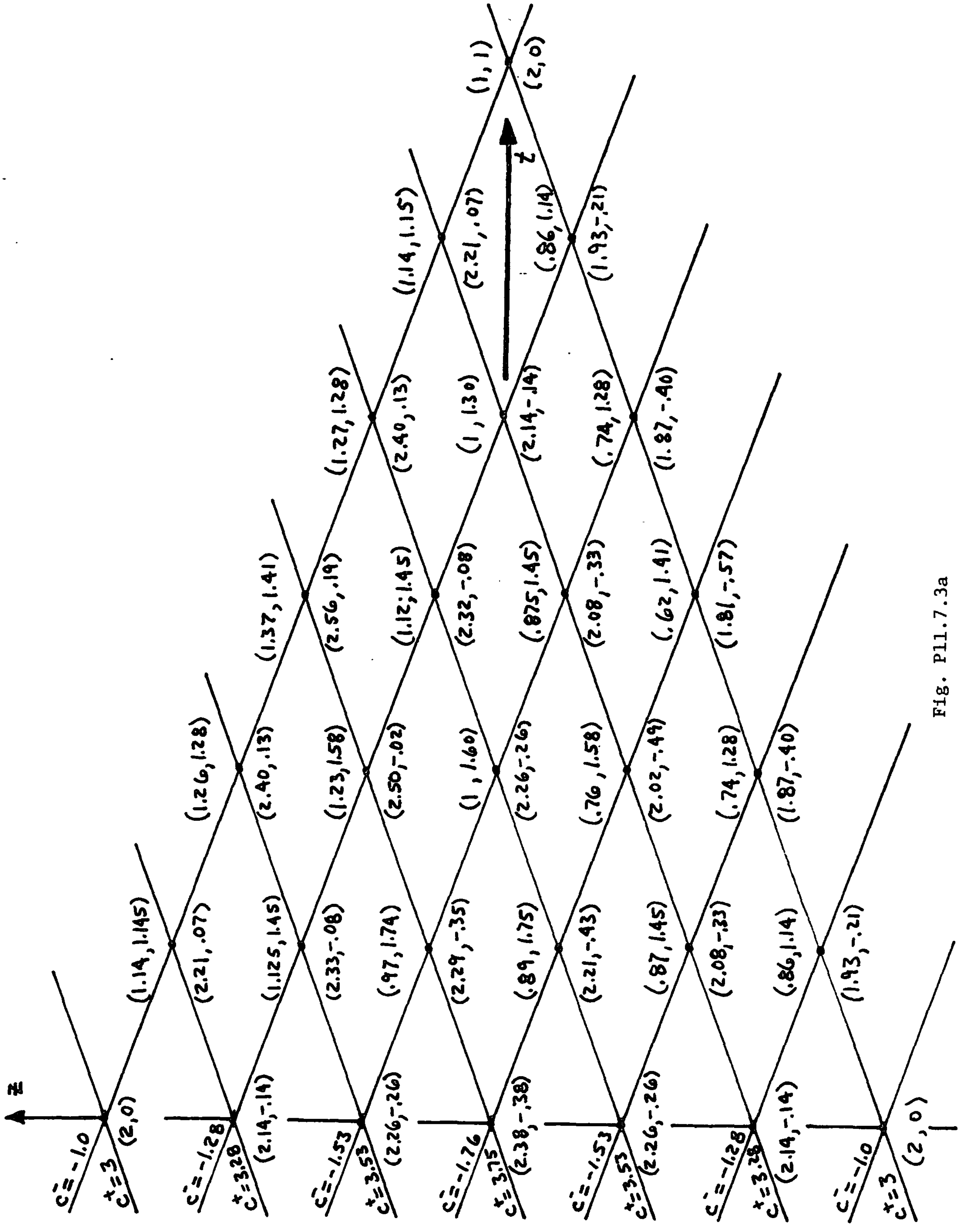
(1,1)
(2,0)
t
(1.14,1.15)
(2.21,.07)
(.86,1.14)
(1.93,-.21)
(1.27,1.28)
(2.40,.13)
(1,1.30)
(2.14,-.14)
(.74,1.28)
(1.87,-.40)
(1.37,1.41)
(2.56,.19)
(1.12,1.45)
(2.32,-.08)
(.875,1.45)
(2.08,-.33)
(.62,1.41)
(1.81,-.57)
(1.26,1.28)
(2.40,.13)
(1.23,1.58)
(2.50,-.02)
(1,1.60)
(2.26,-.26)
(.76,1.58)
(2.02,-.49)
(.74,1.28)
(1.87,-.40)
(1.14,1.145)
(2.21,.07)
(1.125,1.45)
(2.33,-.08)
(.97,1.74)
(2.29,-.35)
(.89,1.75)
(2.21,-.43)
(.87,1.45)
(2.08,-.33)
(.86,1.14)
(1.93,-.21)
z
(2,0)
(2.14,-.14)
(2.26,-.26)
(2.38,-.38)
(2.26,-.26)
(2.14,-.14)
(2,0)
c⁻=-1.0
c⁺=3
c⁻=-1.28
c⁺=3.28
c⁻=-1.53
c⁺=3.53
c⁻=-1.76
c⁺=3.75
c⁻=-1.53
c⁺=3.53
c⁻=-1.28
c⁺=3.28
c⁻=-1.0
c⁺=3

Fig. P11.7.3a

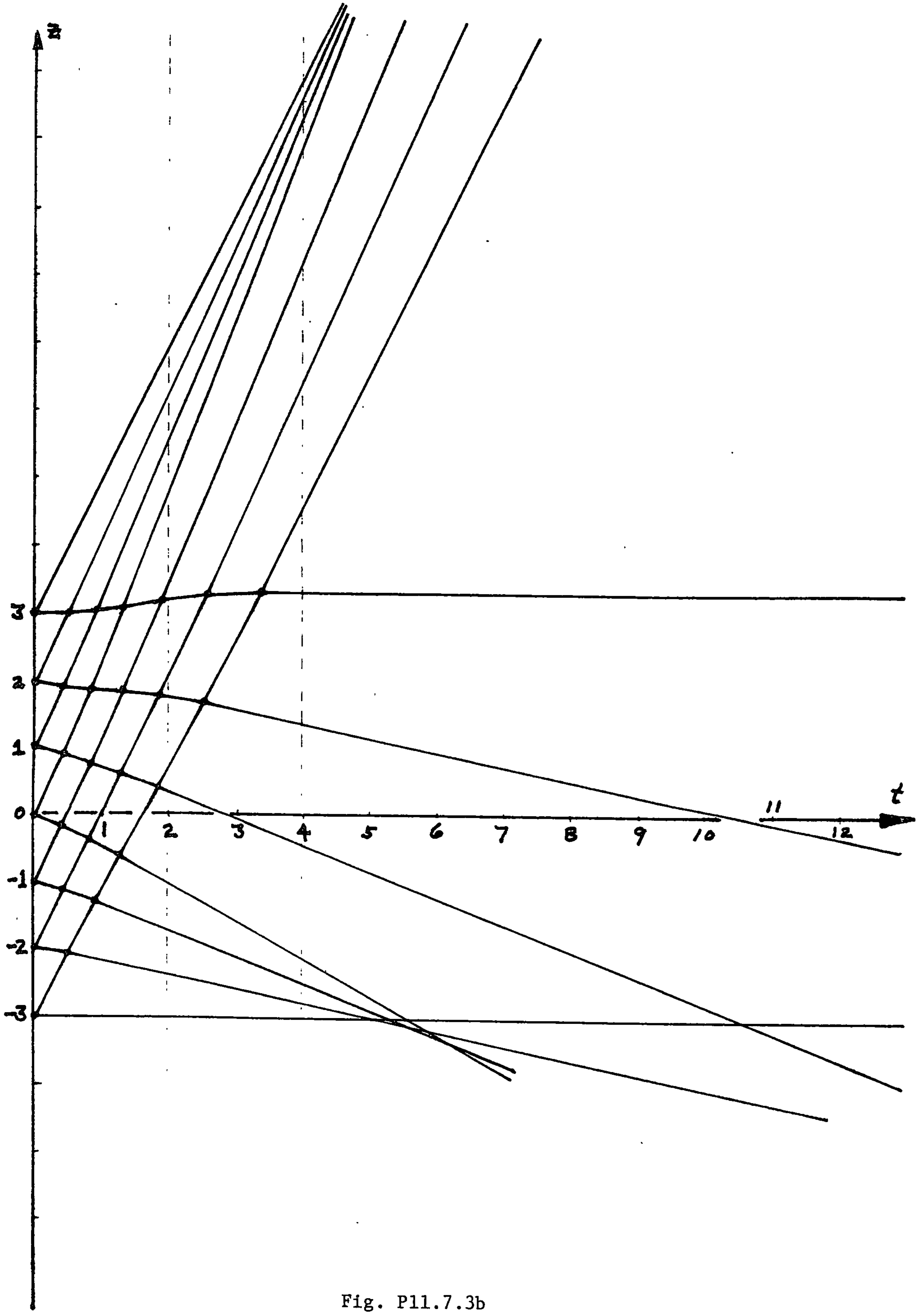

Fig. P11.7.3b

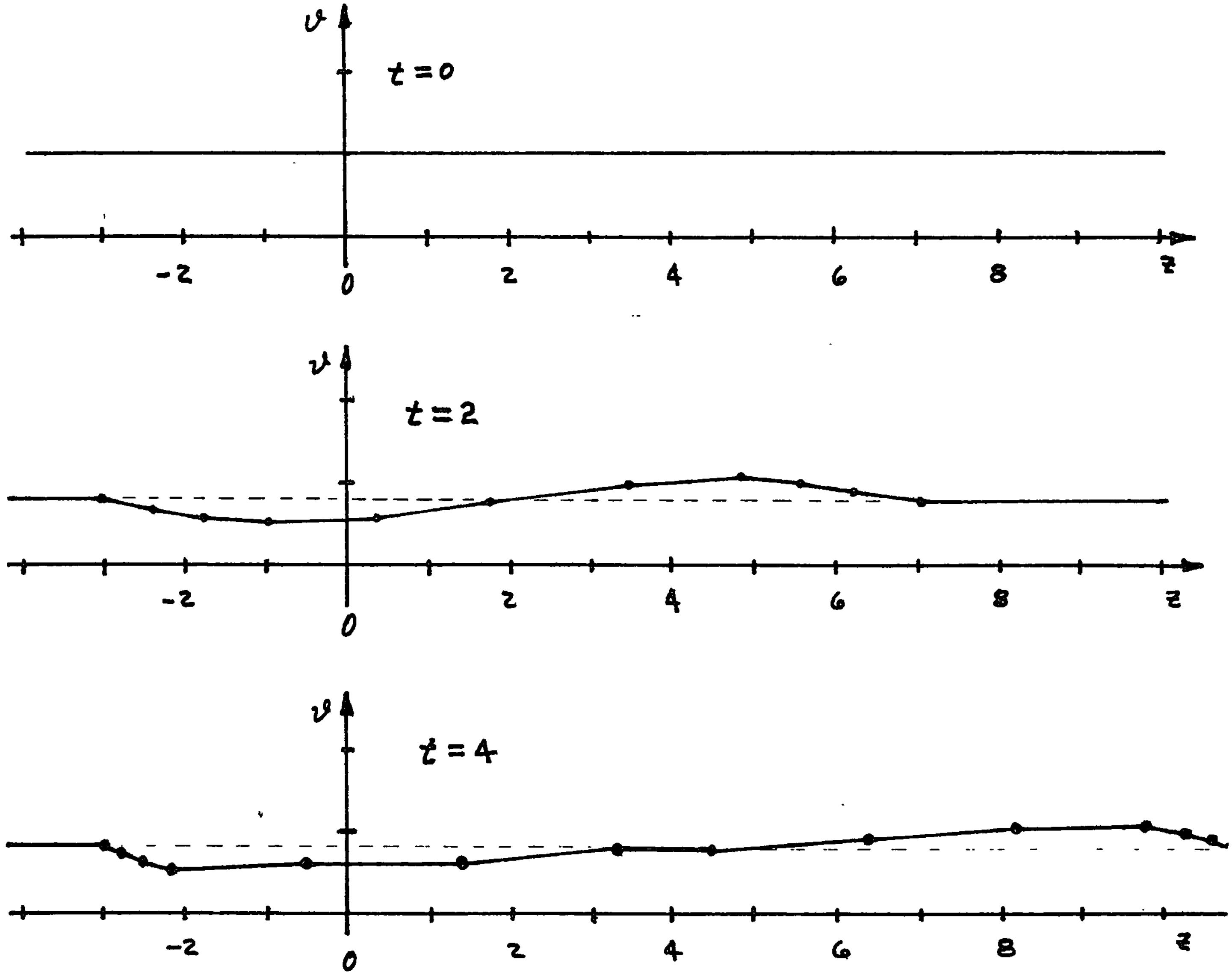

Fig. P11.7.3c

Prob. 11.7.4 (a) Faraday's and Ampere's laws for fields of the given forms reduce to

$$\begin{bmatrix} \bar{i}_x & \bar{i}_y & \bar{i}_z \\ 0 & 0 & \frac{\partial}{\partial z} \\ E & 0 & 0 \end{bmatrix} = \bar{i}_y \frac{\partial E}{\partial z} = -\bar{i}_y \mu_o \frac{\partial H}{\partial t} \tag{1}$$

$$\begin{bmatrix} \bar{i}_x & \bar{i}_y & \bar{i}_z \\ 0 & 0 & \frac{\partial}{\partial z} \\ 0 & H & 0 \end{bmatrix} = -\bar{i}_x \frac{\partial H}{\partial z} = \bar{i}_x \left[\epsilon + 3\delta E^2\right] \frac{\partial E}{\partial t} \tag{2}$$

The fields are transverse and hence solenoidal, as required by the remaining two equations with $\rho_f = 0$.

(b) The characteristic equations follow from

$$\begin{bmatrix} 0 & 1 & \mu_o & 0 \\ \epsilon + 3\delta E^2 & 0 & 0 & 1 \\ dt & dz & 0 & 0 \\ 0 & 0 & dt & dz \end{bmatrix} \begin{bmatrix} E_t \\ E_z \\ H_t \\ H_z \end{bmatrix} = \begin{bmatrix} 0 \\ 0 \\ dE \\ dH \end{bmatrix} \tag{3}$$

The I'st characteristic equations follow by setting the determinant of the coefficients equal to zero. Expanding by minors about the two terms in the first row gives

$$-(dt)^2 + \mu_o (dz)^2 (\epsilon + 3\delta E^2) = 0 \Rightarrow \frac{dz}{dt} = \frac{\pm 1}{\sqrt{\mu_o(\epsilon + 3\delta E^2)}} \quad \text{on} \quad C^{\pm} \tag{4}$$

Prob. 11.7.4 (cont.)

The IInd characteristic equations follow from the determinant formed by substituting the column matrix on the right in Eq. 3 for the first column on the left.

$$\begin{bmatrix} 0 & 1 & \mu_o & 0 \\ 0 & 0 & 0 & 1 \\ dE & dz & 0 & 0 \\ dH & 0 & dt & dz \end{bmatrix} = 0 \tag{5}$$

Expansion about the two terms in the first column gives

$$-dE\,dt - dH(dz\,\mu_o) = 0 \Rightarrow dE + \mu_o dH \frac{dz}{dt} = 0 \tag{6}$$

With dz/dt given by Eq. 4, this becomes

$$dE \pm \sqrt{\frac{\mu_o}{\epsilon + 3\delta E^2}}\, dH = 0 \Rightarrow dH \pm \sqrt{\frac{\epsilon + 3\delta E^2}{\mu_o}}\, dE = 0 \tag{7}$$

This expression is integrated to obtain

$$H \pm \mathcal{R}(E) = c_\pm \tag{8}$$

where

$$\mathcal{R}(E) \equiv \left\{ E\sqrt{E^2 + \frac{\epsilon}{3\delta}} + \frac{\epsilon}{3\delta} \ln\left(E + \sqrt{E^2 + \frac{\epsilon}{3\delta}}\right)\right\} \sqrt{\frac{3\delta}{4\mu_o}}$$

(c) At point A on the t=0 axis the invariant follows from Eq. 8 as

$$c_- = -\mathcal{R}(0) = \frac{-\epsilon}{3\delta} \ln\sqrt{\frac{\epsilon}{3\delta}}\, \sqrt{\frac{3\delta}{4\mu_o}} \tag{9}$$

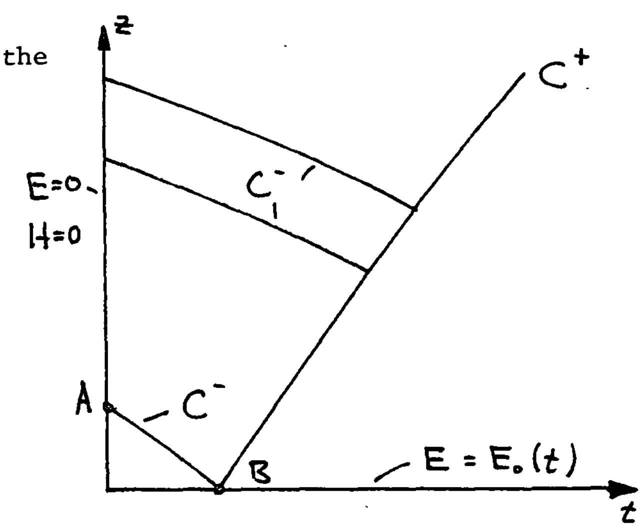

Prob. 11.7.4 (cont.)

Evaluation of the same equation at B when $E = E_o(t)$ then gives

$$H_B - \mathcal{R}(E_o) = -\mathcal{R}(0) \Rightarrow H_B = -\mathcal{R}(0) + \mathcal{R}(E_o) \tag{10}$$

Thus, it is clear that if H were also given $(H_o(t))$ at z=0, the problem would be overspecified.

On the C^+ characteristic, Eqs. 8 and 11 and the fact that $E=E_o$ at B serve to evaluate

$$c_+ = H_B + \mathcal{R}(E_o) = -\mathcal{R}(0) + 2\mathcal{R}(E_o) \tag{11}$$

Because _ is the same for all C^- characteristics coming from the z axis, it follows from Eqs. 8, 9 and 12 that

$$H + \mathcal{R}(E) = -\mathcal{R}(0) + 2\mathcal{R}(E_o) \tag{12}$$

$$H - \mathcal{R}(E) = -\mathcal{R}(0) \tag{13}$$

So, on the C^+ characteristics originating on the t axis,

$$H = \mathcal{R}(E_o) - \mathcal{R}(0) \tag{14}$$

$$\mathcal{R}(E) = \mathcal{R}(E_o) \tag{15}$$

Because the slope of this line is given by Eq. 4

$$\frac{dz}{dt} = \frac{1}{\sqrt{\mu_o(\epsilon + 3\delta E^2)}} \tag{16}$$

evaluated using E inferred from Eq. 16, it follows that the slope is the same at each point on the line.

For $\mu_o = \epsilon = \delta$, the C^+ characteristics have the slopes

$$\frac{dz}{dt} = \frac{1}{\sqrt{1 + 3E_o^2}}$$

and hence values shown in the table. These lines are drawn in the figure. Remember that E is constant along these lines. Thus, it is possible to

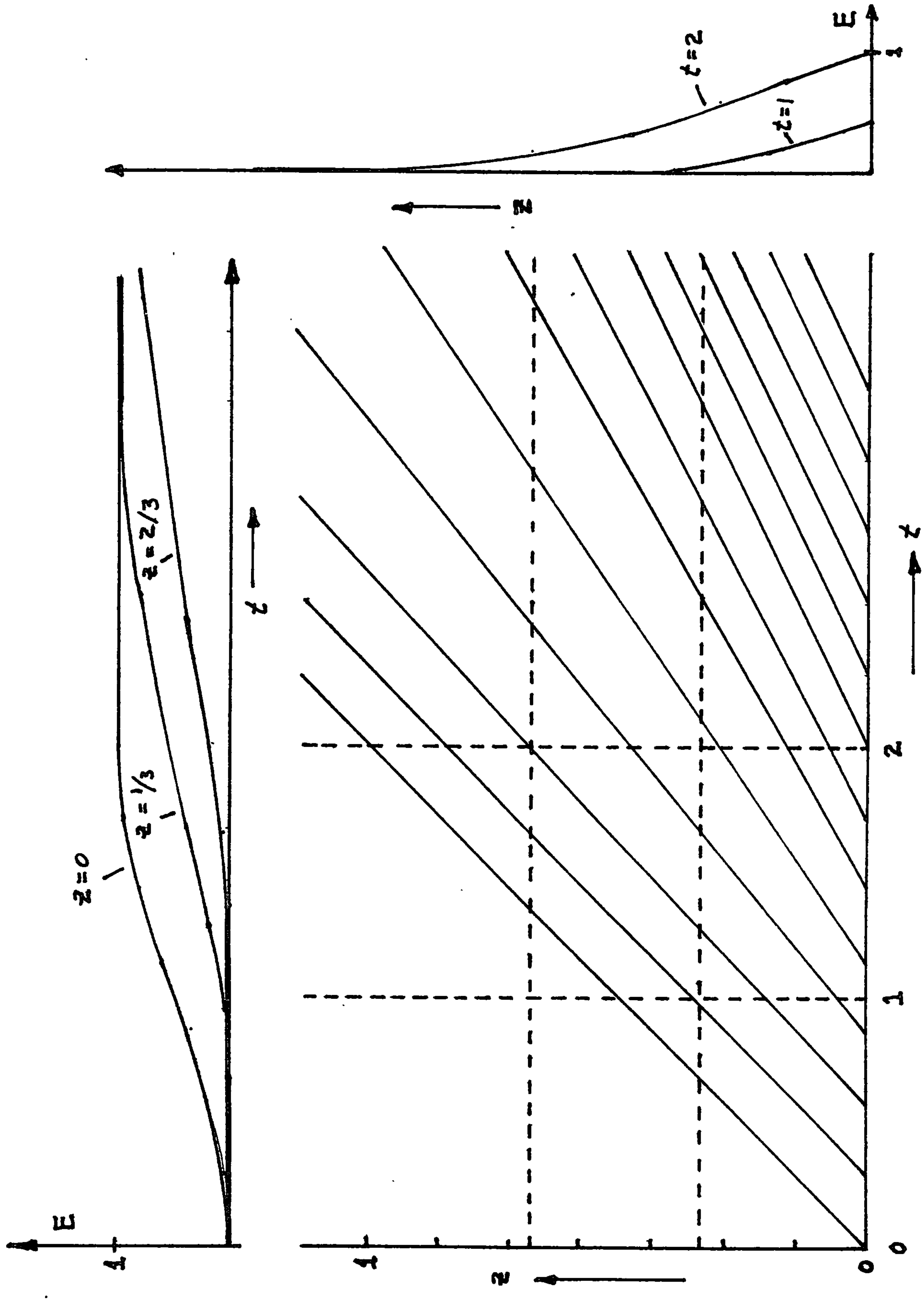
E
t=2
t=1
z
E
4
z=0
z=1/3
z=2/3
t
z
4
0
1
2
t

Prob. 11.7.4 (cont.)

plot either the z or t dependence of E, as shown. Note that the wave front tends to smooth out.

t	E_o	dz/dt
0	0	1
0.285	0.0493	0.996
0.571	0.188	0.951
0.857	0.389	0.829
1.14	0.609	0.688
1.43	0.813	0.579
1.71	0.950	0.519
2.0	1.0	0.50

Prob. 11.7.5 (a) Conservation of total flux requires that

$$B_o \pi (a^2 - \xi_o^2) = B_z \pi (a^2 - \xi^2) \Rightarrow B_z = B_o \frac{(a^2 - \xi_o^2)}{(a^2 - \xi^2)} \tag{1}$$

Thus, for long wave deformations, radial stress equilibrium at the interface requires that

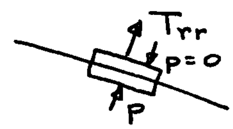

$$p = -T_{rr} = \frac{1}{2}\mu_o B_z^2 = \frac{1}{2}\mu_o \frac{(a^2 - \xi_o^2)}{(a^2 - \xi^2)} \tag{2}$$

By replacing $\pi \xi^2 = A(z)$, the function on the right in Eq. (2) takes the form of Eq. 9.13.5. Thus, the desired equations of motion are Eq. 9.13.9

$$\frac{\partial A}{\partial t} + v\frac{\partial A}{\partial z} + A\frac{\partial v}{\partial z} = 0 \tag{3}$$

and Eq. 9.13.4

$$\frac{\partial v}{\partial t} + v\frac{\partial v}{\partial z} + \frac{c^2}{A}\frac{\partial A}{\partial z} = 0 \tag{4}$$

where

$$c^2 \equiv \frac{B_o^2}{\mu_o \rho} \frac{(\pi a^2 - A_o)^2}{(\pi a^2 - A)^3} A$$

Prob. 11.7.5 (cont.)

Then, the characteristic equations are formed from

$$\begin{bmatrix} 1 & v & 0 & A \\ 0 & \frac{c^2}{A} & 1 & v \\ dt & dz & 0 & 0 \\ 0 & 0 & dt & dz \end{bmatrix} \begin{bmatrix} A_t \\ A_z \\ v_t \\ v_z \end{bmatrix} \begin{bmatrix} 0 \\ 0 \\ dA \\ dv \end{bmatrix} \tag{5}$$

The determinant of the coefficients gives the I'st characteristics

$$\frac{dz}{dt} = v \pm c \tag{6}$$

while the second follows from

$$\begin{bmatrix} 0 & v & 0 & A \\ 0 & \frac{c^2}{A} & 1 & v \\ dA & dz & 0 & 0 \\ dv & 0 & dt & dz \end{bmatrix} = 0 \tag{7}$$

which is

$$dA\left[v\left(\frac{dz}{dt} - v\right) + a^2\right] + dv\left(\frac{dz}{dt} A_o\right) = 0 \tag{8}$$

With the use of Eq. 6, this becomes

$$dv \pm c\frac{dA}{A_o} = 0 \tag{9}$$

The integral of this expression is

$$v \pm \mathcal{R}(A) = C_\pm \tag{10}$$

where

$$\mathcal{R}(A) = \int \frac{c}{A}\, dA = \sqrt{\frac{B_o^2(\pi a^2 - A_o)^2}{\mu_o \rho A_o}}\ \frac{2}{\pi a^2}\sqrt{\frac{A}{\pi a^2 - A}} \tag{11}$$

Prob. 11.7.5 (cont.)

Now, given initial conditions

$$\xi = \xi_o(z) \Rightarrow A = A_o(z) \; ; \; v = 0 \tag{12}$$

where the maximum $A_o(z)$ is A_{max} , invariants follow from Eq. 10 as

$$c_+ = \mathcal{R}(A_B) \; ; \; c_- = -\mathcal{R}(A_c) \tag{13}$$

so solution at D is

$$\mathcal{R}(A_D) = \frac{c_+ - c_-}{2} = \frac{\mathcal{R}(A_B) + \mathcal{R}(A_c)}{2}$$

Thus, the solution R at D is the mean of that at B and C. The largest possible value for A at D is therefore obtained if either B or C is at the maximum in A. Because this implies that the other characteristic comes from a lesser value of A, it follows that A at D is smaller than A_{max}.

Prob. 11.8.1 For "plane-wave" motions of arbitrary orientation, $\bar{v} = \bar{v}(x,t)$ and $\bar{H} = \bar{H}(x,t)$, the general laws are:

Mass Conservation

$$\frac{\partial \rho}{\partial t} + v_x \frac{\partial \rho}{\partial x} + \rho \frac{\partial v_x}{\partial x} = 0 \tag{1}$$

Momentum Conservation (three components)

$$\rho\left(\frac{\partial v_x}{\partial t} + v_x \frac{\partial v_x}{\partial x}\right) + \frac{\partial p}{\partial x} = \frac{\partial T_{xx}}{\partial x} = \frac{\partial}{\partial x}\left[\frac{1}{2}\mu_o\left(H_x^2 - H_y^2 - H_z^2\right)\right] \tag{2}$$

$$\rho\left(\frac{\partial v_y}{\partial t} + v_x \frac{\partial v_y}{\partial x}\right) = \frac{\partial T_{yx}}{\partial x} = \frac{\partial}{\partial x}\left(\mu_o H_x H_y\right) \tag{3}$$

$$\rho\left(\frac{\partial v_z}{\partial t} + v_x \frac{\partial v_z}{\partial x}\right) = \frac{\partial T_{zx}}{\partial x} = \frac{\partial}{\partial x}\left(\mu_o H_x H_z\right) \tag{4}$$

Energy Conservation (which reduces to the insentropic equation of state)

$$\left(\frac{\partial}{\partial t} + v_x \frac{\partial}{\partial x}\right)\left(p \rho^{-\gamma}\right) = 0 \tag{5}$$

The laws of Faraday, Ampere and Ohm (for perfect conductor), Eq. 6.2.3

$$\frac{\partial H_x}{\partial t} = 0 \tag{6}$$

$$\frac{\partial H_y}{\partial t} = \frac{\partial}{\partial x}\left(-v_x H_y + v_y H_x\right) \tag{7}$$

$$\frac{\partial H_z}{\partial t} = \frac{\partial}{\partial x}\left(v_z H_x - v_x H_z\right) \tag{8}$$

These eight equations represent the evolution of the dependent variables

$$(\rho, p, v_x, v_y, v_z, H_x, H_y, H_z)$$

From Eq. 6, (as well as the requirement that $\bar{H}$ is solenoidal) it follows that H_x is independent of both t and x. Hence, H_x can be eliminated from Eq. 2 and considered a constant in Eqs. 3, 4, 7 and 8. Equations 1-5, 7 and 8 are now written as the first 7 of the following 14 equations.

$$
\begin{bmatrix}
1 & v_x & 0 & 0 & 0 & \rho & 0 & 0 & 0 & 0 & 0 & 0 & 0 & 0 \\
0 & 0 & 0 & 1 & \rho & \rho v_x & 0 & 0 & 0 & 0 & 0 & \mu_0 H_y & 0 & \mu_0 H_z \\
0 & 0 & 0 & 0 & 0 & 0 & \rho & \rho v_x & 0 & 0 & 0 & -\mu_0 H_x & 0 & 0 \\
0 & 0 & 0 & 0 & 0 & 0 & 0 & 0 & \rho & \rho v_x & 0 & 0 & 0 & -\mu_0 H_x \\
-\frac{\gamma p}{\rho} & -\frac{\gamma v_x p}{\rho} & 1 & v_x & 0 & 0 & 0 & 0 & 0 & 0 & 0 & 0 & 0 & 0 \\
0 & 0 & 0 & 0 & 0 & -H_y & 0 & H_x & 0 & 0 & -1 & -v_x & 0 & 0 \\
0 & 0 & 0 & 0 & 0 & -H_z & 0 & 0 & 0 & H_x & 0 & 0 & -1 & -v_x \\
dt & dx & 0 & 0 & 0 & 0 & 0 & 0 & 0 & 0 & 0 & 0 & 0 & 0 \\
0 & 0 & dt & dx & 0 & 0 & 0 & 0 & 0 & 0 & 0 & 0 & 0 & 0 \\
0 & 0 & 0 & 0 & dt & dx & 0 & 0 & 0 & 0 & 0 & 0 & 0 & 0 \\
0 & 0 & 0 & 0 & 0 & 0 & dt & dx & 0 & 0 & 0 & 0 & 0 & 0 \\
0 & 0 & 0 & 0 & 0 & 0 & 0 & 0 & dt & dx & 0 & 0 & 0 & 0 \\
0 & 0 & 0 & 0 & 0 & 0 & 0 & 0 & 0 & 0 & dt & dx & 0 & 0 \\
0 & 0 & 0 & 0 & 0 & 0 & 0 & 0 & 0 & 0 & dt & dx & 0 & 0
\end{bmatrix}
\begin{bmatrix}
\rho_{,t} \\ \rho_{,x} \\ p_{,t} \\ p_{,x} \\ v_{x,t} \\ v_{x,x} \\ v_{y,t} \\ v_{y,x} \\ v_{z,t} \\ v_{z,x} \\ H_{y,t} \\ H_{y,x} \\ H_{z,t} \\ H_{z,x}
\end{bmatrix}
=
\begin{bmatrix}
0 \\ 0 \\ 0 \\ 0 \\ 0 \\ 0 \\ 0 \\ d\rho \\ dp \\ dv_x \\ dv_y \\ dv_z \\ dH_y \\ dH_z
\end{bmatrix}
$$

Prob. 11.8.1 (cont.)

Following steps illustrated by Eq. 11.15.19, the determinant of the coefficients is reduced to

$$\begin{vmatrix} v_x-\frac{dx}{dt} & 0 & \rho & 0 & 0 & 0 & 0 \\ 0 & 1 & \rho(v_x-\frac{dx}{dt}) & 0 & 0 & \mu_o H_y & \mu_o H_z \\ 0 & 0 & 0 & \rho(v_x-\frac{dx}{dt}) & 0 & -\mu_o H_x & 0 \\ 0 & 0 & 0 & 0 & \rho(v_x-\frac{dx}{dt}) & 0 & -\mu_o H_x \\ -\frac{\gamma p}{\rho}(v_x-\frac{dx}{dt}) & (v_x-\frac{dx}{dt}) & 0 & 0 & 0 & 0 & 0 \\ 0 & 0 & -H_y & H_x & 0 & -(v_x-\frac{dx}{dt}) & 0 \\ 0 & 0 & -H_z & 0 & H_x & 0 & -(v_x-\frac{dx}{dt}) \end{vmatrix} = 0 \qquad (10)$$

The quantity $v_x - \frac{dx}{dt}$ can be factored out of the fifth row. That row is then subtracted from the second so that there are all zeros in the second column except for the A_{52} term. Expansion by minors about this term then gives

$$(v_x-\frac{dx}{dt})\begin{vmatrix} \rho(v_x-\frac{dx}{dt}) & \rho & 0 & 0 & 0 & 0 \\ \gamma p & \rho(v_x-\frac{dx}{dt}) & 0 & 0 & \mu_o H_y & \mu_o H_z \\ 0 & 0 & \rho(v_x-\frac{dx}{dt}) & 0 & -\mu_o H_x & 0 \\ 0 & 0 & 0 & \rho(v_x-\frac{dx}{dt}) & 0 & -\mu_o H_x \\ 0 & -H_y & H_x & 0 & -(v_x-\frac{dx}{dt}) & 0 \\ 0 & -H_z & 0 & H_x & 0 & -(v_x-\frac{dx}{dt}) \end{vmatrix} = 0 \qquad (11)$$

Multiplication of the second row by $(v_x-\frac{dx}{dt})\rho/\gamma p$ and subtraction from the

Prob. 11.8.1 (cont.)

first generates all zeros in the first row except for the A_{12} term. Expansion about that term then gives

$$\left(v_x-\frac{dx}{dt}\right)\begin{bmatrix} \rho-\frac{\rho^2}{\gamma p}\left(v_x-\frac{dx}{dt}\right)^2 & 0 & 0 & -\frac{\mu_o H_y \rho}{\gamma p}\left(v_x-\frac{dx}{dt}\right) & -\frac{\mu_o H_z \rho}{\gamma p}\left(v_x-\frac{dx}{dt}\right) \\ 0 & \rho\left(v_x-\frac{dx}{dt}\right) & 0 & -\mu_o H_x & 0 \\ 0 & 0 & \rho\left(v_x-\frac{dx}{dt}\right) & 0 & -\mu_o H_x \\ -H_y & H_x & 0 & -\left(v_x-\frac{dx}{dt}\right) & 0 \\ -H_z & 0 & H_x & 0 & -\left(v_x-\frac{dx}{dt}\right) \end{bmatrix} = 0 \qquad (12)$$

Multiplication of the second column by $\mu_o H_x/\rho\left(v_x-\frac{dx}{dt}\right)$ and addition to the fourth column generates all zeros in the second row except for the A_{22} term, while multiplication of the third column by $\mu_o H_x/\rho\left(v_x-\frac{dx}{dt}\right)$ and addition to the last column gives all zeros in the third row except for the A_{33} term. Thus, expansion by minors about the A_{22} and A_{33} terms gives

$$\left(v_x-\frac{dx}{dt}\right)\begin{bmatrix} \rho-\frac{\rho^2}{\gamma p}\left(v_x-\frac{dx}{dt}\right)^2 & -\frac{\mu_o H_y \rho}{\gamma p}\left(v_x-\frac{dx}{dt}\right) & -\frac{\mu_o H_z \rho}{\gamma p}\left(v_x-\frac{dx}{dt}\right) \\ -H_y & -\left(v_x-\frac{dx}{dt}\right)+\frac{\mu_o H_x^2}{\rho\left(v_x-\frac{dx}{dt}\right)} & 0 \\ -H_z & 0 & -\left(v_x-\frac{dx}{dt}\right)+\frac{\mu_o H_x^2}{\rho\left(v_x-\frac{dx}{dt}\right)} \end{bmatrix} = 0 \qquad (13)$$

Prob. 11.8.1 (cont.)

This third order determinant is then expanded by minors to give

$$\frac{\rho^4}{\gamma p}\left(v_x - \frac{dx}{dt}\right)\left[-\left(v_x - \frac{dx}{dt}\right)^2 + \frac{\mu_o H_x^2}{\rho}\right] \cdot \tag{14}$$
$$\left\{\left[\left(v_x - \frac{dx}{dt}\right)^2\right]^2 - \left(v_x - \frac{dx}{dt}\right)^2\left[\frac{\gamma p}{\rho} + \frac{\mu_o}{\rho}\left(H_x^2 + H_y^2 + H_z^2\right)\right] + \frac{\gamma p}{\rho}\frac{\mu_o H_x^2}{\rho}\right\} = 0$$

This expression has been factored to make evident the 7 characteristic lines. First, there is the particle line, evident from the outset (Eq. 5) as the line along which the isentropic invariant propagates.

$$\frac{dx}{dt} = v_x \tag{15}$$

The second represents the two Alfvén waves

$$\frac{dx}{dt} = v_x \pm a_a \quad ; \quad a_a \equiv \sqrt{\frac{\mu_o H_x^2}{\rho}} \tag{16}$$

and the last represents four magnetoacoustic waves

$$\frac{dx}{dt} = v_x \pm \begin{Bmatrix} a_{b+} \\ a_{b-} \end{Bmatrix} \tag{17}$$

where

$$a_{b\pm}^2 \equiv \frac{1}{2}\left(a^2 + a_a^2 + a_b^2\right) \pm \frac{1}{2}\sqrt{\left(a^2 + a_a^2 + a_b^2\right)^2 - 4a^2 a_a^2}$$

$$a \equiv \sqrt{\frac{\gamma p}{\rho}} = \sqrt{\gamma R T}$$

$$a_b \equiv \sqrt{\frac{\mu_o}{\rho}\left(H_y^2 + H_z^2\right)}$$

Prob. 11.9.1   Linearized, Eq. 11.9.17 becomes

$$\frac{d\mathring{e}}{dn} = \frac{-n}{\mathring{e}} \tag{1}$$

Thus,

$$\mathring{e}\, d\mathring{e} = -n\, dn \tag{2}$$

and integration gives

$$\mathring{e}^2 + \mathring{n}^2 = \text{constant} = \mathring{e}_i^2 \tag{3}$$

where the constant of integration is evaluated at the upstream grid where $n=0$ and $\mathring{e}=\mathring{e}_i$.

Prob. 11.9.2   Linearized, Eqs. 11.9.9 and 11.9.10 reduce to

$$\frac{dn}{dt} = -\mathring{e} \tag{1}$$

$$\frac{d\mathring{e}}{dt} = n \tag{2}$$

Elimination of $\underline{e}$ between these gives

$$\frac{d^2 n}{dt^2} + n = 0 \tag{3}$$

The solution to this equation giving $n=0$ when $t=t_o$ is

$$n = A(t_o)\sin(t-t_o) = A\left(t-\frac{z}{U}\right)\sin\left(\frac{z}{U}\right) \tag{4}$$

and it follows from Eq. 1 that

$$\mathring{e} = -A(t_o)\cos(t-t_o) = -A\left(t-\frac{z}{U}\right)\cos\left(\frac{z}{U}\right) \tag{5}$$

To establish $A(t_o)$ it is necessary to use Eq. 11.9.15, which requires that

$$-A(t) = -\frac{V(t)}{U} + \frac{1}{U}\int_0^1\int_0^z A\left(t-\frac{z'}{U}\right)\sin\left(\frac{z'}{U}\right)dz'\,dz \tag{6}$$

For the specific excitation

$$V = \mathrm{Re}\,\hat{V}\exp j\omega t \tag{7}$$

it is reasonable to search for a solution to Eq. 6 in which the phase and amplitude of the response at z=0 are unknown, but the frequency is the same as that of the driving voltage.

Prob. 11.9.2 (cont.)

$$A = \mathrm{Re}\,\hat{A}\exp j\omega t \tag{8}$$

Observe that

$$A\left(t-\frac{z'}{U}\right) = \mathrm{Re}\left(\hat{A}\,e^{j\omega t}e^{-j\frac{\omega z'}{U}}\right) = \frac{1}{2}\hat{A}\,e^{j\left(\omega t-\frac{\omega z'}{U}\right)} + \frac{1}{2}\hat{A}^{*}e^{-j\left(\omega t-\frac{\omega z'}{U}\right)} \tag{9}$$

and

$$\sin\frac{z'}{U} = \frac{1}{2j}\left(e^{j\frac{z'}{U}} - e^{-j\frac{z'}{U}}\right) \tag{10}$$

Thus,

$$\int_0^1\int_0^z A\left(t-\frac{z}{U}\right)\sin\frac{z'}{U}\,dz' =$$

$$\mathrm{Re}\,\frac{U\hat{A}}{2j}e^{j\omega t}\left\{-\frac{\left(e^{j\left(\frac{-\omega+1}{U}\right)}-1\right)}{\frac{1}{U}(-\omega+1)^2} + \frac{\left(e^{-j\left(\frac{\omega+1}{U}\right)}-1\right)}{\frac{1}{U}(\omega+1)^2} - \frac{1}{j(-\omega+1)} - \frac{1}{j(\omega+1)}\right\} \tag{11}$$

Substitution of Eqs. 7, 8 and 11 into Eq. 6 then gives an expression that can be solved for $\hat{A}$.

$$\hat{A} = \frac{\hat{V}}{U}\left\{1-\frac{U}{4j}\left[\frac{\left(e^{j\left(\frac{-\omega+1}{U}\right)}-1\right)U}{(1-\omega)^2} - \frac{\left(e^{-j\left(\frac{\omega+1}{U}\right)}-1\right)U}{(1+\omega)^2} + \frac{2}{j(1-\omega^2)}\right]\right\} \tag{12}$$

Thus, the solution taking the form of Eq. 4 is

$$n(z,t) = \mathrm{Re}\,\hat{A}\,e^{j\omega\left(t-\frac{z}{U}\right)}\sin\left(\frac{z}{U}\right) \tag{13}$$

where $\underline{A}$ is given by Eq. 12.

Prob. 11.10.1 With $p = 0$, Eqs. 11.10.7 and 11.10.8 are

$$d\vartheta + de(M \mp 1) = 0 \tag{1}$$

$$\frac{dz}{dt} = M \pm 1 \quad ; \quad C^{\pm} \tag{2}$$

In this limit, Eq. 1 can be integrated.

$$\vartheta + (M \mp 1)e = c_{\pm} \tag{3}$$

Initial conditions are

$$\xi = \xi_o(z,0) \Rightarrow e = \frac{\partial \xi_o}{\partial z} = e_o(z,0) \tag{4}$$

$$\vartheta = \vartheta_o(z,0) \tag{5}$$

These serve to evaluate $C_{\pm}$ in Eq. 3

$$c_{\pm} = \vartheta_o + (M \mp 1)e_o \tag{6}$$

At a point C where the characteristics cross Eq. 3 can be solved simultaneously to give

$$\begin{bmatrix} 1 & M-1 \\ 1 & M+1 \end{bmatrix}\begin{bmatrix} \vartheta \\ e \end{bmatrix} = \begin{bmatrix} C_+ \\ C_- \end{bmatrix} \Rightarrow \begin{array}{l} \vartheta = \frac{1}{2}\left[(M+1)c_+ - (M-1)c_-\right] \\ e = \frac{1}{2}\left[c_- - c_+\right] \end{array} \tag{7}$$

Integration of Eqs. 2 to give the characteristic lines shown gives

$$z = (M \pm 1)t + z_{\substack{A \\ B}} \tag{8}$$

Prob. 11.10.1 (cont.)

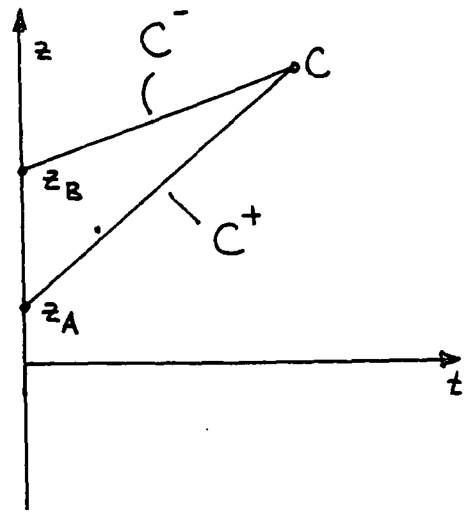

For these lines, the invariants of Eqs. 6 are

$$C_{\pm} = v_o\left(z_{A \atop B}\right) + (M \mp 1)e_o\left(z_{A \atop B}\right) \tag{9}$$

With z_A and z_B evaluated using Eq. 8, these invarients are written in terms of the (z,t) at point C.

$$C_{\pm} = v_o\left[z - (M \pm 1)t\right] + (M \mp 1)e_o\left[z - (M \pm 1)t\right] \tag{10}$$

and, finally, the solutions at C, Eq. 7, are written in terms of the (z,t) at C.

$$\begin{aligned} v = \frac{1}{2}\Big\{&(M+1)v_o\left[z-(M+1)t\right] + (M-1)(M+1)e_o\left[z-(M+1)t\right] \\ &- (M-1)v_o\left[z-(M-1)t\right] - (M+1)(M-1)e_o\left[z-(M-1)t\right] \end{aligned} \tag{11}$$

$$\begin{aligned} e = \frac{1}{2}\Big\{&v_o\left[z-(M-1)t\right] + (M+1)e_o\left[z-(M-1)t\right] \\ &- v_o\left[z-(M+1)t\right] - (M-1)e_o\left[z-(M+1)t\right]\Big\} \end{aligned} \tag{12}$$

Prob. 11.10.2 (a) With $\gamma = 0$, Eqs. 11.10.1 and 11.10.2 combine to give

$$\left(\frac{\partial}{\partial t} + U\frac{\partial}{\partial z}\right)^2 \xi = \frac{\epsilon_o}{2\Delta\rho}\left[\frac{(aE_o^2)}{(a-\xi)^2} - \frac{(aE_o^2)}{(a+\xi)^2}\right] \tag{1}$$

Normalization of this expression is such that

$$\underline{\xi} = \xi/a\ ,\quad \underline{t} = t/\tau\ ,\quad \underline{z} = z/\tau U \tag{2}$$

gives

$$\left(\frac{\partial}{\partial t} + \frac{\partial}{\partial z}\right)^2 \xi = \frac{P}{4}\left[\frac{1}{(1-\xi)^2} - \frac{1}{(1+\xi)^2}\right] \tag{3}$$

where

$$P \equiv 2\epsilon_o E_o^2 \tau^2/\Delta\rho a$$

(b) With the introduction of v as a variable, Eq. 3 becomes

$$\left(\frac{\partial}{\partial t} + \frac{\partial}{\partial z}\right) v = -\frac{\partial \mathcal{E}}{\partial \xi} \tag{4}$$

$$\left(\frac{\partial}{\partial t} + \frac{\partial}{\partial z}\right) \xi = v \tag{5}$$

where

$$\mathcal{E} = -\frac{P}{4}\left(\frac{1}{1-\xi} + \frac{1}{1+\xi}\right)$$

The characteristics could be found by one of the approaches outlined, but here they are obvious. On the I'st characteristics

$$\frac{dz}{dt} = 1 \tag{6}$$

the II'nd characteristic equations both apply and are

Prob. 11.10.2 (cont.)

$$\frac{d\upsilon}{dt} = -\frac{\partial E}{\partial \xi} \tag{7}$$

$$\frac{d\xi}{dt} = \upsilon \tag{8}$$

Multiply the left-hand side of Eq. 7 by the right-hand side of Eq. 8 and similarly, the right-hand side of Eq. 7 by the left-hand side of Eq. 8.

$$\upsilon\frac{d\upsilon}{dt} = -\frac{\partial E}{\partial \xi}\frac{d\xi}{dt} \Rightarrow \frac{d}{dt}\left[\frac{1}{2}\upsilon^2 + E(\xi)\right] = 0 \tag{9}$$

(c) It follows from Eq. 9 that

$$\frac{1}{2}\upsilon^2 + E(\xi) = \frac{1}{2}\upsilon_o^2 + E(\xi_o) \tag{10}$$

or specifically

$$\frac{1}{2}\upsilon^2 - \frac{P}{4}\left[\frac{1}{1-\xi} + \frac{1}{1+\xi}\right] = \frac{1}{2}\upsilon_o^2 - \frac{P}{4}\left[\frac{1}{1-\xi_o} + \frac{1}{1+\xi_o}\right]$$

Phase-plane plots are shown in the first quandrant. Reflecting the unstable nature of the dynamics, the trajectories are open for $P > 1$, showing a deflection that has $\upsilon \rightarrow \infty$ as $\xi \rightarrow 1$ (the sheet approaches one or the other of the electrodes). The oscillatory nature of the response with $P = -1$ is apparent from the closed trajectories.

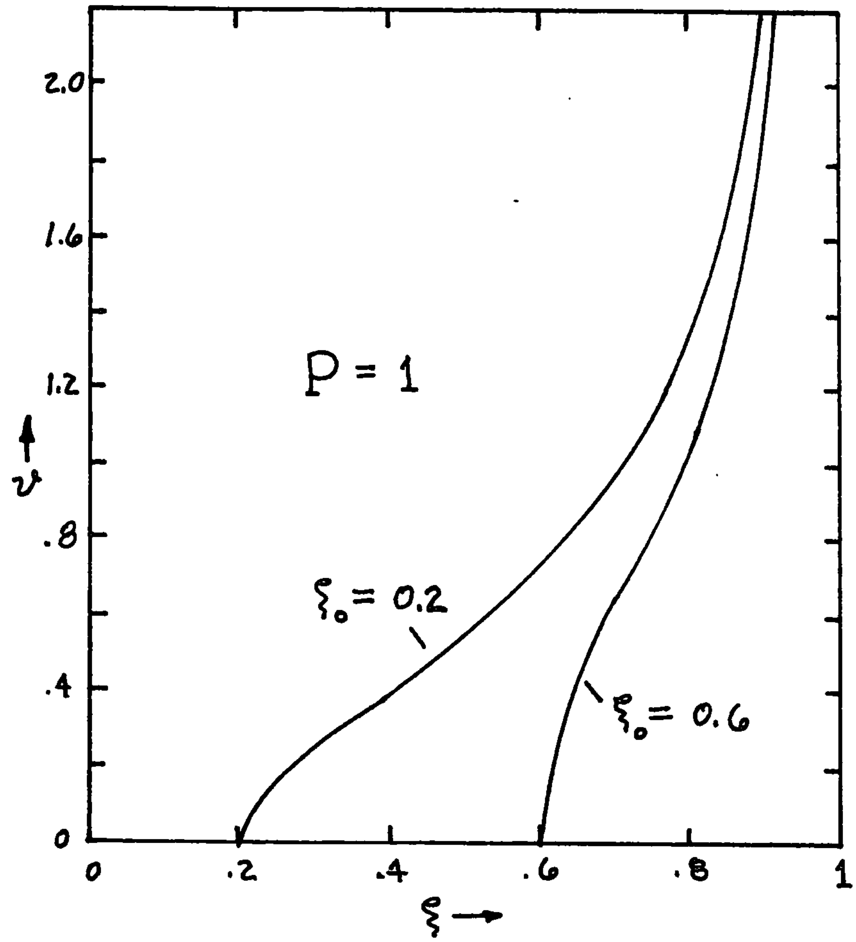
2.0
1.6
1.2
.8
.4
0
0
.2
.4
.6
.8
1
$\xi \rightarrow$
$\uparrow v$
P = 1
$\xi_0 = 0.2$
$\xi_0 = 0.6$

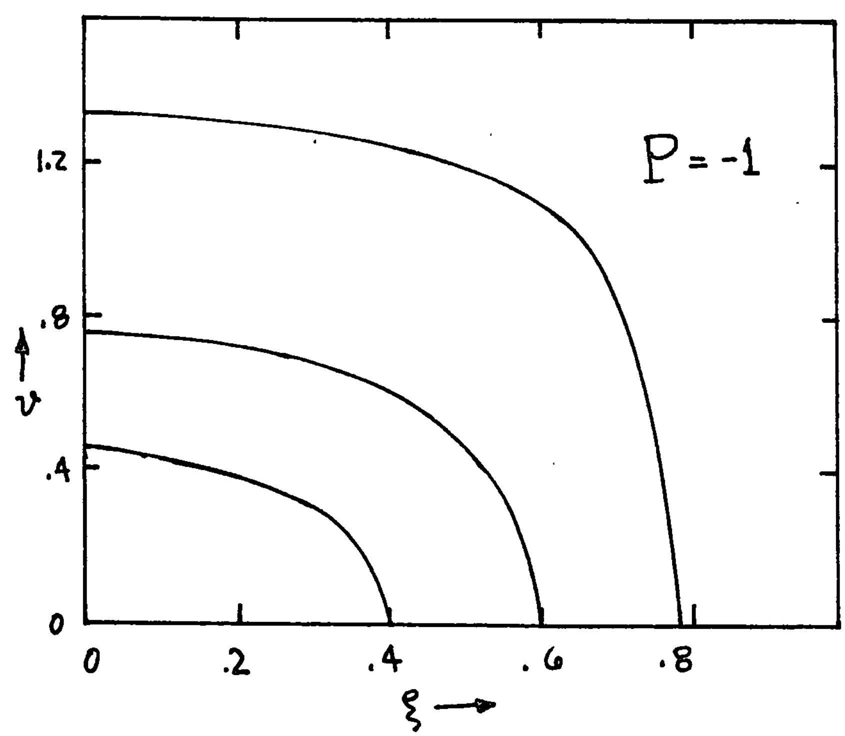
1.2
.8
.4
0
0
.2
.4
.6
.8
$\xi \rightarrow$
$\uparrow v$
P = -1

Prob. 11.10.3 The characteristic equations follow from Eqs. 11.10.19-11.10.22 written as

$$\begin{bmatrix} 1 & M_1 & M_1 & M_1^2-1 & 0 & 0 & 0 & 0 \\ 0 & 1 & -1 & 0 & 0 & 0 & 0 & 0 \\ dt & dz & 0 & 0 & 0 & 0 & 0 & 0 \\ 0 & 0 & dt & dz & 0 & 0 & 0 & 0 \\ 0 & 0 & 0 & 0 & 1 & M_2 & M_2 & M_2^2-1 \\ 0 & 0 & 0 & 0 & 0 & 1 & -1 & 0 \\ 0 & 0 & 0 & 0 & dt & dz & 0 & 0 \\ 0 & 0 & 0 & 0 & 0 & 0 & dt & dz \end{bmatrix} \begin{bmatrix} v_{1,t} \\ v_{1,z} \\ e_{1,t} \\ e_{1,z} \\ v_{2,t} \\ v_{2,z} \\ e_{2,t} \\ e_{2,z} \end{bmatrix} = \begin{bmatrix} Pf_1 \\ 0 \\ dv_1 \\ de_1 \\ Pf_2 \\ 0 \\ dv_2 \\ de_2 \end{bmatrix} \qquad (1)$$

Also included are the 4 equations representing the differentials $dv_1 \cdots de_2$. These expressions have been written in such an order that the lack of coupling between streams is exploited. Thus, the determinant of the coefficients can be reduced by independently manipulating the first 4 rows and first 4 columns or the second 4 rows and second four columns. Thus, the determinant is reduced by dividing the third rows by dt and subtracting from the first and adding the third column to the second.

$$\begin{bmatrix} 0 & 2M_1-\frac{dz}{dt} & M_1 & M_1^2-1 \\ 0 & 0 & -1 & 0 \\ dt & dz & 0 & 0 \\ 0 & dt & dt & dz \end{bmatrix} \begin{bmatrix} 0 & 2M_2-\frac{dz}{dt} & M_2 & M_2^2-1 \\ 0 & 0 & -1 & 0 \\ dt & dz & 0 & 0 \\ 0 & dt & dt & dz \end{bmatrix} \qquad (2)$$

$$= \left[\left(2M_1-\frac{dz}{dt}\right)dz-(M_1^2-1)dt\right]\left[\left(2M_2-\frac{dz}{dt}\right)dz-(M_2^2-1)dt\right]=0$$

Prob. 11.10.3 (cont.)

This expression reduces to

$$(dt)^2\left[\left(\frac{dz}{dt}-M_1\right)^2-1\right]\left[\left(\frac{dz}{dt}-M_2\right)^2-1\right]=0 \tag{3}$$

and it follows that the Ist characteristic equations are Eqs. 11.10.24 and 11.10.26.

The IInd characteristics follow from

$$\begin{bmatrix} Pf_1 & M_1 & M_1 & M_1^2-1 & 0 & 0 & 0 & 0 \\ 0 & 1 & -1 & 0 & 0 & 0 & 0 & 0 \\ d\vartheta_1 & dz & 0 & 0 & 0 & 0 & 0 & 0 \\ de_1 & 0 & dt & dz & 0 & 0 & 0 & 0 \\ Pf_2 & 0 & 0 & 0 & 1 & M_2 & M_2 & M_2^2-1 \\ 0 & 0 & 0 & 0 & 0 & 1 & -1 & 0 \\ d\vartheta_2 & 0 & 0 & 0 & dt & dz & 0 & 0 \\ de_2 & 0 & 0 & 0 & 0 & 0 & dt & dz \end{bmatrix}=0 \tag{4}$$

Expanded by minors about the left column, this determinant becomes

$$\begin{aligned} &Pf_1(-dz)(-1)dz\,D_2+d\vartheta_1(-1)\left[2M_1dz-dt\,(M_1^2-1)\right]D_2 \\ &-de_1(dz)(1)(M_1^2-1)D_2=0 \end{aligned} \tag{5}$$

Thus, so long as $D_2 \neq 0$ (not on the second characteristic equation) Eq. 5 reduces to

$$d\vartheta_1\left[2M_1\frac{dz}{dt}-(M_1^2-1)\right]+(M_1^2-1)\frac{dz}{dt}de_1=Pf_1\frac{(dz)^2}{dt}$$

In view of Eq. 2, this becomes

$$d\vartheta_1\left(\frac{dz}{dt}\right)^2+(M_1^2-1)\frac{dz}{dt}de_1=Pf_1\frac{(dz)^2}{dt} \tag{6}$$

Prob. 11.10.3 (cont.)

Now, using Eq. 5a,

$$d\vartheta_1(M_1 \pm 1)^2 + (M_1-1)(M_1+1)(M_1 \pm 1)de_1 = Pf_1(M_1 \pm 1)^2 dt \tag{7}$$

and finally, Eq. 11.10.23 is obtained

$$d\vartheta_1 + (M_1 \mp 1)de_1 = Pf_1 dt \tag{8}$$

These equations apply on $C_1^{\pm}$ respectively. To recover the IInd characteristics, which apply where $D_2 = 0$ and hence Eq. 4 degenerates, substitute the column on the right in Eq. 1 for the fifth column on the left. The situation is then analogous to the one just considered. The characteristic equations are written with $d\vartheta_1 \rightarrow \Delta\vartheta_{1A}$ on C^+ originating at A, etc. The subscripts A, B, C and D designate the change in the variable along the line originating at the subscript point. The superscripts designate the positive or negative characteristic lines. Thus, Eqs. 11.10.23 and 11.10.25 become the first, second, fifth and sixth of the following eight equations.

$$\begin{bmatrix} 1 & 0 & M_1-1 & 0 & 0 & 0 & 0 & 0 \\ 0 & 1 & 0 & M_1+1 & 0 & 0 & 0 & 0 \\ 1 & -1 & 0 & 0 & 0 & 0 & 0 & 0 \\ 0 & 0 & 1 & -1 & 0 & 0 & 0 & 0 \\ 0 & 0 & 0 & 0 & 1 & 0 & M_2-1 & 0 \\ 0 & 0 & 0 & 0 & 0 & 1 & 0 & M_2+1 \\ 0 & 0 & 0 & 0 & 1 & -1 & 0 & 0 \\ 0 & 0 & 0 & 0 & 0 & 0 & 1 & -1 \end{bmatrix} \begin{bmatrix} \Delta\vartheta_{1A}^+ \\ \Delta\vartheta_{1B}^- \\ \Delta e_{1A}^+ \\ \Delta e_{1B}^- \\ \Delta\vartheta_{2C}^+ \\ \Delta\vartheta_{2D}^- \\ \Delta e_{2C}^+ \\ \Delta e_{2D}^- \end{bmatrix} = \begin{bmatrix} Pf_1(\xi_{1A}, \xi_{2A})\Delta t \\ Pf_1(\xi_{1B}, \xi_{2B})\Delta t \\ -(\vartheta_{1A} - \vartheta_{1B}) \\ -(e_{1A} - e_{1B}) \\ Pf_2(\xi_{1C}, \xi_{2C})\Delta t \\ Pf_2(\xi_{1D}, \xi_{2D})\Delta t \\ -(\vartheta_{2C} - \vartheta_{2D}) \\ -(e_{2C} - e_{2D}) \end{bmatrix} \tag{9}$$

Prob. 11.10.3 (cont.)

The third, fourth and last two equations require that

$$\vartheta_{1E} = \vartheta_{1A} + \Delta\vartheta_{1A}^{+} = \vartheta_{1B} + \Delta\vartheta_{1B}^{-} ; \Delta e_{1E} = e_{1A} + \Delta e_{1A}^{+} = e_{1B} + \Delta e_{1B}^{-}$$
$$\vartheta_{2E} = \vartheta_{2C} + \Delta\vartheta_{2C}^{+} = \vartheta_{2D} + \Delta\vartheta_{2D}^{-} ; \Delta e_{2E} = e_{2C} + \Delta e_{2C}^{+} = e_{2D} + \Delta e_{2D}^{-} \qquad (10)$$

Clearly, the first four equations are coupled to the second four only through the inhomogeneous terms. Thus, solution for $\Delta\vartheta_{1A}^{+}$ and Δe_{1A}^{+} involves the inversion of the first 4 expressions.

The determinant of the respective 4x4 coefficients are

$$D_1 = -2 \ ; \ D_2 = -2 \qquad (11)$$

and hence

$$\Delta\vartheta_{1A}^{+} = -\frac{1}{2}\begin{vmatrix} Pf_1(\xi_{1A},\xi_{2A})\Delta t & 0 & M_1-1 & 0 \\ Pf_1(\xi_{1B},\xi_{2B})\Delta t & 1 & 0 & M_1+1 \\ -(\vartheta_{1A}-\vartheta_{1B}) & -1 & 0 & 0 \\ -(e_{1A}-e_{1B}) & 0 & 1 & -1 \end{vmatrix}$$

$$= -\frac{1}{2}\begin{vmatrix} Pf_1(\xi_{1A},\xi_{2A})\Delta t & 0 & M_1-1 & 0 \\ Pf_1(\xi_{1B},\xi_{2B})\Delta t-(\vartheta_{1A}-\vartheta_{1B}) & 0 & 0 & M_1+1 \\ -(\vartheta_{1A}-\vartheta_{1B}) & -1 & 0 & 0 \\ -(e_{1A}-e_{1B}) & 0 & 1 & -1 \end{vmatrix} \qquad (12)$$

$$= -\frac{1}{2}\Big[-Pf_1(\xi_{1A},\xi_{2A})\Delta t(M_1+1) + Pf_1(\xi_{1B},\xi_{2B})(M_1-1)\Delta t$$
$$-(\vartheta_{1A}-\vartheta_{1B})(M_1-1) - (e_{1A}-e_{1B})(M_1-1)(M_1+1)\Big]$$

Prob. 11.10.3 (cont.)

which is Eq. 11.10.27. Similarly,

$$\Delta e^{+}_{1A} = -\frac{1}{2}\begin{vmatrix} 1 & 0 & Pf_{1A}\Delta t & 0 \\ 0 & 1 & Pf_{1B}\Delta t & M_1+1 \\ 1 & -1 & -(v_{1A}-v_{1B}) & 0 \\ 0 & 0 & -(e_{1A}-e_{1B}) & -1 \end{vmatrix}$$

$$= -\frac{1}{2}\begin{vmatrix} 0 & 1 & Pf_{1A}\Delta t+(v_{1A}-v_{1B}) & 0 \\ 0 & 1 & Pf_{1B}\Delta t & M_1+1 \\ 1 & -1 & -(v_{1A}-v_{1B}) & 0 \\ 0 & 0 & -(e_{1A}-e_{1B}) & -1 \end{vmatrix} \qquad (\underline{13})$$

$$= -\frac{1}{2}\begin{vmatrix} 0 & Pf_{1A}\Delta t+(v_{1A}-v_{1B})-Pf_{1B}\Delta t & -(M_1+1) \\ 1 & Pf_{1B}\Delta t & M_1+1 \\ 0 & -(e_{1A}-e_{1B}) & -1 \end{vmatrix}$$

$$= \frac{1}{2}\Big[-P(f_{1A}-f_{1B})\Delta t - (v_{1A}-v_{1B}) - (M_1+1)(e_{1A}-e_{1B})\Big]$$

which is the same as Eq. 11.10.28.

The expressions for Δv^{+}_{2C} and Δe^{+}_{2C} are found in the same way from the second set of 4 equations rather than the first. The calculation is the same except that $A \to C$, $B \to D$, $1 \to 2$ and $2 \to 1$.

Prob. 11.11.1 In the long-wave limit, the magnetic field intensity above and below the sheet is given by the statement of flux conservation

$$\mu_o H_z(a \mp \xi) = -\mu_o H_o a \pm A_d(t) \tag{1}$$

Thus, the x-directed force per unit area on the sheet is

$$T = -\frac{1}{2}\mu_o [\![H_z^2]\!] = -\frac{1}{2}\mu_o \left[\frac{(-\mu_o H_o a + A_d)^2}{\mu_o^2 (a-\xi)^2} - \frac{(-\mu_o H_o a - A_d)^2}{\mu_o^2 (a+\xi)^2} \right] \tag{2}$$

This expression is linearized to obtain

$$\begin{aligned} T \cong -\frac{1}{2}\frac{1}{\mu_o} \Big\{ & [(-\mu_o H_o a)^2 + 2(-\mu_o H_o a) A_d][\frac{1}{a^2} + \frac{\xi}{a^3}] \\ & - [(-\mu_o H_o a)^2 + 2(-\mu_o H_o a)(-A_d)][\frac{1}{a^2} - \frac{\xi}{a^3}] \Big\} \\ \cong & \frac{2 H_o A_d}{a} - \frac{2\mu_o H_o^2 \xi}{a} \end{aligned} \tag{3}$$

Thus, the equation of motion for the sheet is

$$\Delta\rho \left(\frac{\partial}{\partial t} + U\frac{\partial}{\partial z}\right)^2 \xi = 2\gamma \frac{\partial^2 \xi}{\partial z^2} - 2\mu_o H_o^2 \frac{\xi}{a} + \frac{2 H_o A_d}{a} \tag{4}$$

Normalization such that

$$t = \underline{t}\,\tau, \quad z = \underline{z}\,\tau V, \quad V \equiv \sqrt{2\gamma/\Delta\rho} \tag{5}$$

gives

$$\left(\frac{\partial}{\partial \underline{t}} + \frac{U}{V}\frac{\partial}{\partial \underline{z}}\right)^2 \underline{\xi} = \frac{2\gamma\tau^2}{\Delta\rho(\tau V)^2}\frac{\partial^2 \underline{\xi}}{\partial \underline{z}^2} - \frac{2\mu_o H_o^2 \tau^2 \underline{\xi}}{\Delta\rho a} + \frac{2\mu_o H_o^2 \tau^2 A_d}{\Delta\rho a \mu_o H_o a} \tag{6}$$

which becomes the desired result, Eq. 11.11.3

$$\left(\frac{\partial}{\partial t} + M\frac{\partial}{\partial z}\right)^2 \xi = \frac{\partial^2 \xi}{\partial z^2} + P\xi - Pf \tag{7}$$

where

$$\underline{P} = -\frac{2\mu_o H_o^2 \tau^2}{\Delta\rho a}; \quad M = \frac{U}{V}; \quad f = A_d/\mu_o H_o a$$

<u>Prob. 11.11.2</u> The transverse force equation for the "wire" is written by considering the incremental length Δz shown in the figure

$$\Delta z\, m \frac{\partial^2 \xi}{\partial t^2} = T\left[\frac{\partial \xi}{\partial z}\bigg|_{z+\Delta z} - \frac{\partial \xi}{\partial z}\bigg|_{z}\right] + f(z)\Delta z \tag{1}$$

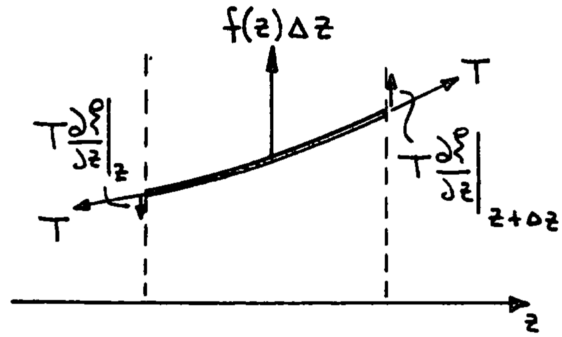

Divided by Δz and in the limit $\Delta z \rightarrow 0$, this expression becomes

$$m\frac{\partial^2 \xi}{\partial t^2} = T\frac{\partial^2 \xi}{\partial z^2} + f(z) \tag{2}$$

The force per unit length is

$$f = (\bar{I}\times\bar{B})_x = I\,\bar{i}_z \times\left[\frac{B_o}{d}(y\,\bar{i}_x + x\,\bar{i}_y)\right]_x = \frac{IB_o}{d}x \tag{3}$$

Evaluated at the location of the wire, $x = \xi$, this expression is inserted into Eq. 2 to give

$$m\frac{\partial^2 \xi}{\partial t^2} = T\frac{\partial^2 \xi}{\partial z^2} + \frac{IB_o}{d}\xi \tag{4}$$

This takes the form of Eq. 11.11.3 with $M = 0$ and $f = 0$ with $t = \underline{t}\,\tau$, $z = \underline{z}\,\tau V$, $V \equiv \sqrt{T/m}$ and

$$P \equiv \frac{IB_o\tau^2}{md} \tag{5}$$

Prob. 11.11.3 The solution is given by evaluating $\hat{A}$ and $\hat{B}$ in Eq. 11.11.9. With the deflection made zero at $z = \ell$, the first of the following two equations is obtained ($z = \ell \Rightarrow \underline{z} = \underline{\ell}$ where $\underline{\ell} \equiv \ell/\tau V$)

$$\begin{bmatrix} e^{-jk_1\ell} & e^{-jk_2\ell} \\ 1 & 1 \end{bmatrix} \begin{bmatrix} \hat{A} \\ \hat{B} \end{bmatrix} = \begin{bmatrix} 0 \\ \hat{\xi}_d \end{bmatrix} \tag{1}$$

The second assures that $\xi(0,t) = Re\, \hat{\xi}_d\, e^{j\omega_o t}$. Solution for $\hat{A}$ and $\hat{B}$ gives

$$\hat{A} = \frac{-\hat{\xi}_d\, e^{-jk_2\ell}}{e^{-jk_1\ell} - e^{-jk_2\ell}} \; ; \; \hat{B} = \frac{\hat{\xi}_d\, e^{-jk_1\ell}}{e^{-jk_1\ell} - e^{-jk_2\ell}} \tag{2}$$

and Eq. 11.11.9 becomes

$$\xi = Re\, \hat{\xi}_d \frac{-e^{-jk_1z}e^{-jk_2\ell} + e^{-jk_2z}e^{-jk_1\ell}}{e^{-jk_1\ell} - e^{-jk_2\ell}}\, e^{j\omega_o t} \tag{3}$$

With the definitions

$$k_{\substack{1\\2}} = \eta \pm \gamma \; ; \; \eta \equiv \frac{\omega_o M}{M^2 - 1} \; ; \; \gamma = \frac{\sqrt{\omega_o^2 + P(1 - M^2)}}{M^2 - 1} \tag{4}$$

Eq. 3 is written as Eq. 11.11.13

$$\xi = -Re\, \hat{\xi}_d \frac{\left[e^{-j(\gamma z - \gamma\ell)} - e^{j(\gamma z - \gamma\ell)}\right]}{e^{-j\gamma\ell} - e^{j\gamma\ell}}\, e^{j(\omega_o t - \eta z)} = -Re\, \hat{\xi}_d \frac{\sin\gamma(z-\ell)}{\sin\gamma\ell}\, e^{j(\omega_o t - \eta z)} \tag{5}$$

For $\omega_o^2 > P\,(M^2 - 1)$ (sub-magnetic, $P < 0$ and $M^2 < 1$), γ is real. The deflection is then as sketched

Prob. 11.11.3 (cont.)

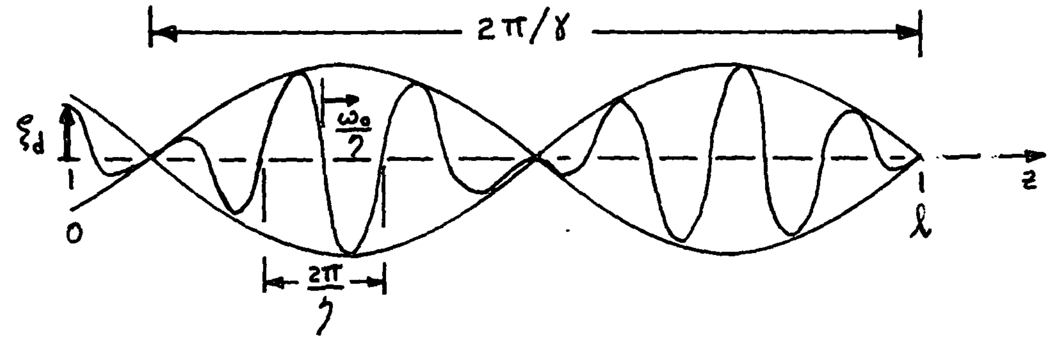

Note that for $M^2 < 1$, $\zeta < 1$ and the phases propagate in the -z direction. The picture is for the wavelength of the envelope greater than that of the propagating wave ($2\pi/\gamma > 2\pi/\zeta \Rightarrow |\gamma| < |\zeta|$). The relationship of wavelengths depends on ω_o , as shown in the figure, and is as sketched in the frequency range $\omega_c < \omega_o < \sqrt{-P}$. For frequencies $\omega_o > \sqrt{-P}$, the deflections are more complex to picture because the wavelength of the envelope is shorter than that of the traveling wave. With the frequency below cut-off, γ becomes imaginary. Let $\gamma = j\alpha$ and Eq. 5 becomes

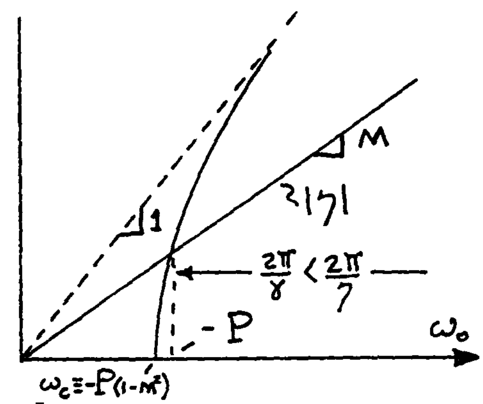

$$\xi = -\mathcal{R}e\, \hat{\xi}_d \frac{\sinh \alpha(z-\ell)}{\sinh \alpha\ell}\, e^{j(\omega_o t - \zeta z)} \qquad (6)$$

Now, the picture is as shown below

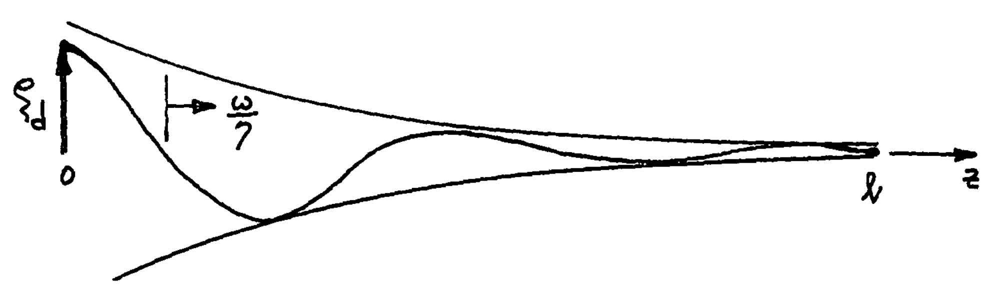

Again, the phases propogate upstream. The decay of the envelope is likely to be so rapid that the traveling wave would be difficult to discern.

Prob. 11.11.4 Solutions have the general form of Eq. 11.11.9 where $\hat{f} = 0$.

$$\xi = \mathcal{R}e\left(\hat{A}\, e^{-jk_1 z} + \hat{B}\, e^{-jk_2 z}\right) e^{j\omega_o t} \qquad (1)$$

Thus

$$\frac{\partial \xi}{\partial z} = \mathcal{R}e\left(-jk_1 \hat{A}\, e^{-jk_1 z} - jk_2 \hat{B}\, e^{-jk_2 z}\right) e^{j\omega_o t} \qquad (2)$$

and the boundary conditions that $\xi(0,t) = \mathcal{R}e\, \hat{\xi}_d\, e^{j\omega_o t}$ and $\partial \xi/\partial z$ evaluated at $z = 0$ be zero require that

$$\begin{bmatrix} 1 & 1 \\ -jk_1 & -jk_2 \end{bmatrix} \begin{bmatrix} \hat{A} \\ \hat{B} \end{bmatrix} = \begin{bmatrix} \hat{\xi}_d \\ 0 \end{bmatrix} \qquad (3)$$

so that

$$\hat{A} = \frac{k_2 \hat{\xi}_d}{k_2 - k_1}\ ; \quad \hat{B} = \frac{-k_1 \hat{\xi}_d}{k_2 - k_1} \qquad (4)$$

and Eq. 1 becomes

$$\xi = \mathcal{R}e\, \hat{\xi}_d \frac{\left(k_2 e^{-jk_1 z} - k_1 e^{-jk_2 z}\right)}{k_2 - k_1} e^{j\omega_o t} \qquad (5)$$

With the definitions

$$k_{\substack{1\\2}} = \eta \pm \gamma\ ; \quad \eta = \frac{\omega_o M}{M^2 - 1}\ ; \quad \gamma = \frac{\sqrt{\omega_o^2 + P(1 - M^2)}}{M^2 - 1} \qquad (6)$$

Eq. 5 becomes

Prob. 11.11.4 (cont.)

$$\xi = \mathcal{R}e\, \hat{\xi}_d \frac{(\mathcal{R}_2 e^{-j\gamma z} - \mathcal{R}_1 e^{j\gamma z})}{-2\gamma} e^{j(\omega_o t - \eta z)} \tag{7}$$

For $\omega_o^2 + P(1 - M^2) < 1$ (super electric below "cut-off") γ is imaginary, $\gamma = j\alpha$. Then, Eq. 7 becomes

$$\xi = \mathcal{R}e\, \hat{\xi}_d \frac{(\mathcal{R}_2 e^{\alpha z} - \mathcal{R}_1 e^{-\alpha z})}{-2j\alpha} e^{j(\omega_o t - \eta z)} \tag{8}$$

Note that the phases propagate downstream with an envelope that eventually is an increasing exponential, as sketched.

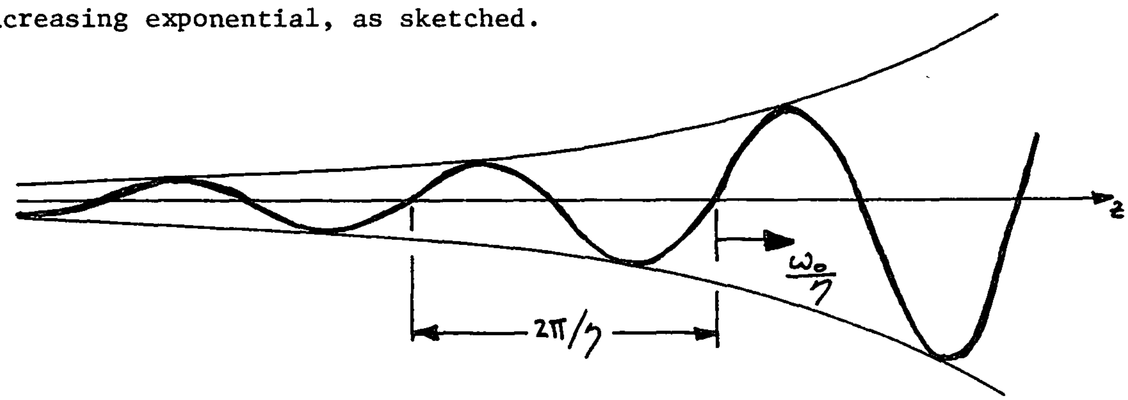

This is illustrated by the experiment of Fig. 11.11.5. If the frequency is so high that $\omega_o^2 + P(1 - M^2) > 0$, the envelope is a standing wave

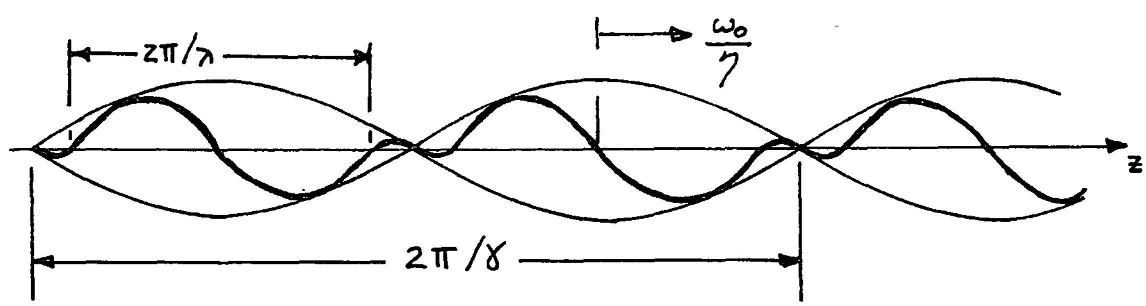

Note that at cut-off, where $\omega_o^2 = P(M^2 - 1)$, the envelope has an infinite wavelength. As the frequency is raised, this wavelength shortens. This is illustrated with $P = 0$ by the experiment of Fig. 11.11.4.

Prob. 11.11.5 (a) The analysis is as described in Prob. 8.13.1 except that there is now a coaxial cylinder. Thus, instead of Eq. 10 from the solution to Prob. 8.13.1, the transfer relation is Eq. (a) of Table 2.16.2 with $\hat{\Phi}^{\alpha} = 0$ because the outer electrode is an equipotential.

$$\hat{e}_r^a = f_m(a,R)\hat{\Phi}^a \tag{1}$$

Then it follows that (m=1)

$$-(\omega - kU)^2 \rho F_1(0,R) = \frac{\epsilon_o E_o^2}{R} - \epsilon_o E_o^2 f_1(a,R) + \frac{\gamma}{R^2}(kR)^2 \tag{2}$$

(b) In the long-wave limit,

$$F_m(0,R) = -\frac{J_m(jkR)}{jk\,J_m'(jkR)} = f_m^{-1}(0,R) \tag{3}$$

and in view of Eqs. 28, for $kR << 1$ and $m = 0$

$$F_1(0,R) \to -R \tag{4}$$

To take the long-wave limit of $f_1(a,R)$, use Eqs. 2.16.24

$$J_1(ju) \to \frac{1}{2}ju \; ; \; H_1(ju) \to \frac{2}{j\pi(ju)}$$
$$J_1'(ju) \to \frac{1}{2} \; ; \; H_1'(ju) \to \frac{-2}{j\pi(ju)^2} \tag{5}$$

to evaluate

$$f_1(a,R) \to \frac{R^2 + a^2}{R^2(a-R)} \tag{6}$$

so that Eq. 2 becomes

$$(\omega - kU)^2 \pi\rho R^2 = \pi\epsilon E_o^2\left[1 - \frac{R^2+a^2}{R(a-R)}\right] + \pi R k^2 \tag{7}$$

The equivalent "string" equation is

$$\pi\rho R^2\left(\frac{\partial}{\partial t} + U\frac{\partial}{\partial z}\right)^2\xi = \pi R\gamma\frac{\partial^2\xi}{\partial z^2} + \pi\epsilon E_o^2\left[\frac{R^2+a^2}{R(a-R)} - 1\right]\xi \tag{8}$$

Normalization, as introduced with Eq. 11.11.3, shows that

$$V = \sqrt{\frac{\gamma}{\rho R}} \; ; \; M = \frac{U}{V} \; ; \; P = \frac{\epsilon E_o^2 \Upsilon^2}{\rho R^2}\left[\frac{R^2+a^2}{R(a-R)} - 1\right] \tag{9}$$

Prob. 11.12.1 The equation of motion is

$$\frac{\partial^2 \xi}{\partial t^2} = V^2 \frac{\partial^2 \xi}{\partial z^2} + f(z,t) \tag{1}$$

and the temporal and spatial transforms are respectively defined as

$$\hat{\xi}(z,\omega) = \int_{-\infty}^{+\infty} \xi(z,t)\, e^{-j\omega t}\, d\omega \Leftrightarrow \xi(z,t) = \int_{-\infty-j\sigma}^{\infty-j\sigma} \hat{\xi}(z,\omega)\, e^{j\omega t} \frac{d\omega}{2\pi} \tag{2}$$

$$\hat{\xi}(k,\omega) = \int_{-\infty}^{+\infty} \hat{\xi}(z,\omega)\, e^{jkz}\, dk \Leftrightarrow \hat{\xi}(z,\omega) = \int_{-\infty}^{+\infty} \hat{\xi}(k,\omega)\, e^{-jkz} \frac{dk}{2\pi} \tag{3}$$

The excitation force is an impulse of width Δz and amplitude f_o in space and a cosinusoid that is turned on when t=0.

$$f(z,t) = \Delta z\, u_o(z)\, f_o \cos \omega_o t\, u_{-1}(t) \tag{4}$$

It follows from Eq. 2 that

$$\hat{f}(z,\omega) = \Delta z\, u_o(z) f_o \left[\frac{1}{2j(\omega_o - \omega)} - \frac{1}{2j(\omega_o + \omega)} \right] \tag{5}$$

In turn, Eq. 3 transforms this expression to

$$f(k,\omega) = \Delta z\, f_o \left[\frac{1}{2j(\omega_o - \omega)} - \frac{1}{2j(\omega_o + \omega)} \right] \tag{6}$$

With the understanding that this is the Fourier-Laplace transform of f(z,t), it follows from Eq. 1 that the transform of the response is given by

$$\hat{\xi} = \frac{\hat{f}}{V^2 D(\omega,k)} \tag{7}$$

where

$$D(\omega,k) = k^2 - \left(\frac{\omega}{V}\right)^2 = \left(k - \frac{\omega}{V}\right)\left(k + \frac{\omega}{V}\right) \tag{8}$$

Now, to invert this transform, Eq. 3b is used to write

$$\hat{\xi} = \frac{\Delta z f_o}{2\, V^2} \left[\frac{1}{j(\omega_o - \omega)} - \frac{1}{j(\omega_o + \omega)} \right] \int_{-\infty}^{\infty} \frac{e^{-jkz}}{D(\omega,k)} \frac{dk}{2\pi} \tag{9}$$

Prob. 11.12.1 (cont.)

This integration is carried out using the residue theorem

$$\oint_C \frac{N(k)}{D(k)}\,dk = 2\pi j\left[K_1 + K_2 + \cdots\right];\; K_n = \frac{N(k_n)}{D'(k_n)} \tag{9}$$

It follows from Eq. 7 that

$$D(\omega, k_n) = 0 \Rightarrow k_n = k_{\substack{1\\-1}} = \pm\frac{\omega}{V} \tag{10}$$

and therefore

$$D'(\omega, k_{\substack{1\\-1}}) = \left(k_{\substack{1\\-1}} + \frac{\omega}{c}\right) + \left(k_{\substack{1\\-1}} - \frac{\omega}{c}\right) = \pm 2\frac{\omega}{V} \tag{11}$$

The open integral called for with Eq. 8 is equivalent to the closed contour integral that can be evaluated using Eq. 9 on the respective contours shown in Fig. 11.12.4. Poles, $D(\omega, k) = 0$, in the k plane have the locations shown to the right for values of ω on the Laplace contour, because they are given in terms of ω by Eq. 10. The ranges of z associated with the respective contours are those required to make the additional parts of the integral added to make the contours closed ones make zero contribution, Thus, Eq. 8 becomes

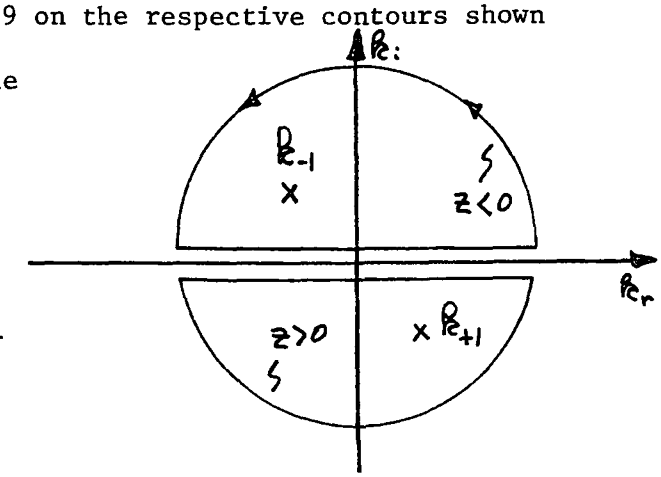

$$\hat{\xi} = \frac{\Delta z\, f_o}{2V^2}\left[\frac{1}{\omega_o - \omega} - \frac{1}{\omega_o + \omega}\right]\frac{e^{-jk_{\substack{-1\\+1}} z}}{2\left(\frac{\omega}{c}\right)} \tag{12}$$

Here, and in the following discussion, the upper and lower signs respectively refer to $z < 0$ and $z > 0$.

The Laplace inversion, Eq. 2b, is evaluated using Eq. 12

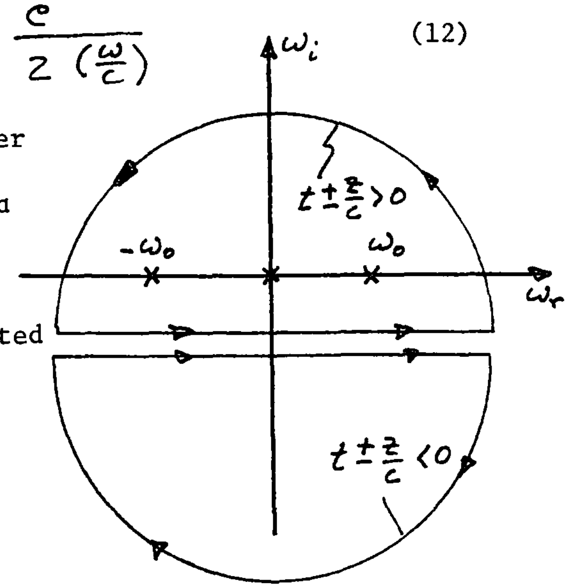

Prob. 11.12.1 (cont.)

$$\xi(z,t)=\frac{\Delta z f_o}{4V}\int_{-\infty-j\sigma}^{+\infty-j\sigma}\left[\frac{1}{\omega_o-\omega}-\frac{1}{\omega_o+\omega}\right]\frac{e^{\pm j\frac{\omega}{c}t}\,e^{j\omega t}}{\omega}\frac{d\omega}{2\pi} \tag{13}$$

Choice of the contour used to close the integral is aided by noting that

$$e^{j(\omega t\pm\frac{\omega}{V}z)}=e^{j(\omega_r t\pm\frac{\omega_r}{V}z)}\,e^{-\omega_i(t\pm\frac{z}{V})} \tag{14}$$

and recognizing that if the addition to the original open integral is to be zero, $t\pm\frac{z}{V}>0$ on the upper contour and $t\pm\frac{z}{V}<0$ on the lower one.

The integral on the lower contour encloses no poles (by definition so that causality is preserved) and so the response is zero for

$$t<\mp\frac{z}{V} \tag{15}$$

Conversely, closure in the upper half plane is appropriate for

$$t>\mp\frac{z}{V} \tag{16}$$

By the residue theorem, Eq. 9, Eq. 13 becomes

$$\xi(z,t)=\frac{\Delta z f_o}{4V}\oint_C\left[\frac{e^{\pm j\frac{\omega}{c}z}\,e^{j\omega t}}{(\omega_o-\omega)\,\omega}-\frac{e^{\pm j\frac{\omega}{c}z}\,e^{j\omega t}}{(\omega_o+\omega)\,\omega}\right]\frac{d\omega}{2\pi} \tag{17}$$

$$D'(\omega)=-\omega+(\omega_o-\omega)\qquad D'(\omega)=\omega+(\omega_o+\omega)$$

$$=\frac{\Delta z f_o}{4V}j\left[\frac{1}{-\omega_o}e^{j(\omega_o t\pm j\frac{\omega_o}{c}z)}+\frac{1}{\omega_o}-\frac{1}{-\omega_o}e^{-j(\omega_o t\pm\frac{\omega_o}{c}z)}-\frac{1}{\omega_o}\right]$$

This function simplifies to a sinusoidal traveling wave. To encapsulate Eqs. 15 and 16, Eq. 17 is multiplied by the step function

$$\xi(z,t)=\frac{\Delta z f_o}{2V\omega_o}\sin\left[\omega_o\left(t\pm\frac{z}{V}\right)u_{-1}\left(t\pm\frac{z}{V}\right)\right];\ z\lessgtr 0 \tag{18}$$

Prob. 11.12.2 The dispersion equation, without the long-wave approximation, is given by Eq. 8. Solved for ω it gives one root

$$\omega = k + j\frac{k}{U}\tanh k \qquad (1)$$

That is, there is only one temporal mode and it is stable. This is sufficient condition to identify all spatial modes as evanescent.

The long-wave limit, if represented by Eq. 11, is not self-consistent. This is evident from the fact that the expression is quadratic in ω and it is clear that an extraneous root has been introduced by the polynomial approximation to the transcendental functions. In fact, two higher order terms must be omitted to make the -k relation self-consistent, and Eq. 5.7.11 becomes

$$k_{\mp} = j\frac{U}{2} \pm \sqrt{-\frac{U^2}{4} - j\omega U} \qquad (2)$$

Solved for ω , this expression gives

$$\omega = k\left(1 + \frac{jk}{U}\right) \qquad (3)$$

which is directly evident from Eq. 1. To plot the loci of k for fixed values of ω_r as σ goes from ∞ to zero, Eq. 2 is written as

$$k_{\mp} = j\left[\frac{U}{2} \pm \sqrt{\left(\frac{U^2}{4} + \sigma U\right) + j\omega_r U}\right] \qquad (4)$$

The loci of k are illustrated by the figure with $U = 0.2$.

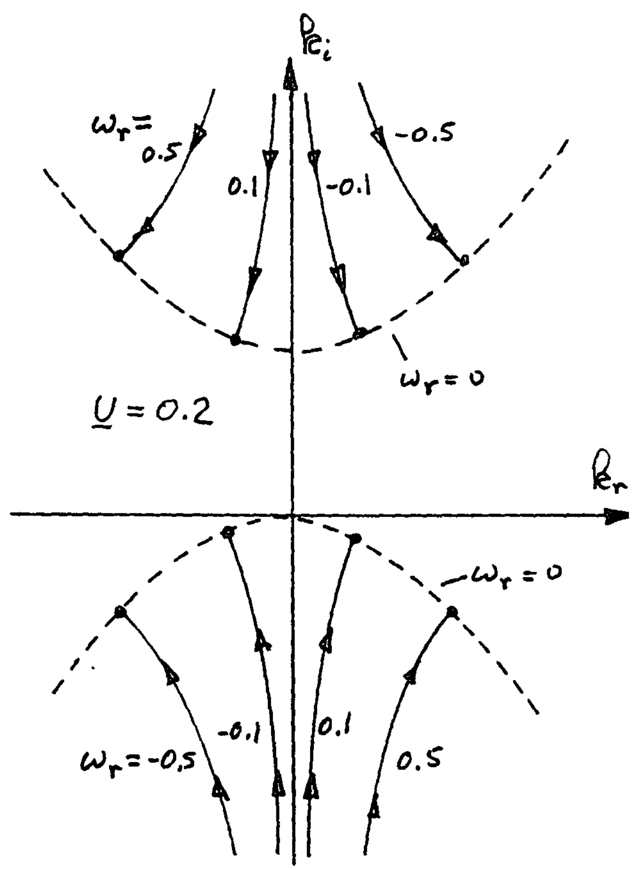

Prob.11.13.1 With the understanding that the total solution is the superposition of this solution and one gotten following the prescription of Eq. 11.12.5, the desired limit is

$$\lim_{t\to\infty} \xi(z,t) = \lim_{t\to\infty} \pm \int_{C_L''} \frac{f(\omega)\sum_n j g(k_n)}{D'(\omega,k_n)} e^{j(\omega t - k_n z)} \frac{d\omega}{2\pi} \tag{1}$$

where Eqs. 11.13.8 and 11.13.9 supply

$$f(\omega) = \frac{1}{j(\omega-\omega_o)} \tag{2}$$
$$g(k) = \frac{P\hat{f}_o}{2} \frac{[e^{j(k-\beta)\ell} - 1]}{j(k-\beta)} \tag{3}$$

The contour of integration is shown to the right (Fig. 11.13.4). Calculated here is the response outside the range $z<0,z>\ell$ so that the summation is either n=1 or n=-1. For the particular case where P $>$ 0 and M $<$ 1 (sub-electric) Eq. 11.13.16 is

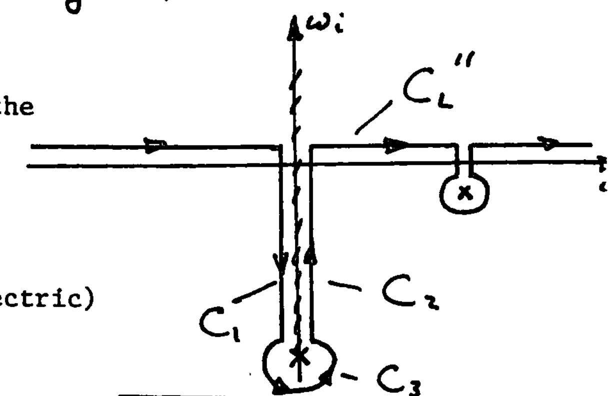

$$D'(k_\pm) = \mp 2\sqrt{(\omega - j\sigma_s)(\omega + j\sigma_s)}\ ;\ \sigma_s = \sqrt{P(1-M^2)} \tag{4}$$

Note that at the branch point, roots k_n coalesce at k_s in the k plane. From Eq. 11.13.15,

$$k_s = \frac{\omega M}{M^2-1} = \frac{-j\sigma_s M}{M^2-1} \tag{5}$$

as shown graphically by the coalescence of roots in Fig. 11.13.3. As $t\to\infty$, the contributions to the integration on the contour just above the ω_r axis go to zero. ($\omega = \omega_r + j\omega_i$ makes the time dependence of the integrand in Eq. 1 $(\exp j\omega_r t)(\exp -\omega_i t)$ and because $\omega_i > 0$, the integrand goes to zero as $t\to\infty$.) Contributions from the integration around the pole (due to f(ω)) at $\omega = \omega_o$ are finite and hence dominated by the instability now represented by the integration around the half of the branch-cut projecting into the lower half plane.

The integration around the branch-cut is composed of parts C_1 and C_2 paralleling the cut along the imaginary axis and a apart C_3 around the lower branch point. Because D' on C_2 is the negative of that on C_1, and C_1 and C_2

Prob. 11.13.1 (cont.)

are integrations in opposite directions, the contributions on C_1+C_2 are twice that on C_1. Thus, for C_1 and C_2, Eq. 1 is written in terms of $\sigma(\omega = -j\sigma)$

$$-2\int_{\sigma_o}^{\sigma_s} f(-j\sigma)\sum_n \frac{jg(k_n)\, e^{\sigma t} e^{-jk_n z}}{2j\sqrt{(\sigma-\sigma_s)(\sigma+\sigma_s)}}\frac{(-jd\sigma)}{2\pi} \tag{6}$$

In evaluating this expression approximately (for $t\to\infty$) let σ_s be the origin by using $\sigma-\sigma_s$ as a new variable $\sigma^{\#}\equiv -\sigma+\sigma_s \Rightarrow d\sigma = -d\sigma^{\#}$ Then, Eq. 6 becomes

$$\frac{e^{\sigma_s t}}{2\pi}\int_{\sigma_o+\sigma_s}^{0} \frac{f(-j\sigma)\sum_n jg(k_n)e^{-jk_n z}\, e^{-\sigma^{\#}t}\, d\sigma^{\#}}{\sqrt{\sigma^{\#}-2\sigma_s}\,\sqrt{\sigma^{\#}}} \tag{7}$$

Note that $\sigma^{\#}<0$ as the integration is carried out. Thus, as $t\to\infty$, contributions to the integration are confined to regions where $\sqrt{\sigma^{\#}}\to 0$. The remainder of the integrand, which varies slowly with σ, is approximated by its value at $\sigma=\sigma_s$. Also, σ_o is taken to ∞ so the integral of Eq. 7 becomes ($k_1\to k_{-1}\to k_s$)

$$\frac{e^{\sigma_s t}\, e^{-jk_s z} f(-j\sigma_s)\, jg(k_s)}{2\pi\sqrt{-2\sigma_s}}\int_{\infty}^{0}\frac{e^{-\sigma^{\#}t}\, d\sigma^{\#}}{\sqrt{\sigma^{\#}}} \tag{8}$$

The definite integration called for here is given in standard tables as

$$-\sqrt{\pi}/\sqrt{t} \tag{9}$$

The integration around the branch point is again in a region where all but the $\sqrt{\omega - j\sigma_s}$ in the denominator is essentially constant. Thus, with $\Omega\equiv\omega+j\sigma_s$, the integration on C_3 of Eq. 1 becomes essentially

$$\lim_{t\to\infty} -\frac{f(j\sigma_s)\, jg(k_s)}{4\pi}\,\frac{e^{-jk_s z}\, e^{-\sigma_s t}}{\sqrt{-2j\sigma_s}}\oint\frac{e^{j\Omega t}}{\sqrt{\Omega}}\,d\Omega \tag{10}$$

Let $\Omega = R\exp j\phi$ and the integral from Eq. 9 becomes

$$\oint_{-3\pi/2}^{\pi/2}\frac{jR\, e^{j\phi}\, e^{j\Omega t}}{\sqrt{R}\, e^{\frac{j\phi}{2}}}\,d\phi = \int_{-3\pi/2}^{\pi/2} j\sqrt{R}\, e^{\frac{j\phi}{2}}\, e^{j\Omega t}\,d\phi \tag{11}$$

In the limit $R\to 0$, this integration gives no contribution. Thus, the asymptotic response is given by the integrations on C_1+C_2 alone.

Prob. 11.13.1 (cont.)

$$\lim_{t\to\infty} \xi(z,t) = -\frac{f(-j\sigma_s)g(k_s)}{2\sqrt{\pi}\sqrt{2\sigma_s}} \frac{e^{\sigma_s t - jk_s z}}{\sqrt{t}} \tag{12}$$

The same solution applies for both $z < 0$ and $\ell < z$. The z dependence in Eq. 11 renders the solution non-symmetric in z. This is the result of the convection, as can be seen from the fact that as $\bar{M} \to 0$, $k_s \to 0$.

Prob. 11.13.2 (a) The dispersion equation is simply

$$(\omega - kU)^2 = V^2 k^2 + j\omega\nu \tag{1}$$

Solved for ω, this expression gives the frequency of the temporal modes.

$$\omega = kU + \frac{j\nu}{2} \pm \sqrt{\left(k^2V^2 - \frac{\nu^2}{4}\right) + j\nu kU} \tag{2}$$

Alternatively, Eq. 1 can be normalized such that

$$\underline{\omega} = \omega/\nu, \quad M = U/V, \quad \underline{k} = kV/\nu \tag{3}$$

and Eqs. 1 and 2 become

$$\begin{gathered} \omega^2 - 2M\omega k + k^2(M^2 - 1) - j\omega = 0 \\ \omega = Mk + \frac{j}{2} \pm \sqrt{\left(k^2 - \frac{1}{4}\right) + jMk} \end{gathered} \tag{4}$$

To see that $U > V$ $(M > 1)$ implies instability, observe that for "small" ν, Eq. 2 becomes

$$\omega = k(U \pm V) + \frac{j\nu}{2}(1 \pm M) \tag{5}$$

Thus, there is an $\omega_i < 0$ if $M > 1$. Another examination of Eq.5 is based on an expansion of M about M=1, showing that instability depends on having $|M|>1$.

Prob. 11.13.2 (cont.)

Complex ω as a function of real k are illustrated in Fig. 11.3.2a.

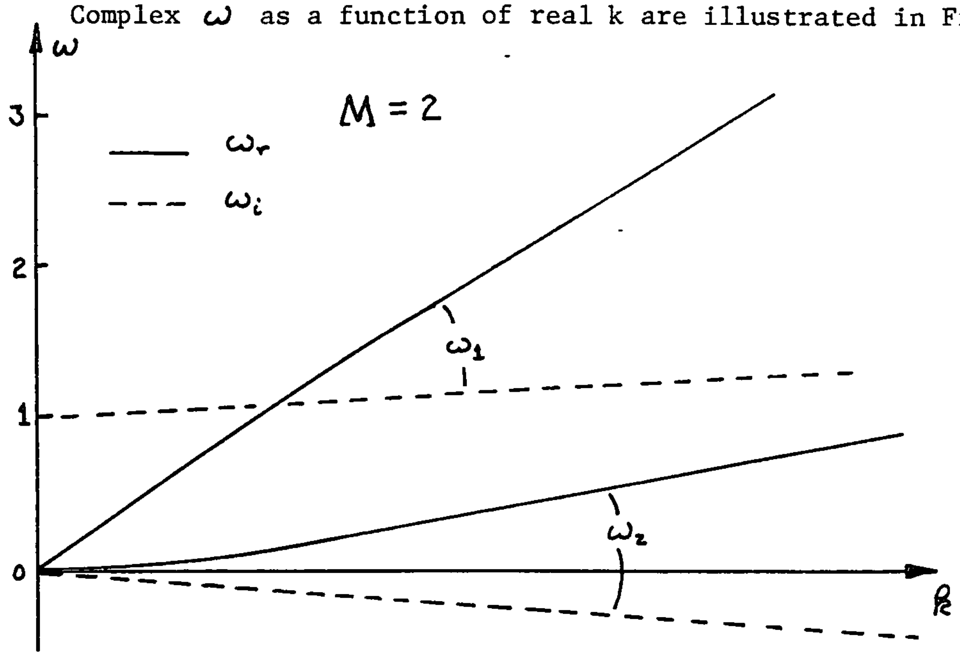

Fig. 11.3.2a

(b) To determine the nature of the instability, Eq. 4 is solved for complex k as a function of $\omega = \omega_r - j\sigma$.

$$k = \frac{M\omega \pm \sqrt{j\omega(M^2-1) + \omega^2}}{M^2-1} \tag{7}$$

or

$$k = \frac{M(\omega_r - j\sigma) \pm \sqrt{[\omega_r^2 - \sigma^2 + \sigma(M^2-1)] + j[\omega_r(M^2-1) - 2\omega_r\sigma]}}{M^2-1} \tag{8}$$

Note that as $\sigma \to \infty$

$$k \to \frac{M(\omega_r - j\sigma) \pm j\sigma}{M^2-1} = \frac{M\omega_r - j\sigma(M \pm 1)}{M^2-1} \tag{9}$$

and for $M > 1$ both roots go to $k_i \to -\infty$. Thus, the loci of complex k for σ varying from $-\infty$ to zero at fixed ω_r move upward through the lower half plane. The two roots to Eq. 7 pass through the k_r axis where ω reaches the values shown in Fig. 11.3.2a. Thus, one of the roots passes into the upper half plane while the other remains in the lower half plane. There is no possibility that they coalesce to form a saddle point, so the instability is convective.

Prob. 11.14.1 (a) Stress equilibrium at the equilibrium interface

$$p^d - p^e = \frac{1}{2}\epsilon E_o^2 \quad ; \quad E_o \equiv V/a \tag{1}$$

In the stationary state,

$$p = \Pi_a - \frac{1}{2}\rho U^2$$
$$p = \Pi_b \tag{2}$$

and so, Eq. (1) requires that

$$\Pi_a - \frac{1}{2}\rho U^2 - \Pi_b = \frac{1}{2}\epsilon E_o^2 \tag{3}$$

All other boundary conditions and bulk relations are automatically satisfied by the stationary state where $\bar{v} = U\bar{i}_z$ in the upper region, $\bar{v} = 0$ in the lower region and

$$p = \begin{cases} \Pi_a - \frac{1}{2}\rho U^2 \\ \Pi_b \end{cases} \tag{4}$$

(b) The alteration to the derivation in Sec. 11.14 comes from the additional electric stress at the perturbed interface. The mechanical bulk relations are again

$$\begin{bmatrix} \hat{p}^c \\ \hat{p}^d \end{bmatrix} = \frac{j(\omega - k_z U)\rho_a}{k} \begin{bmatrix} -\coth ka & \frac{1}{\sinh ka} \\ \frac{-1}{\sinh ka} & \coth ka \end{bmatrix} \begin{bmatrix} \hat{v}_x^c \\ \hat{v}_x^d \end{bmatrix} \tag{5}$$

$$\begin{bmatrix} \hat{p}^e \\ \hat{p}^f \end{bmatrix} = \frac{j\omega\rho_b}{k} \begin{bmatrix} -\coth kb & \frac{1}{\sinh kb} \\ \frac{-1}{\sinh kb} & \coth kb \end{bmatrix} \begin{bmatrix} \hat{v}_x^e \\ \hat{v}_x^f \end{bmatrix} \tag{6}$$

The electric field takes the form $\bar{E} = E_o\bar{i}_x + \bar{e}$, $\bar{e} = -\nabla\Phi$ and perturbations, $\bar{e}$, are represented by

Prob. 11.14.1 (cont.)

$$\begin{bmatrix} \hat{e}_x^c \\ \hat{e}_x^d \end{bmatrix} = k \begin{bmatrix} -\coth ka & \frac{1}{\sinh ka} \\ \frac{-1}{\sinh ka} & \coth ka \end{bmatrix} \begin{bmatrix} \hat{\Phi}^c \\ \hat{\Phi}^d \end{bmatrix} \tag{7}$$

in the upper region. There is no $\bar{E}$ in the lower region.

Boundary conditions reflect mass conservation,

$$\hat{v}_x^d = j(\omega - k_z U)\hat{\xi},\ \hat{v}_x^e = j\omega\hat{\xi},\ \hat{v}_x^c = 0,\ \hat{v}_x^f = 0 \tag{8}$$

that the interface and the upper electrode are equipotentials,

$$\begin{vmatrix} \bar{i}_x & \bar{i}_y & \bar{i}_z \\ 1 & -\frac{\partial \xi}{\partial y} & -\frac{\partial \xi}{\partial z} \\ E_o + e_x & e_y & e_z \end{vmatrix} = 0 \Rightarrow e_z^d = -E_o \frac{\partial \xi}{\partial z} \Rightarrow \hat{\Phi}^d = E_o \hat{\xi};\ \hat{\Phi}^c = 0 \tag{9}$$

and that stress equilibrium prevail in the x direction at the interface

$$-(\rho_a - \rho_b)g\hat{\xi} + \hat{p}^d - \hat{p}^e - E_o \hat{e}_x^d + \gamma k^2 \hat{\xi} = 0 \tag{10}$$

The desired dispersion equation is obtained by substituting Eqs. 8 into Eqs. 5b and 6a, and these expressions for $\hat{p}^d$ and $\hat{p}^e$ into Eq. 10, and Eq. 9 into Eq. 7b and the latter into Eq. 10.

$$\hat{\xi}\Big[-(\rho_a - \rho_b)g - \frac{(\omega - k_z U)^2 \rho_a \coth ka}{k} - \frac{\omega^2 \rho_b}{k}\coth kb - \epsilon E_o^2 k \coth ka + \gamma k^2 = 0 \tag{11}$$

To make $\hat{\xi} \neq 0$, the term in brackets must be zero, so

$$[(\omega - k_z U)^2 \rho_a \coth ka/k] + [\omega^2 \rho_b \coth kb/k] = \gamma k^2 + (\rho_b - \rho_a)g - \epsilon E_o^2 k \coth ka \tag{12}$$

This is simply Eq. 11.14.9 with an added term reflecting the self-field-effect of the electric stress. In solving for ω, group this additional term with those due to surface tension and gravity ($\gamma k^2 + (\rho_b - \rho_a)g \rightarrow \gamma k^2 + (\rho_b - \rho_a)g - \epsilon E_o^2 k \coth ka$). It then follows that instability

Prob. 11.14.1 (cont.)

results if (Eq. 11.14.11)

$$U^2 > \left[\frac{\tanh kb}{\rho_b} + \frac{\tanh ka}{\rho_a}\right]\left[\gamma k^2 + g(\rho_b - \rho_a)k - \epsilon E_o^2 k^2 \coth ka\right]\frac{1}{k_z^2} \qquad (13)$$

For short waves $(|kb| >> 1, |ka| >> 1)$ this condition becomes

$$U^2 > \left[\frac{1}{\rho_b} + \frac{1}{\rho_a}\right]\left[\gamma k + \frac{g(\rho_b - \rho_a)}{k} - \epsilon E_o^2\right] \qquad (14)$$

The electric field contribution has no k dependence in this limit, thus making it clear that the most critical wavelength for instability remains the Taylor wavelength

$$k = k^* \equiv \sqrt{\frac{g(\rho_b - \rho_a)}{\gamma}} \qquad (15)$$

Insertion of Eq. 15 for k in Eq. 14 gives the critical velocity

$$U^* = \left(\frac{1}{\rho_b} + \frac{1}{\rho_a}\right)\left(2\sqrt{g\gamma(\rho_b - \rho_a)} - \epsilon E_o^2\right) \qquad (16)$$

By making

$$\epsilon E_o^2 = 2\sqrt{g\gamma(\rho_b - \rho_a)} \qquad (17)$$

the critical velocity becomes zero because the interface is unstable in the Rayleigh-Taylor sense of Secs. 8.9 and 8.10.

In the long-wave limit $(|ka| << 1, |kb| << 1)$ the electric field has the same effect as gravity. That is $\gamma k^2 + (\rho_b - \rho_a)g \rightarrow \gamma k^2 + [(\rho_b - \rho_a)g - \epsilon E_o^2/a]$ and the k dependence of the gravity and electric field terms is the same.

(c) Because the long-wave field effect can be lumped with that due to gravity, the discussion of absolute vs. convective instability given in Sec. 11.14 pertains directly.

Prob. 11.14.2 (a) This problem is similar to Prob. 11.14.1. The equilibrium pressure is now less above than below, because the surface force density is now down rather than up.

$$\Pi_a - \tfrac{1}{2}\rho U^2 - \Pi_b = -\tfrac{1}{2}\mu H_o^2 \tag{1}$$

The analysis then follows the same format except that at the boundaries of the upper region, the conditions are $(\bar{n}\cdot\mu_o\bar{H} = 0)$

$$\left[\bar{i}_x - \frac{\partial\xi}{\partial y}\bar{i}_y - \frac{\partial\xi}{\partial z}\bar{i}_z\right]\left[h_x\bar{i}_x + h_y\bar{i}_y + (H_o + h_z)\bar{i}_z\right] \tag{2}$$
$$\Rightarrow h_x^d = H_o\frac{\partial\xi}{\partial z} \Rightarrow \hat{h}_x^d = -jk_z H_o\hat{\xi}$$

and

$$\hat{h}_x^c = 0 \tag{3}$$

Thus, the magnetic transfer relations for the upper region are

$$\begin{bmatrix}\hat{\psi}^c \\ \hat{\psi}^d\end{bmatrix} = \frac{1}{k}\begin{bmatrix} -\coth ka & \dfrac{1}{\sinh ka} \\ \dfrac{-1}{\sinh ka} & \coth ka\end{bmatrix}\begin{bmatrix} 0 \\ -jk_z H_o\hat{\xi}\end{bmatrix} \tag{4}$$

The stress balance for the perturbed interface requires $(\hat{h}_z = jk\hat{\psi})$

$$-(\rho_a - \rho_b)g\hat{\xi} + \hat{p}^d - \hat{p}^e + j\mu H_o k_z\hat{\psi}^d + \gamma k^2\hat{\xi} = 0 \tag{5}$$

Substitution from the mechanical transfer relations for $\hat{p}^d$ and $\hat{p}^e$ (Eqs. 5, 6 and 8 of Prob. 11.14.1) and for $\hat{\psi}^d$ from Eq. 4 gives the desired dispersion equation.

$$-(\rho_a - \rho_b)g - \frac{(\omega - k_z U)^2\rho_a\coth ka}{k} - \frac{\omega^2\rho_b\coth kb}{k}$$
$$+\frac{\mu H_o^2 k_z^2}{k}\coth ka + \gamma k^2 = 0 \tag{6}$$

Thus, the dispersion equation is Eq. 11.14.9 with $\gamma k^2 + g(\rho_b - \rho_a) \rightarrow \gamma k^2 + g(\rho_b - \rho_a) + \mu_o H_o^2 k_z^2\coth ka/k$. Because the effect of streaming is on perturbations propagating in the z direction, consider $k = k_z$. Then, the problem is the anti-dual of Prob. 11.14.2 (as discussed in Sec. 8.5) and results from Prob. 11.14.1 carry over directly with the substitution $-\epsilon E_o^2 \rightarrow \mu_o H_o^2$.

Prob. 11.14.3 The analysis parallels that of Sec. 8.12. There is now an appreciable mass density to the initially static fluid surrounding the now streaming plasma column. Thus, the mechanical transfer relations are (Table 7.9.1).

$$\begin{bmatrix} \hat{p}^b \\ \hat{p}^c \end{bmatrix} = j\omega\rho_v \begin{bmatrix} F_m(R,a) & G_m(a,R) \\ G_m(R,a) & F_m(a,R) \end{bmatrix} \begin{bmatrix} 0 \\ j\omega\hat{\xi} \end{bmatrix} \tag{1}$$

$$\hat{p}^d = -(\omega - kU)^2 \rho F_m(0,R)\hat{\xi} \tag{2}$$

where substituted on the right are the relations $\hat{v}_r^c = j\omega\hat{\xi}$ and $\hat{v}_r^d = j(\omega - kU)\hat{\xi}$. The magnetic boundary conditions remain the same with $\mathcal{H} = 0$ (no excitation at exterior boundary). Thus, the stress equilibrium equation (Eq. 8.12.10 with $\hat{p}^c$ included)

$$\hat{p}^c - \hat{p}^d = \frac{\mu_o H_t^2}{R}\hat{\xi} - j\mu_o\left(\frac{m}{R}H_t + kH_a\right)\hat{\psi}^c \tag{3}$$

is evaluated using Eqs. 1b, and 2, for $\hat{p}^c$ and $\hat{p}^d$ and Eqs. 8.12.4b, 8.12.7 and $\hat{h}_r^b = 0$ for $\hat{\psi}^c$ to give

$$-\omega^2\rho_v F_m(a,R) + (\omega - kU)^2\rho F_m(0,R) = \frac{\mu_o H_t^2}{R} - \mu_o\left(\frac{m}{R}H_t + kH_a\right)^2 F_m(a,R) \tag{4}$$

This expression is solved for ω.

$$\omega = \frac{-\rho kU F_m(0,R) \pm \left\{\left[\rho_v F_m(a,R) - \rho F_m(0,R)\right]\left[\mu_o\left(\frac{m}{R}H_t + kH_a\right)^2 F_m(a,R) - \frac{\mu_o H_t^2}{R}\right] + k^2U^2\rho_v\rho F_m(0,R)F_m(a,R)\right\}^{1/2}}{\rho_v F_m(a,R) - \rho F_m(0,R)} \tag{5}$$

to give an expression having the same form as Eq. 11.14.10

Prob. 11.14.3 (cont.)

$$(F_m(0,R)<0,\ F_m(a,R)>0 .$$

The system is unstable for those wavenumbers making the radicand negative, that is for

$$U^2 > \frac{[\rho_v F_m(a,R) - \rho F_m(0,R)][\mu_o(\frac{m}{R}H_t + kH_a)^2 F_m(a,R) - \frac{\mu_o H_t^2}{R}]}{-k^2 \rho_v \rho F_m(0,R) F_m(a,R)} \quad (6)$$

Prob. 11.14.4 (a) The alteration to the analysis as presented in Sec. 8.14 is in the transfer relations of Eq. 8.14.12, which become

$$\begin{bmatrix} \hat{\pi}^c \\ \\ \hat{\pi}^d \end{bmatrix} = j\frac{(\omega - k_z U)\rho_a}{k} \begin{bmatrix} -\coth ka & \frac{1}{\sinh ka} \\ \\ \frac{-1}{\sinh ka} & \coth ka \end{bmatrix} \begin{bmatrix} 0 \\ \\ j(\omega - k_z U)\hat{\xi} \end{bmatrix} \quad (1)$$

where boundary conditions inserted on the right require that and $\hat{v}_x^c = 0$, $\hat{v}_x^d = j(\omega - k_z U)\hat{\xi}$. Then evaluation of the interfacial stress equilibrium condition, using Eq. 1, requires that

$$\frac{(\omega - k_z U)^2 \rho_a \coth ka}{k} + \frac{\omega^2 \rho_b \coth kb}{\rho} \quad (2)$$
$$= g(\rho_b - \rho_a) + E_o(q_a - q_b) + \frac{(q_a - q_b)^2}{\epsilon_o k(\coth ka + \coth kb)}$$

(b) To obtain a temporal mode stability condition, Eq. 2 is solved for ω.

$$\omega = \frac{k_z U \frac{\rho_a \coth ka}{k} \pm \left\{ \left[\frac{\rho_a \coth ka}{k} + \frac{\rho_b \coth kb}{k}\right]\left[g(\rho_b - \rho_a) + E_o(q_a - q_b) + \frac{(q_a - q_b)^2}{\epsilon_o k(\coth ka + \coth kb)}\right] - \frac{\rho_a \rho_b}{k^2} \coth kb\, k_z^2 U^2 \coth ka \right\}^{1/2}}{(\rho_a \coth ka + \rho_b \coth kb)/k} \quad (3)$$

Prob. 11.14.4 (cont.)

Thus, instability results if

$$U^2 > \frac{k\left[\rho_a \coth ka + \rho_b \coth kb\right]\left[g(\rho_b - \rho_a) + E_o(q_a - q_b) + \dfrac{(q_a - q_b)^2}{\epsilon_o k(\coth ka + \coth kb)}\right]}{\rho_a \rho_b k_z^2 \coth kb \coth ka} \tag{4}$$

Prob. 11.15.1 Equations 11.15.1 and 11.15.2 become

$$\left(\frac{\partial}{\partial t}+M\frac{\partial}{\partial z}\right)^2\xi_1=\frac{\partial^2\xi_1}{\partial z^2}+P\xi_1-\frac{1}{2}P\xi_2 \qquad (1)$$

$$\left(\frac{\partial}{\partial t}-M\frac{\partial}{\partial z}\right)^2\xi_2=\frac{\partial^2\xi_2}{\partial z^2}+P\xi_2-\frac{1}{2}P\xi_1 \qquad (2)$$

Thus, these relations are written in terms of complex amplitudes as

$$\begin{bmatrix}[-(\omega-Mk)^2+k^2-P] & \frac{1}{2}P\\ \frac{1}{2}P & [-(\omega+Mk)^2+k^2-P]\end{bmatrix}\begin{bmatrix}\xi_1\\ \xi_2\end{bmatrix}=0 \qquad (3)$$

and it follows that the dispersion equation is

$$[(\omega-Mk)^2-k^2+P][(\omega+Mk)^2-k^2+P]-\frac{P^2}{4}=0 \qquad (4)$$

Multiplied out and arranged as a polynomial in ω, this expression is

$$\omega^4+\omega^2[2P-2k^2(M^2+1)]+[(M^2-1)^2k^4+2P(M^2-1)k^2+P^2\tfrac{3}{4}]=0 \qquad (5)$$

Similarly, written as a polynomial in k, Eq. 4 is

$$k^4[M^2-1]^2+k^2[2P(M^2-1)-2\omega^2(M^2+1)]+[\omega^4+2\omega^2P+P^2\tfrac{3}{4}]=0 \qquad (6)$$

These last two expressions are biquadratic in ω and k respecively, and can be conveniently solved for these variables by using the quadratic formula twice.

$$\omega=\pm\left\{k^2(M^2+1)-P\pm\sqrt{4k^2M^2(k^2-P)+\tfrac{1}{4}P^2}\right\}^{1/2} \qquad (7)$$

$$k=\pm\left\{\frac{\omega^2(M^2+1)-P(M^2-1)\pm\sqrt{[P(M^2-1)-\omega^2(M^2+1)]^2-(M^2-1)^2[\omega^4+2\omega^2P+\frac{3}{4}P^2]}}{(M^2-1)}\right\}^{\frac{1}{2}} \qquad (8)$$

First, in plotting complex ω for real k, it is helpful to observe that in the limit $k\to\pm\infty$, Eq. 7 takes the asymptotic form

$$\omega\to\pm k(M\pm 1) \qquad (9)$$

These are shown in the four cases of Fig. 11.15.1a as the light straight lines. Because the dispersion relation is biquadradic in both ω and k, it is clear that for each root given, its negative is also a root. Also, only the complex ω is given as a function of positive k, because the plots must be symmetric in k.

Prob. 11.15.1 (cont.)

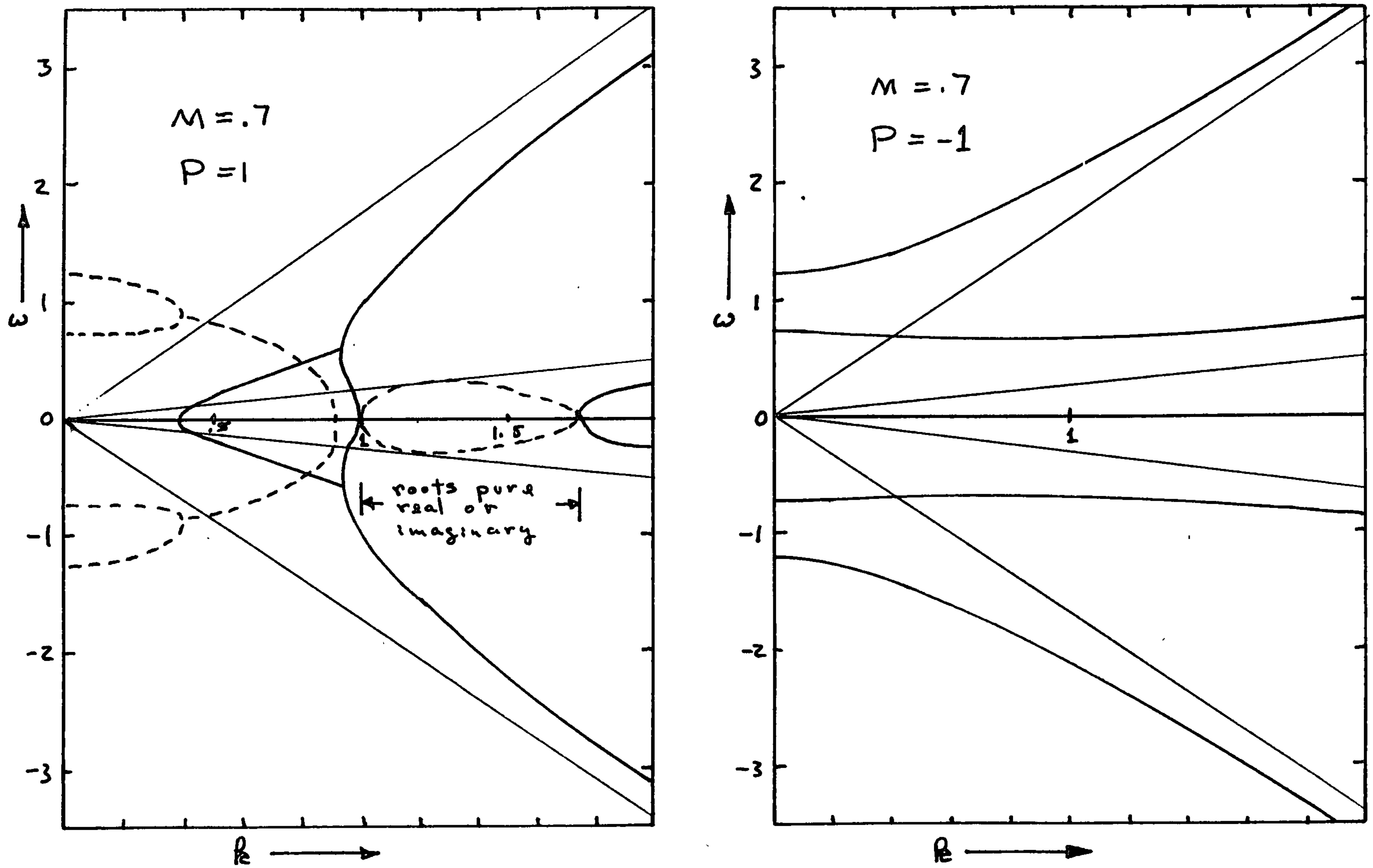

Complex ω as a function of real k for subcritical electric-field (P=1) and magnetic-field (P=-1) coupled counterstreaming streams.

Prob. 11.15.1 (cont.)

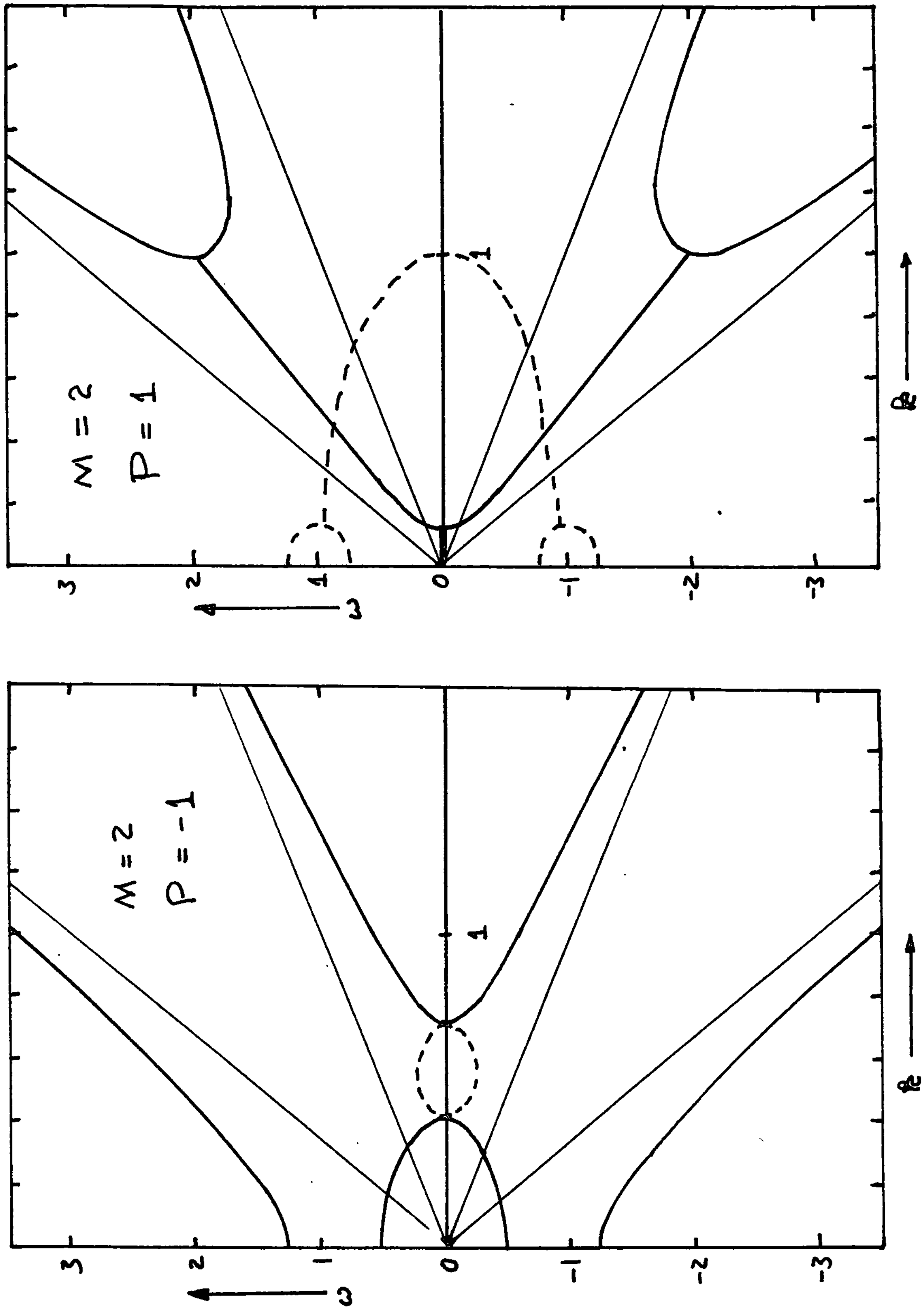

Complex ω as a function of real k for supercritical magnetic-field (P=-1) and electric-field (P=1) coupled counterstreaming streams.

Prob. 11.15.1 (cont.)

The subcritical magnetic case shows no "unstable" values of ω for real k, so there is no question about whether the instability is absolute or convective. For the subcritical electric case, the figure below shows the critical plot of complex k as ω is varied along the trajectory shown at the right. The plot makes it clear that the instabilities are absolute, as would be expected from the fact that the streams are subcritical.

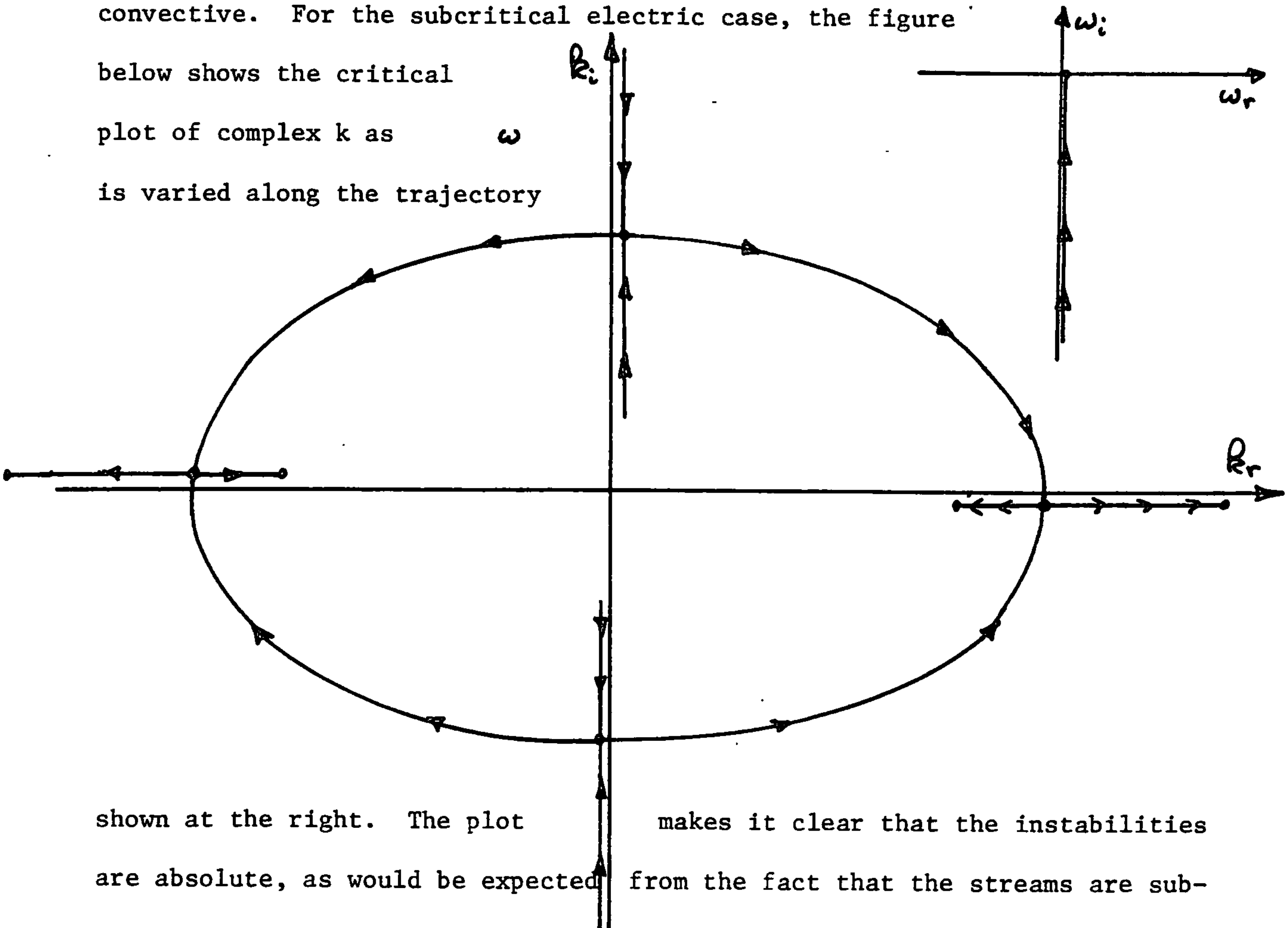

Probably the most interesting case is the supercritical magnetic one, because the individual streams then tend to be stable. In the map of complex k shown on the next figure, there are also roots of k that are the negatives of those shown. Thus, there is a branching on the k_r axis at both $k_r \approx .56$ and at $k_r \approx -.56$. Again, the instability is clearly absolute. Finally, the last figure shows the map for a super-electric case. As might be expected, from the fact that the two stable (P=-1) streams become unstable when coupled, this super-electric case is also absolutely unstable.

Prob. 11.15.1 (cont.)

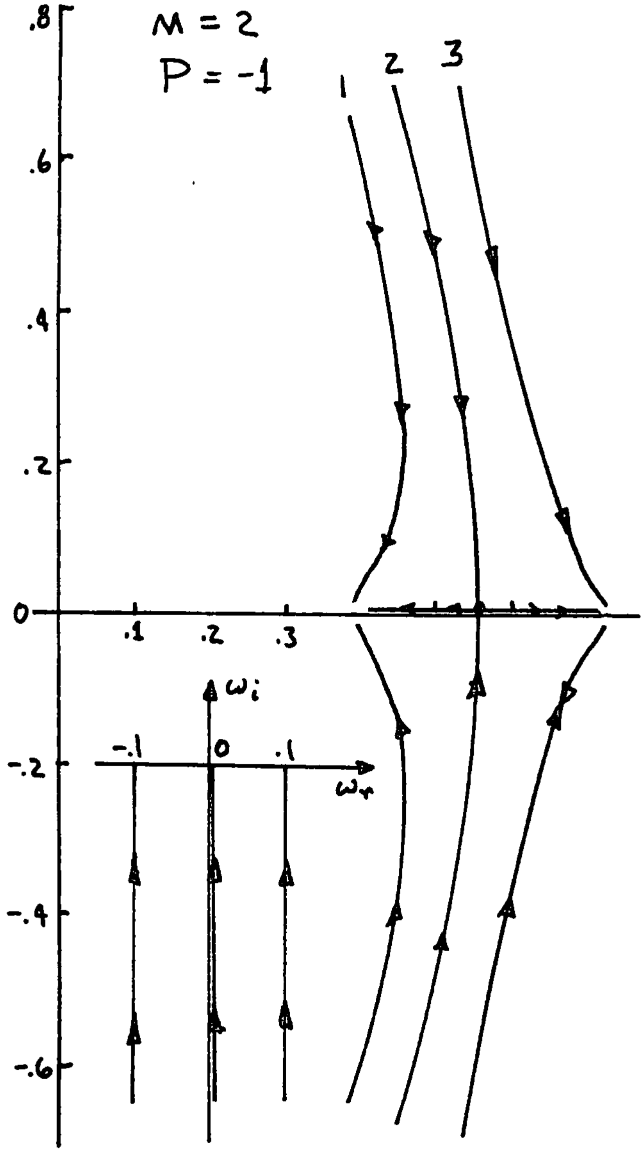

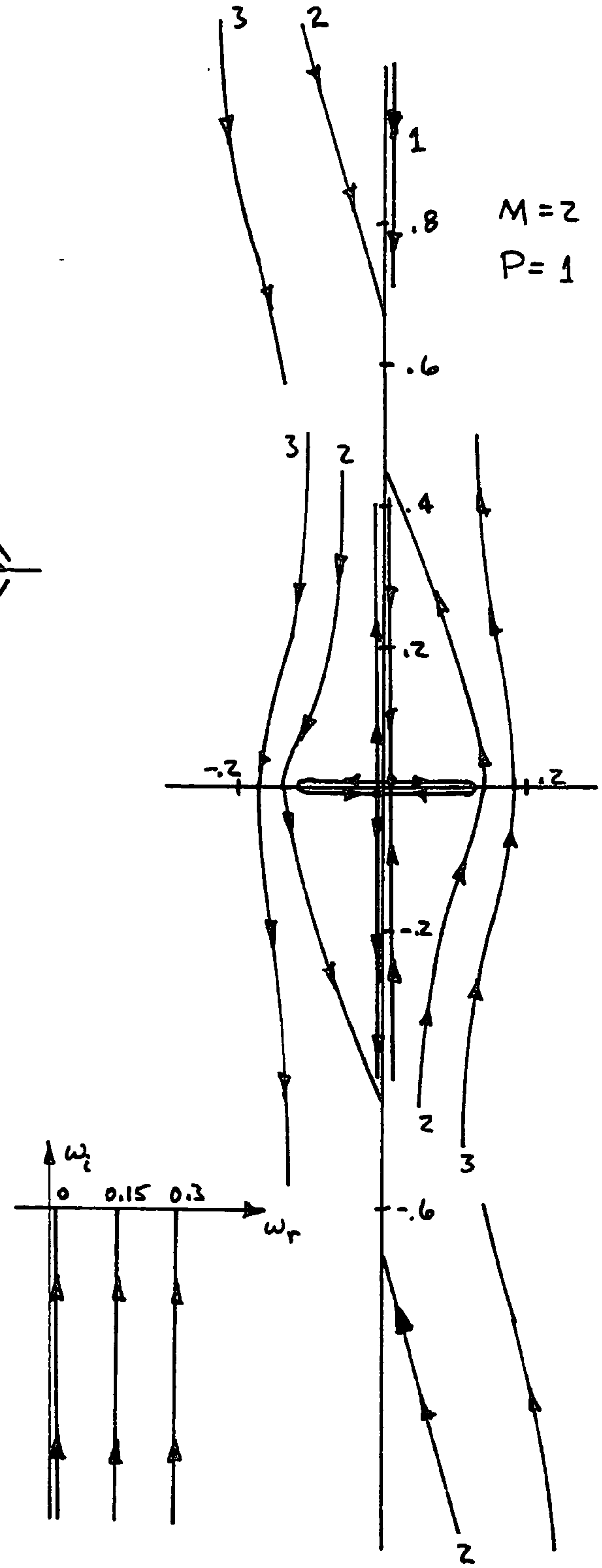

Prob. 11.16.1 With homogeneous boundary conditions, the amplitude of an eigenmode is determined by the specific initial conditions. Each eigenmode can be thought of as the response to initial conditions having just the distribution required to excite that mode. To determine that distribution, one of the amplitudes in Eq. 11.16.6 is arbitrarily set. For example, suppose A_1 is given. Then the first three of these equations require that

$$\begin{bmatrix} 1 & 1 & 1 \\ e^{-jk_2 l} & e^{-jk_3 l} & e^{-jk_4 l} \\ Q_2 & Q_3 & Q_4 \end{bmatrix} \begin{bmatrix} A_2 \\ A_3 \\ A_4 \end{bmatrix} = \begin{bmatrix} -A_1 \\ -e^{-jk_1 l} A_1 \\ -QA_1 \end{bmatrix} \qquad (1)$$

and the fourth is automatically satisfied because, for each mode, ω is such that the determinant of the coefficients of Eq. 11.16.6 is zero. With A_1 set, A_2, A_3 and A_4 are determined by inverting Eqs. 1. Thus, within a multiplicative factor, namely A_1, the coefficients needed to evaluate Eq. 11.16.2 are determined.

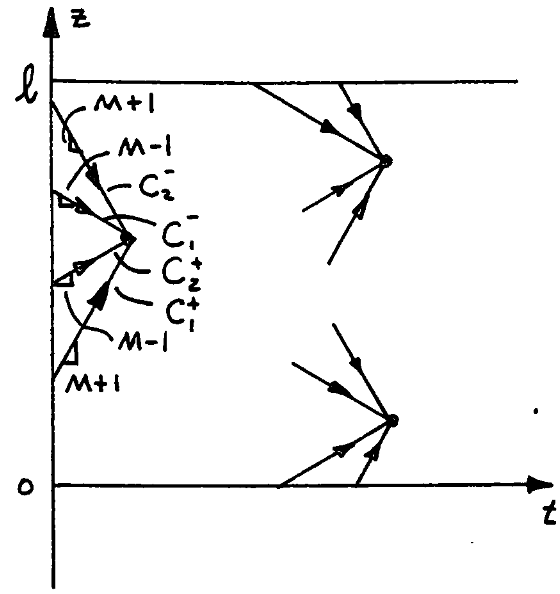

Prob. 11.16.2 (a) With $M_1 = -M_2 = M$ and $|M| < 1$, the characteristic lines are as shown in the figure. Thus, by the arguments given in Sec. 11.10, Causality and Boundary Condition, a point on either boundary has two "incident" characteristics. Thus, two conditions can be imposed at each boundary with the result dynamics that do not require initial conditions implied by subsequent (later) boundary conditions.

The eigenfrequency equation follows from evaluation of the solutions

$$\xi_2 = \mathcal{R}e \sum_{n=1}^{4} A_n e^{-jk_n z} e^{j\omega t} \tag{1}$$

$$\xi_1 = \mathcal{R}e \sum_{n=1}^{4} Q_n A_n e^{-jk_n z} e^{j\omega t} \tag{2}$$

where (from Eq. 11.15.2)

$$Q_n = \frac{2}{\underline{P}}\left[(\omega + Mk)^2 - k^2 + \underline{P}\right] \tag{3}$$

Thus,

$$\begin{bmatrix} 1 & 1 & 1 & 1 \\ e^{-jk_1 \ell} & e^{-jk_2 \ell} & e^{-jk_3 \ell} & e^{-jk_4 \ell} \\ Q_1 & Q_2 & Q_3 & Q_4 \\ Q_1 e^{-jk_1 \ell} & Q_2 e^{-jk_2 \ell} & Q_3 e^{-jk_3 \ell} & Q_4 e^{-jk_4 \ell} \end{bmatrix} \begin{bmatrix} A_1 \\ A_2 \\ A_3 \\ A_4 \end{bmatrix} = \begin{bmatrix} 0 \\ 0 \\ 0 \\ 0 \end{bmatrix} \tag{4}$$

Prob. 11.16.2 (cont.)

Given the dispersion equation, $D(\omega, k) \Rightarrow k_n = k_n(\omega)$, this is an eigenfrequency equation.

$$\mathrm{Det}\,(\omega) = 0 \tag{5}$$

In the limit $M \to 0$, Eqs. 11.15.1 and 11.15.2 require that

$$\begin{bmatrix} \omega^2 - k^2 + P & -\frac{P}{2} \\ -\frac{P}{2} & \omega^2 - k^2 + P \end{bmatrix} \begin{bmatrix} \hat{\xi}_1 \\ \hat{\xi}_2 \end{bmatrix} \begin{bmatrix} 0 \\ 0 \end{bmatrix} \tag{6}$$

For $\hat{\xi}_1 = \hat{\xi}_2$, both of these equations are satisfied if

$$\omega^2 - k^2 + P\left(1 - \frac{1}{2}\right) = 0 \Rightarrow k_1 = \sqrt{\omega^2 + \frac{P}{2}} \;,\; k_2 = -\sqrt{\omega^2 + P} \tag{7}$$

and for $\hat{\xi}_1 = -\hat{\xi}_2$,

$$\omega^2 - k^2 + \frac{3}{2}P = 0 \Rightarrow k_3 = \sqrt{\omega^2 + \frac{3}{2}P} \;,\; k_4 = -\sqrt{\omega^2 + \frac{3}{2}P} \tag{8}$$

and it follows that

$$Q_1 = 1 \;,\; Q_2 = 1 \;,\; Q_3 = -1 \;,\; Q_4 = -1 \tag{9}$$

Thus, in this limit, Eq. 4 becomes

$$\begin{bmatrix} 1 & 1 & 1 & 1 \\ e^{-jk_1 l} & e^{jk_1 l} & e^{-jk_2 l} & e^{jk_2 l} \\ 1 & 1 & -1 & -1 \\ e^{-jk_1 l} & e^{jk_1 l} & e^{-jk_2 l} & e^{jk_2 l} \end{bmatrix} = 0 \tag{10}$$

Prob. 11.16.2 (cont.)

and reduces to

$$\sin k_1 \ell \, \sin k_2 \ell = 0 \tag{11}$$

The roots follow from

$$k_1 = \frac{n\pi}{\ell} \;, \quad k_2 = \frac{m\pi}{\ell} \;, \quad m = 1,2,3\ldots \tag{12}$$

and hence from Eqs. 7 and 8

$$\omega = \pm\sqrt{\left(\frac{n\pi}{\ell}\right)^2 - \frac{P}{2}} \;; \qquad \omega = \pm\sqrt{\left(\frac{m\pi}{\ell}\right)^2 - \frac{3}{2}P} \tag{13}$$

Instability is incipient in the odd $m=1$ mode when

$$P = \frac{2}{3}\left(\frac{\pi}{\ell}\right)^2 \tag{14}$$

(b) For $M > 1$, the characteristics are as shown in the figure. Each boundary has two incident characteristics. Thus, two conditions can be imposed at each boundary. In the limit where $P \to 0$, the streams become uncoupled and it is most likely that conditions would be imposed on the streams where they (and hence their associated characteristics) enter the region of interest.

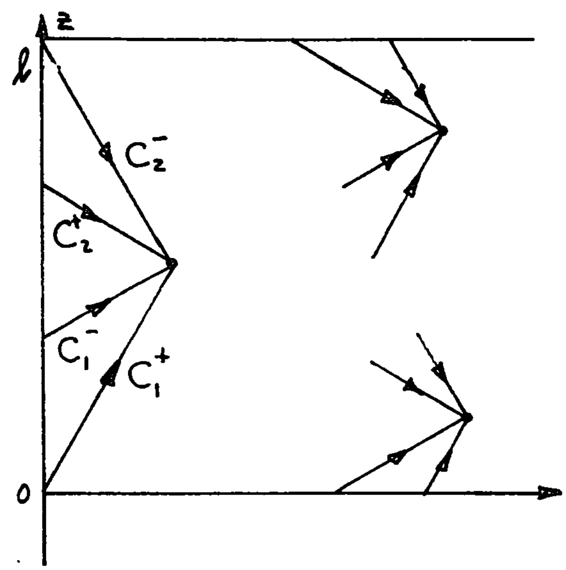

From Eqs. 11.15.2 and 11.15.5

$$\frac{\partial \xi_2}{\partial z} = \mathrm{Re} \sum_{n=1}^{4} -jk_n A_n e^{-jk_n z} e^{j\omega t} \tag{15}$$

$$\frac{\partial \xi_1}{\partial z} = \mathrm{Re} \sum_{n=1}^{4} -jk_n Q_n A_n e^{-jk_n z} e^{j\omega t} \tag{16}$$

Prob. 11.16.2 (cont.)

Evaluation of Eqs. 11.15.2, 15, 11.15.5 and 16 at the respective boundaries where the conditions are specified then results in the desired eigenfrequency equation.

$$\begin{bmatrix} Q_1 & Q_2 & Q_3 & Q_4 \\ k_1 Q_1 & k_2 Q_2 & k_3 Q_3 & k_4 Q_4 \\ e^{-jk_1 l} & e^{-jk_2 l} & e^{-jk_3 l} & e^{-jk_4 l} \\ k_1 e^{-jk_1 l} & k_2 e^{-jk_2 l} & k_3 e^{-jk_3 l} & k_4 e^{-jk_4 l} \end{bmatrix} \begin{bmatrix} A_1 \\ A_2 \\ A_3 \\ A_4 \end{bmatrix} = 0 \tag{17}$$

Given that $k_n = k_n(\omega)$, the determinant of the coefficients comprises a complex equation in the complex unknown, ω .

Prob. 11.17.1 The voltage and current circuit equations are

$$v(y,t) = \Delta y\, L \frac{\partial i}{\partial t} - nw\Delta y \frac{\partial B_x}{\partial t} + v(y+\Delta y, t) \tag{1}$$

$$i(y,t) = \Delta y\, C \frac{\partial v}{\partial t} + i(y+\Delta y, t) \tag{2}$$

In the limit $\Delta y \to 0$, these become the first two of the given expressions. In addition, the surface current density is given by

$$K_z = \frac{n\, i(y+\Delta y, t) - n\, i(y)}{\Delta y} \tag{3}$$

and in the limit $\Delta y \to 0$, this becomes

$$[\![H_y]\!] = n \frac{\partial i}{\partial y} \tag{4}$$

By Ampere's law, $[\![H_y]\!] = K_z$ and the third expression follows.

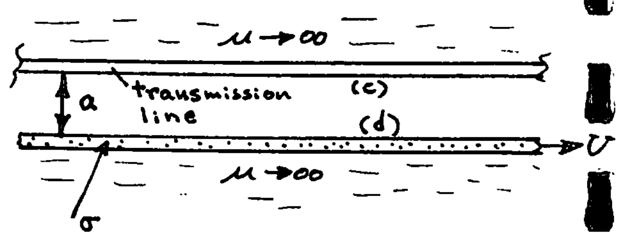

Prob. 11.17.2 With amplitudes designated as in the figure, the boundary conditions representing the distributed coils and transmission line (the equations summarized in Prob. 11.17.1) are

$$jk\hat{v} = j\omega L\hat{i} - j\omega n w \hat{B}_x^c \tag{1}$$

$$jk\hat{i} = j\omega C\hat{v} \tag{2}$$

$$-\hat{H}_y^c = -jkn\hat{i} \tag{3}$$

The resistive sheet is represented by the boundary condition of Eq. (a) from Table 6.3.1.

$$-k^2\hat{H}_y^d = -\sigma_s k(\omega - kU)\hat{B}_x^d \tag{4}$$

The air-gap fields are represented by the transfer relations, Eqs. (a), from Table 6.5.1 with $\gamma \to k$.

$$\begin{bmatrix} \hat{H}_y^c \\ \hat{H}_y^d \end{bmatrix} = \frac{j}{\mu_0}\begin{bmatrix} -\coth ka & \frac{1}{\sinh ka} \\ \frac{-1}{\sinh ka} & \coth ka \end{bmatrix}\begin{bmatrix} \hat{B}_x^c \\ \hat{B}_x^d \end{bmatrix} \tag{5}$$

These expressions are now combined to obtain the dispersion equation. Equations 1 and 2 give the first of the following three equations

$$\begin{bmatrix} j\left(\omega L - \frac{k^2}{\omega C}\right) & -jnw\omega & 0 \\ -jkn & -\frac{j}{\mu_0}\coth ka & \frac{j}{\mu_0}\frac{1}{\sinh ka} \\ 0 & -\frac{j}{\mu_0}\frac{1}{\sinh ka} & \frac{j}{\mu_0}\coth ka - \frac{\sigma_s(\omega - kU)}{k} \end{bmatrix} = \begin{bmatrix} \hat{i} \\ \hat{B}_x^c \\ \hat{B}_x^d \end{bmatrix} \tag{6}$$

The second of these equations is Eq. 5a with $\hat{H}_y^c$ given by Eq. 3. The third is Eq. 5b with Eq. 4 substituted for $\hat{H}_y^d$. The dispersion equation follows from the condition that the determinant of the coefficients vanish.

Prob. 11.17.2 (cont.)

$$\left(\omega^2 LC - k^2\right)\left[\frac{\mu_o \sigma_s (\omega - kU)}{k} \coth ka - j\right]$$

$$+ \mu_o k n^2 w \omega^2 C\left[\frac{\mu_o \sigma_s (\omega - kU)}{k} - j \coth ka\right] = 0 \quad (7)$$

As should be expected, as $n \rightarrow 0$ (so that coupling between the transmission line and the resistive moving sheet is removed), the dispersion equations for the transmission line waves and convective diffusion mode are obtained. The coupled system is represented by the cubic obtained by expanding Eq. 7. In terms of characteristic times respectively representing the transite of electromagnetic waves on the line (without the effect of the coupling coils), material transport, magnetic diffusion and coupling,

$$\tau_{em} \equiv a\sqrt{LC}, \; \tau_v \equiv \frac{a}{U}, \; \tau_m \equiv \mu_o \sigma_s a, \; \tau_c \equiv \sqrt{\mu_o w a C n^2} \quad (8)$$

and the normalized frequency and wavenumber

$$\omega = \underline{\omega} / \tau_{em}, \; k = \underline{k} / a \quad (9)$$

the dispersion equation is

$$(\omega)^3\left[\frac{\tau_m}{\tau_{em}} \frac{\coth k}{k} + \frac{\tau_c^2 \tau_m}{\tau_{em}^3}\right] \quad (10)$$

$$(\omega)^2\left[-\frac{\tau_m}{\tau_v} \coth k - j - \frac{\tau_c^2 \tau_m}{\tau_v \tau_{em}^2} k - j \frac{\tau_c^2}{\tau_{em}^2} k \coth k\right]$$

$$(\omega)\left[-\frac{\tau_m}{\tau_{em}} k \coth k\right] + \left[\frac{\tau_m}{\tau_v} k^2 \coth k + j k^2\right] = 0$$

Prob. 11.17.2 (cont.)

The long-wave limit of Eq. 10 is

$$(\omega)^3\left[\frac{\tau_m}{\tau_{em}}+\frac{\tau_c^2\tau_m k^2}{\tau_{em}^3}\right]+(\omega)^2\left[-\frac{\tau_m}{\tau_v}k-jk^2-\frac{\tau_c^2\tau_m}{\tau_v\tau_{em}^2}k^3-j\frac{\tau_c^2k^2}{\tau_{em}^2}\right] \tag{11}$$

$$+\ \omega\left[-\frac{\tau_m}{\tau_{em}}k^2\right]+\left[\frac{\tau_m}{\tau_v}k^3+jk^4\right]=0$$

In the form of a polynomial in k, this is

$$k^4-k^3\left[j\frac{\tau_m}{\tau_v}-j\omega^2\frac{\tau_c^2\tau_m}{\tau_v\tau_{em}^2}\right]$$

$$+\,k^2\left[\frac{j\omega\tau_m}{\tau_{em}}-\frac{\omega^2\tau_c^2}{\tau_{em}^2}-j\frac{\omega^3\tau_c^2\tau_m}{\tau_{em}^3}-\omega^2\right] \tag{12}$$

$$+\,k\left[j\omega^2\frac{\tau_m}{\tau_v}\right]-\left[j\omega^3\frac{\tau_m}{\tau_{em}}\right]=0$$

where it must be remembered that $\underline{k} << 1$

As would be expected for the coupling of two systems that individually have two spatial modes, the coupled transmission line and convecting sheet are represented by a quartic dispersion equation. The complex values of for real k are shown in Fig. 11.17.2a. One of the three modes is indeed unstable for the parameters used. Note that these are assigned to make the material velocity exceed that of the uncoupled transmission-line wave. It is unfortunate that the system exhibits instability even as k is increased beyond the range of validity for the long-wave approximation $\underline{k}<\underline{1}$. The mapping of complex shown in Fig. 11.17.2b is typical of a convective instability. Note that for $\omega_r = 0.5$ the root crosses the k_r axis. Of course, a rigerous proof that there are no absolute instabilities requires considering all possible values of $\sigma > 0$.

Prob. 11.17.2a (cont.)

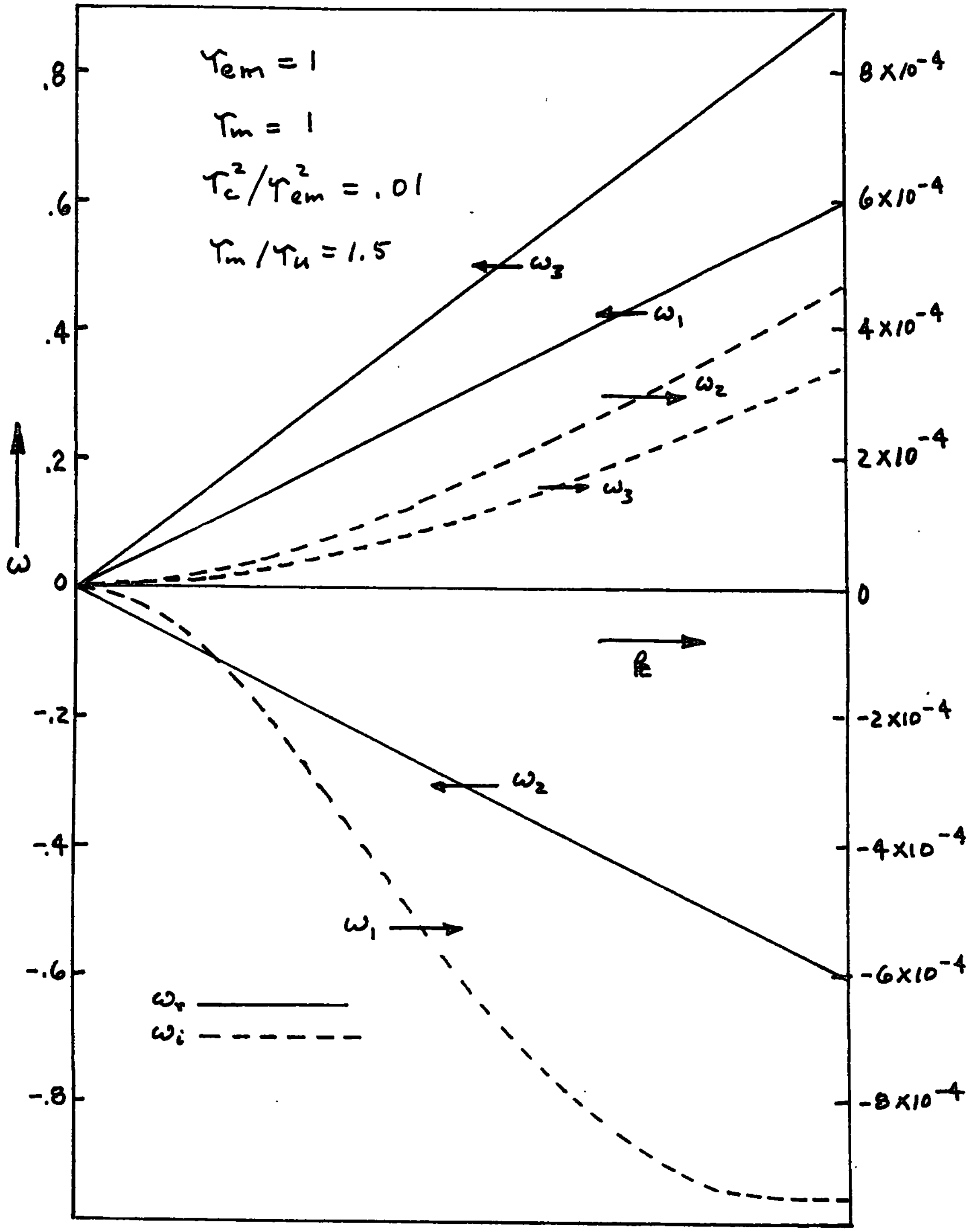

Fig. 11.17.2a Complex ω for real k.

Prob. 11.17.2 (cont.)

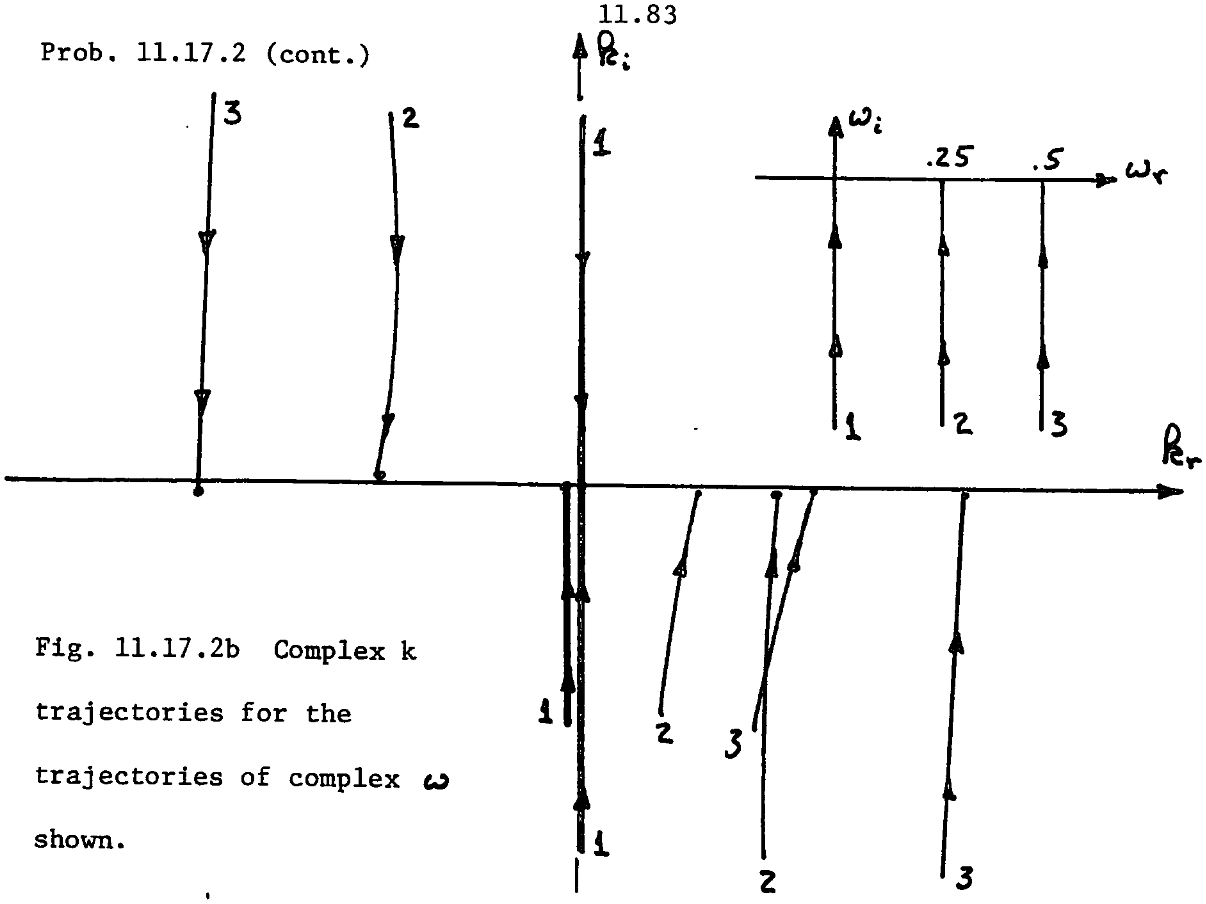

Fig. 11.17.2b Complex k trajectories for the trajectories of complex ω shown.

Prob. 11.17.3 The first relation requires that the drop in voltage across the inductor be

$$v(z) - v(z+\Delta z) = L\,\Delta z \frac{\partial i}{\partial t} \tag{1}$$

Divided by Δz and in the limit where $\Delta z \to 0$ this becomes

$$-\frac{\partial v}{\partial z} = L\frac{\partial i}{\partial t} \tag{2}$$

The second requires that the sum of currents into the mode at $z + \Delta z$ be zero.

$$i(z) - i(z+\Delta z) = C\,\Delta z\frac{\partial v}{\partial t} + \frac{\partial}{\partial t}(\sigma_f w \Delta z) \tag{3}$$

where σ_f is the net charge per unit area on the electrode

$$\sigma_f = [\![D_x]\!] \tag{4}$$

Divided by Δz and in the limit $\Delta z \to 0$, Eq. 3 becomes

$$-\frac{\partial i}{\partial z} = C\frac{\partial v}{\partial t} + w\frac{\partial \sigma_f}{\partial t} \tag{5}$$

Prob. 11.17.4 (a) The beam and air-gaps are represented by Eq. 11.5.11, which is ($k_y=0, k_z=k$)

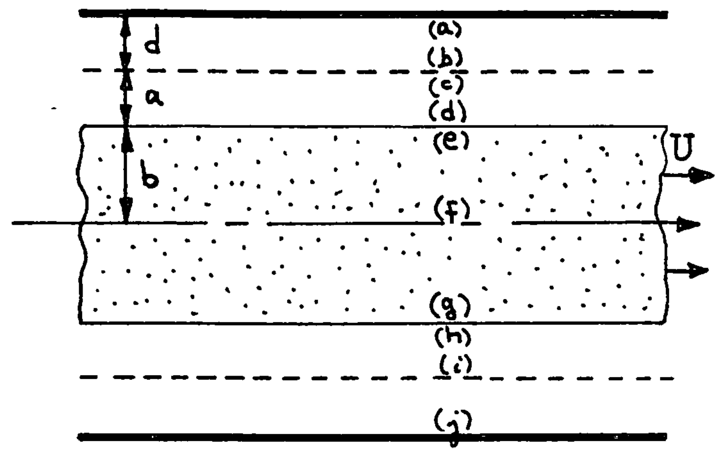

$$\hat{D}_x^c = \frac{-\epsilon k(k+\gamma\coth ka\tanh\gamma b)\,\hat{\Phi}^c}{k\coth ka+\gamma\tanh\gamma b} \qquad (1)$$

$$\gamma^2 \equiv k^2[1-\omega_p^2/(\omega-kU)^2]$$

The transfer relations for the region a-b, with $\hat{\Phi}^a=0$ require that

$$\hat{D}_x^b = \epsilon k\coth kd\,\hat{\Phi}^b \qquad (2)$$

With the recognition that $\hat{v}\rightarrow\hat{\Phi}^b=\hat{\Phi}^c$, the traveling-wave structure equations from Prob. 11.17.3 require that

$$jk\hat{\Phi}^c = j\omega L\hat{i} \qquad (3)$$

$$jk\hat{i} = j\omega C\hat{\Phi}^c + j\omega w(\hat{D}_x^b-\hat{D}_x^c) \qquad (4)$$

The dispersion equation follows from substitution of Eqs. 1 and 2 (for $\hat{D}_x^c$ and $\hat{D}_x^b$) and Eq. 3 (for $\hat{i}$) into Eq. 4.

$$\frac{k^2}{\omega L} = \omega C + \omega w\epsilon k\left[\coth kd + \frac{(k+\gamma\coth ka\tanh\gamma b)}{k\coth ka+\gamma\tanh\gamma b}\right] \qquad (5)$$

As a check, in the limit where $L\rightarrow\infty$ and $C\rightarrow 0$ this expression should be the dispersion relation for the electron beam (D=o in Eq. 11.5.11) with a of that problem replaced by a+d. (This follows by using the identity $(\coth kd+\coth ka)/(\coth ka\coth kd+1) = \tanh k(a+d)$.)

In taking the long-wave limit of Eq. 5, where $kd\ll 1$, $ka\ll 1$ and $\gamma b\ll 1$,

Prob. 11.17.4 (cont.)

the object is to retain the dominant modes of the uncoupled systems. These are the transmission line and the electron beam. Each of these is represented by a dispersion equation that is quadratic in ω and in k. Thus, the appropriate limit of Eq. 5 should retain terms in ω and k of sufficient order that the resulting dispersion equation for the coupled system is quartic in ω and in k. With $C' \equiv C + w\epsilon/d$, Eq. 5 becomes

$$\left(\frac{k^2}{L} - C'\omega^2\right)\left[\frac{(\omega - kU)^2}{a} - b k^2 \omega_p^2\right] = w\epsilon k^2 \omega^2\left[(\omega - kU)^2\left(1 + \frac{b}{a}\right) - \frac{b}{a}\omega_p^2\right] \tag{6}$$

With normalization

$$\underline{k} = kb \qquad c^2 = (\omega_p^2 L b^2 C')^{-1}$$

$$\underline{\omega} = \omega/\omega_p$$

$$\underline{U} = U/b\omega_p \qquad K = \frac{w\epsilon}{C'b}$$

this expression becomes

$$(k^2c^2 - \omega^2)\left[(\omega - kU)^2\frac{b}{a} - k^2\right] - K k^2\omega^2\left[(\omega - kU)^2\left(1 + \frac{b}{a}\right) - \frac{b}{a}\right] = 0 \tag{7}$$

Written as a polynomial in ω, this expression is

$$\left[\frac{b}{a} + K k^2\left(1 + \frac{b}{a}\right)\right]\omega^4 - 2\left[\frac{b}{a}kU + K k^3 U\left(1 + \frac{b}{a}\right)\right]\omega^3 + \left[k^2\frac{b}{a}(U^2 - c^2) - k^2 + K k^4 U\left(1 + \frac{b}{a}\right) - K k^2\frac{b}{a}\right]\omega^2 + \left[2\frac{b}{a}k^3 U c^2\right]\omega + \left[k^4 c^2\left(1 - U^2\frac{b}{a}\right)\right] = 0 \tag{8}$$

Prob. 11.17.4 (cont.)

This expression can be numerically solved for ω to determine if the system is unstable, convective or absolute. A typical plot of complex ω for real k, shown in Fig. P11.17.4a, shows that the system is indeed unstable.

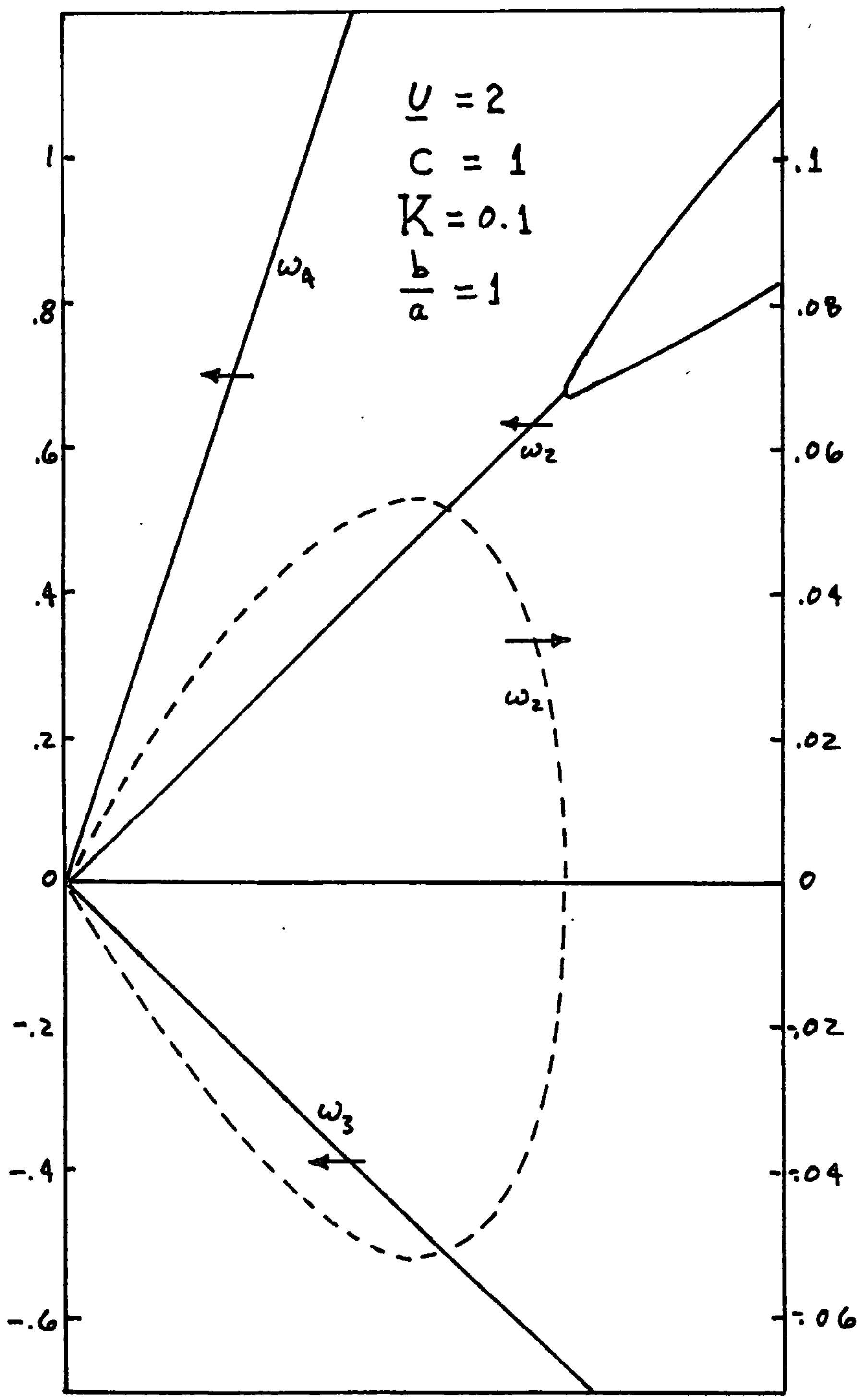

Prob. 11.17.4(cont.)

To determine whether the instability is convective or absolute, it is necessary to map the loci of complex k as a function of complex $\omega = \omega_r - j\sigma$. Typical trajectories for the values of ω shown by the inset are shown in Fig. 11.17.4b.

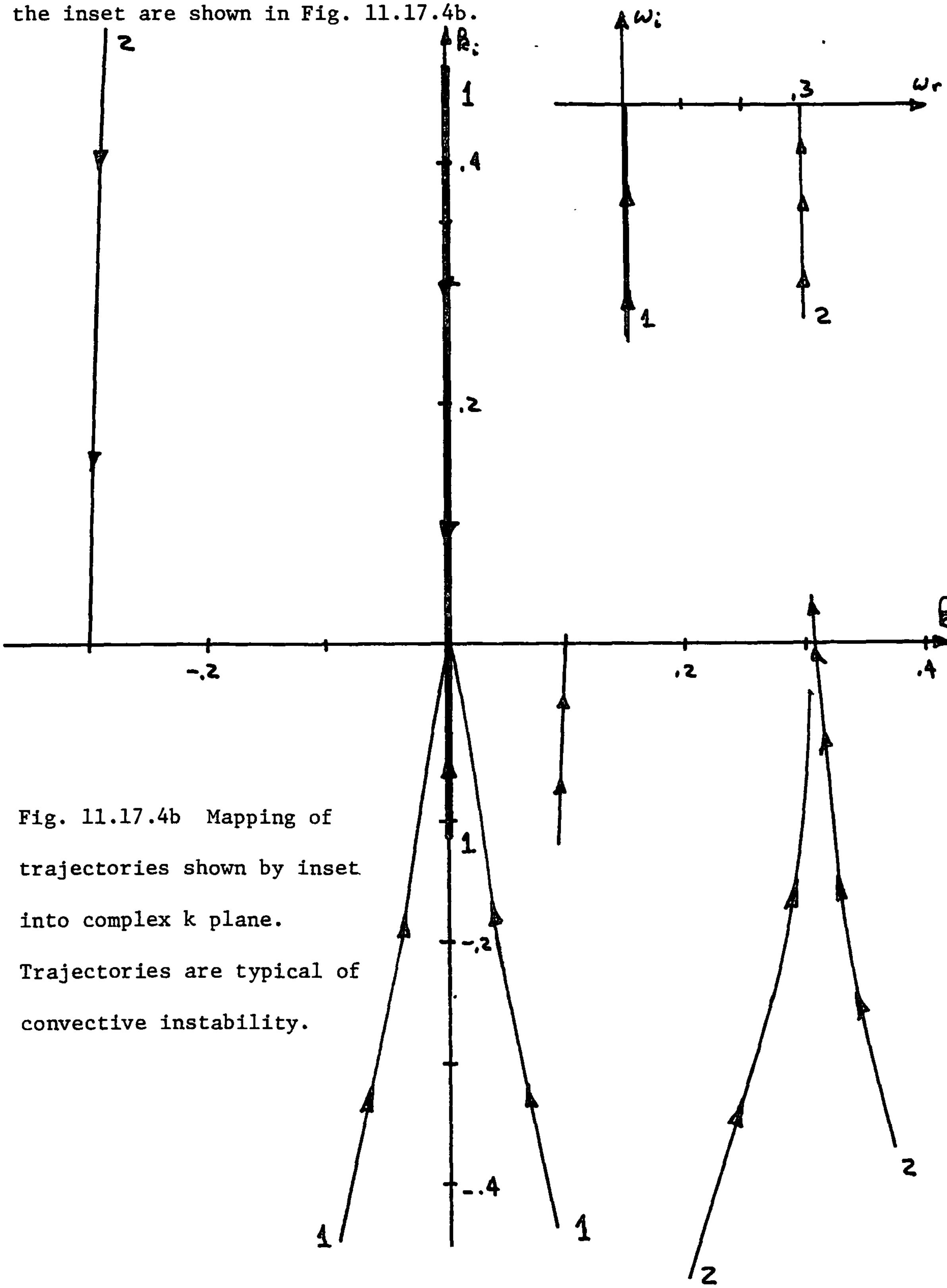

Fig. 11.17.4b Mapping of trajectories shown by inset into complex k plane. Trajectories are typical of convective instability.

<u>Prob. 11.17.5</u> (a) In a state of stationary equilibrium, $\bar{v} = U\bar{i}_y$ and $p = \Pi$ = constant, to satisfy mass and momentum conservation conditions in the fluid bulk. Boundary conditions are automatically satisfied, with normal stress equilibrium at the interfaces making

$$\Pi = \frac{1}{2}\mu_o H_o^2 \qquad (1)$$

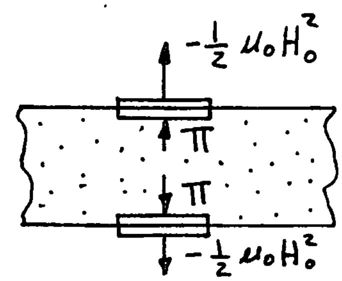

where the pressure in the low mass density media surrounding the jet is taken as zero.

(b) <u>Bulk relations</u> describe the magnetic perturbations in the free-space region and the fluid motion in the stream. From Eqs. (a) of Table 2.16.1, with

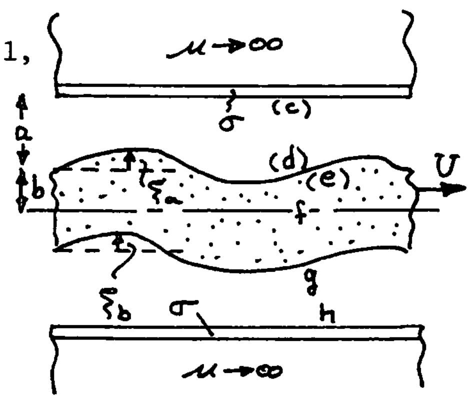

$$\bar{H} = H_o\bar{i}_y + \bar{h}\,;\ \bar{h} = -\nabla\psi \qquad (2)$$

$$\begin{bmatrix} \hat{h}_x^c \\ \hat{h}_x^d \end{bmatrix} = k \begin{bmatrix} -\coth ka & \dfrac{1}{\sinh ka} \\ \dfrac{-1}{\sinh ka} & \coth ka \end{bmatrix} \begin{bmatrix} \hat{\psi}^c \\ \hat{\psi}^d \end{bmatrix} \qquad (3)$$

and from Table 7.9.1, Eq. (c),

$$\begin{bmatrix} \hat{p}^e \\ \hat{p}^f \end{bmatrix} = j\frac{(\omega - k_y U)}{k} \begin{bmatrix} -\coth kb & \dfrac{1}{\sinh kb} \\ \dfrac{-1}{\sinh kb} & \coth kb \end{bmatrix} \begin{bmatrix} \hat{v}_x^e \\ \hat{v}_x^f \end{bmatrix} \qquad (4)$$

Because only the kinking motions are to be described, Eq. 4 has been written with position (f) at the center of the stream. From the symmetry of the system, it can be argued that for the kinking motions the perturbation pressure at the center-plane must valish. Thus, Eq. 4b requires that

$$\hat{v}_x^f = \frac{\hat{v}_x^e}{\sinh kb\ \coth kb} = \frac{\hat{v}_x^e}{\cosh kb} \qquad (5)$$

so that Eq. 4a becomes

Prob. 11.17.5 (cont.)

$$\hat{p}^e = j\frac{(\omega - k_y U)\rho}{k}\left(-\coth kb + \frac{1}{\sinh kb \cosh kb}\right)\hat{v}_x^e \tag{6}$$

or

$$\hat{p}^e = -j\frac{(\omega - k_y U)\rho}{k}\tanh kb\, \hat{v}_x^e = \frac{(\omega - kU)^2}{k}\rho \tanh kb\, \hat{\xi}$$

where the last equality introduces the fact that $\hat{v}_x = j(\omega - kU)\hat{\xi}$.

Boundary conditions begin with the resistive sheet, described by Eq. (a) of Table 6.3.1.

$$k_y^2 \hat{h}_y^c = -\sigma_s(-jk_y)(j)\omega\mu_o \hat{h}_x^c \tag{7}$$

which is written in terms of $\hat{\Psi}^c$ as $(\hat{h}_y = jk_y\hat{\Psi})$.

$$\hat{\Psi}^c = \frac{j\mu_o\sigma_s}{k_y^2}\omega \hat{h}_x^c \tag{8}$$

At the perfectly conducting interface, $\left(\bar{n} \simeq \bar{i}_x - \frac{\partial\xi}{\partial y}\bar{i}_y - \frac{\partial\xi}{\partial z}\bar{i}_z\right)$

$$\bar{n}\cdot\bar{H} = 0 \Rightarrow \hat{h}_x^d + jk_y H_o\hat{\xi} = 0 \tag{9}$$

Stress equilibrium for the perturbed interface is written for the x component, with the others identically satisfied to first order because the interface is free of shear stress. From Eq. 7.7.6 with $i \to x$

$$[\![p]\!]n_x = [\![T_{xj}]\!]n_j - \gamma(\nabla\cdot\bar{n})n_x \tag{10}$$

Linearization gives

$$-\hat{p}^e = -\mu_o H_o \hat{h}_y^d - \gamma k^2\hat{\xi} \tag{11}$$

where Eq. (d) of Table 7.6.2 has been used for the surface tension term.

With $\hat{h}_y = jk\hat{\Psi}$, Eq. 5 becomes

$$\hat{p}^e = jk_y\mu_o H_o\hat{\Psi}^d + \gamma k^2\hat{\xi} \tag{12}$$

Now, to combine the boundary conditions and bulk relations, Eq. 8 is expressed using Eq. 3a as the first of the three relations

Prob. 11.17.5 (cont.)

$$\begin{bmatrix} 1+\dfrac{j\mu_o\sigma_s k}{k_y^2}\omega\coth ka & \dfrac{-j\mu_o k\sigma_s\omega}{k_y^2\sinh ka} & 0 \\ \dfrac{-k}{\sinh ka} & k\coth ka & jk_y H_o \\ 0 & -jk_y\mu_o H_o & \dfrac{(\omega-k_yU)^2}{k}\rho\tanh kb - \gamma k^2 \end{bmatrix}\begin{bmatrix}\hat{\psi}^c \\ \hat{\psi}^d \\ \hat{\xi}\end{bmatrix}=0 \qquad (13)$$

The second is Eq. 9 with $\hat{H}_x^d$ expressed using Eq. 3b. The third is Eq. 12 with $\hat{p}^e$ given by Eq. 6.

Expansion by minors gives

$$-k_y^2 H_o^2\mu_o\left[1+\frac{j\mu_o\sigma_s k}{k_y^2}\omega\coth ka\right]+$$

$$k\left[\frac{(\omega-k_yU)^2}{k}\rho\tanh kb-\gamma k^2\right]\left[\coth ka+\frac{j\mu_o\sigma_s k\omega}{k_y^2}\right]=0 \qquad (14)$$

Some limits of interest are:

$H_o\to 0$ so that mechanics and magnetic diffusion are uncoupled. Then, Eq. 14 factors into dispersion equations for the capillary jet and the magnetic diffusion

$$(\omega-k_yU)^2=\gamma k^3/\rho\tanh kb \qquad (15)$$

$$\omega=\frac{jk_y^2}{\mu_o\sigma_s k}\coth ka \qquad (16)$$

The latter gives modes similar to those of Sec. 6.10 except that the wall opposite the conducting sheet is now perfectly conducting rather than

Prob. 11.17.5 (cont.)

infinitely permeable.

$\sigma \to \infty$, so that Eq. 14 can be factored into the dispersion equations

$$\omega = \tag{17}$$

$$(\omega - k_y U)^2 \rho \tanh kb = \gamma k^3 + k_y^2 \mu_o H_o^2 \coth ka \tag{18}$$

This last expression agrees with the kink mode dispersion equation (with $\gamma \to 0$) of Prob. 8.12.1.

In the long-wave limit, $\coth ka \to 1/ka$, $\tanh kb \to kb$ and Eq. 14 becomes

$$-k_y^2 \frac{\mu_o H_o^2}{k}\left(1 + j\frac{\mu_o \sigma_s}{k_y^2 a}\omega\right) + \left[(\omega - k_y U)^2 \rho b - \gamma k^2\right]\left[\frac{1}{ka} + j\frac{\mu_o \sigma_s \omega}{k_y^2}\right] = 0 \tag{19}$$

In general, this expression is cubic in ω. However, with interest limited to frequencies such that

$$ka \frac{\mu_o \sigma_s \omega}{k} << 1 \tag{20}$$

and $k = k_y$, the expression reduces to

$$\omega^2 - \omega\left(2kU + jV_a^2 \frac{\mu_o \sigma_s}{a}\right) + k^2\left(U^2 - V^2 - V_a^2\right) \tag{21}$$

where $V^2 \equiv \gamma/\rho b$ and $V_a^2 \equiv (\mu_o H_o^2/\rho)(a/b)$. Thus, in this long-wave low frequency approximation,

$$\omega = kU + jV_a^2 \frac{\mu_o \sigma_s}{2a} \pm \left\{\left(kU + jV_a^2 \frac{\mu_o \sigma_s}{2a}\right)^2 - k^2\left(U^2 - V^2 - V_a^2\right)\right\}^{1/2} \tag{22}$$

Prob. 11.17.5 (cont.)

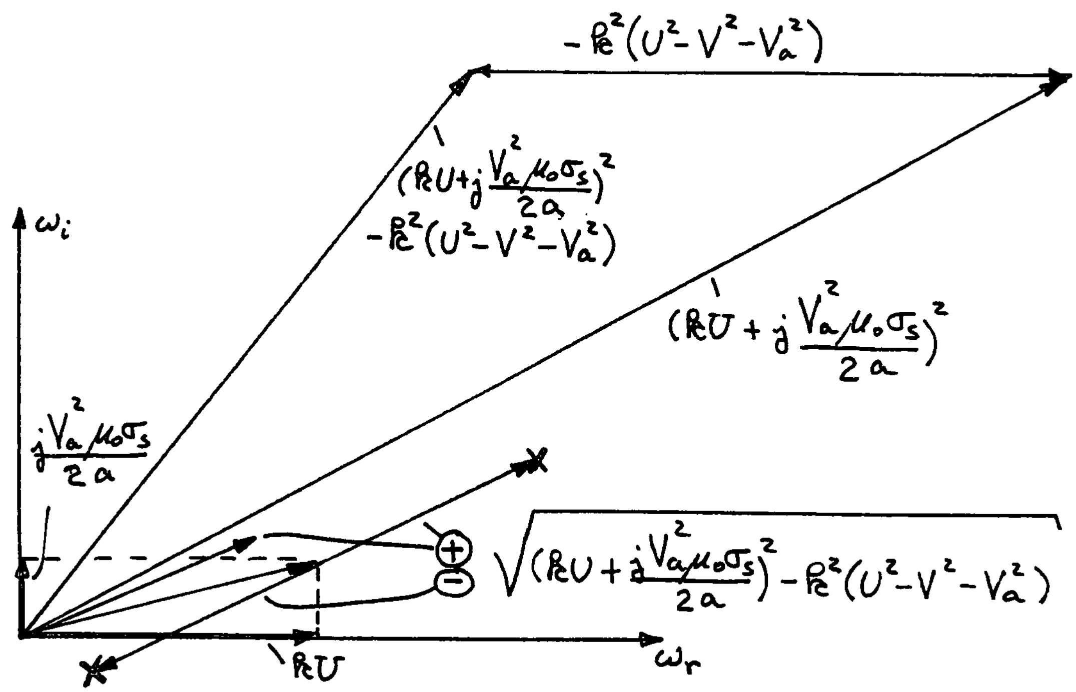

It follows from the diagram that if $U>\sqrt{V^2+V_a^2}$, the system is unstable. To explore the nature of the instability, Eq. 21 is written as a polynomial in k.

$$(U^2-V^2-V_a^2)k^2 - 2\omega U k + \omega\left(\omega - j\frac{V_a^2\mu_o\sigma_s}{a}\right) = 0 \tag{23}$$

This quadratic in k is solved to give

$$k = \frac{\omega U \pm \sqrt{\omega^2(V^2+V_a^2) + j(U^2-V^2-V_a^2)V_a^2\frac{\mu_o\sigma_s\omega}{a}}}{(U^2-V^2-V_a^2)} \tag{24}$$

With $\omega=\omega_r-j\sigma$, this becomes

$$k = \frac{\omega_r U - j\sigma U \pm \sqrt{A+jB}}{U^2-V^2-V_a^2} \tag{25}$$

Prob. 11.17.5 (cont.)

where

$$A \equiv (\omega_r^2 - \sigma^2)(V^2 + V_a^2) + (U^2 - V^2 - V_a^2)\frac{V_a^2 \mu_o \sigma_s}{a}\sigma$$

$$B \equiv \left[(U^2 - V^2 - V_a^2)\frac{V_a^2 \mu_o \sigma_s}{a} - 2\sigma(V^2 + V_a^2)\right]\omega_r$$

The loci of complex k at fixed ω_r as σ is varied from ∞ to 0 for $U^2 > (V^2 + V_a^2)$ could be plotted in detail. However, it is already known that one of these passes through the k_r axis when $\sigma < 0$ (that one temporal mode is unstable). To see that the instability is convective it is only necessary to observe that both families of loci originate at $k_i \rightarrow -\infty$. That is, in the limit $\sigma \rightarrow \infty$, Eq. 25 gives

$$k \rightarrow \frac{-j\sigma U \pm j\sigma\sqrt{V^2 + V_a^2}}{U^2 - V^2 - V_a^2} \tag{26}$$

and if $U^2 > V^2 + V_a^2$ it follows that for both roots $k \rightarrow -j\infty$ as $\sigma \rightarrow \infty$. Thus, the loci have the character of Fig. 11.12.8. The "unstable" root crosses the k_r axis into the upper half-plane. Because the "stable" root never crosses the k_r axis, these two loci cannot coalesce, as required for an absolute instability.

Note that the same conclusion follows from reverting to a z-t model for the dynamics. The long-wave model represented by Eq. 21 is equivalent to a "string" having the equation of motion

$$\left(\frac{\partial}{\partial t} + U\frac{\partial}{\partial z}\right)^2 \xi = (V^2 + V_a^2)\frac{\partial^2 \xi}{\partial z^2} - V_a^2 \frac{\mu_o \sigma_s}{a}\frac{\partial \xi}{\partial t} \tag{27}$$

The characteristics for this expression are

$$\frac{dz}{dt} = U \pm \sqrt{V^2 + V_a^2} \tag{28}$$

and it follows that if $U > \sqrt{V^2 + V_a^2}$, the instability must be convective.

Prob. 11.17.6 (a) With the understanding that the potential represents an electric field that is in common to both beams, the linearized longitudinal force equations for the respective one-dimensional overlapping beams are

$$\frac{\partial v_{z1}}{\partial t} + U_1 \frac{\partial v_{z1}}{\partial z} = \frac{e}{m}\frac{\partial \Phi}{\partial z} \tag{1}$$

$$\frac{\partial v_{z2}}{\partial t} + U_2 \frac{\partial v_{z2}}{\partial z} = \frac{e}{m}\frac{\partial \Phi}{\partial z} \tag{2}$$

To write particle conservation, first observe that the longitudinal current density for the first beam is

$$\bar{J}_1 = -e n_o U_1 \bar{i}_z - e(n_1 U_1 + n_o v_{z1}) \tag{3}$$

and hence particle conservation for that beam is represented by

$$\frac{\partial n_1}{\partial t} + U_1 \frac{\partial n_1}{\partial z} + n_{o1}\frac{\partial v_{z1}}{\partial z} = 0 \tag{4}$$

Similarly, the conservation of particles on the second beam is represented by

$$\frac{\partial n_2}{\partial t} + U_2 \frac{\partial n_2}{\partial z} + n_{o2}\frac{\partial v_{z2}}{\partial z} = 0 \tag{5}$$

Finally, perturbations of charge density in each of the beams contribute to the electric field, and the one-dimensional form of Gauss' Law is

$$\frac{\partial^2 \Phi}{\partial z^2} = \frac{e}{\epsilon_o}(n_1 + n_2) \tag{6}$$

The five dependent variables $v_{z1}, v_{z2}, \Phi, n_1$, and n_2 are described by Eqs. 1, 2, 4 and 5. In terms of complex amplitudes, these expressions are represented by the five algebraic statements summarized by

$$\begin{bmatrix} \omega - kU_1 & 0 & \frac{ek}{m} & 0 & 0 \\ 0 & \omega - kU_2 & \frac{ek}{m} & 0 & 0 \\ -kn_{o1} & 0 & 0 & \omega - kU_1 & 0 \\ 0 & -kn_{o2} & 0 & 0 & \omega - kU_2 \\ 0 & 0 & k^2 & \frac{e}{\epsilon_o} & \frac{e}{\epsilon_o} \end{bmatrix} \begin{bmatrix} \hat{v}_{z1} \\ \hat{v}_{z2} \\ \hat{\Phi} \\ \hat{n}_1 \\ \hat{n}_2 \end{bmatrix} = \begin{bmatrix} 0 \\ 0 \\ 0 \\ 0 \\ 0 \end{bmatrix} \tag{7}$$

Prob. 11.17.6 (cont.)

The determinant of the coefficients reduces to the desired dispersion equation.

$$1 = \frac{\omega_{p1}^2}{(\omega - kU_1)^2} + \frac{\omega_{p2}^2}{(\omega - kU_2)^2} \tag{8}$$

where the respective beam plasma frequencies are defined as

$$\omega_{p1} = \sqrt{\frac{n_{01} e^2}{\epsilon_o m}} \;;\; \omega_{p2} = \sqrt{\frac{n_{02} e^2}{\epsilon_o m}} \tag{9}$$

(b) In the limit where the second "beam" is actually a plasma (formally equivalent to making U_2=0), the dispersion equation, Eq. 8, becomes the polynomial,

$$\underline{k}^2 - 2\underline{\omega}\underline{k} + \underline{\omega}^2\left(1 - \frac{r}{\underline{\omega}^2 - 1}\right) = 0 \tag{10}$$

where $r \equiv (\omega_{p1}/\omega_{p2})^2$, $\underline{\omega} \equiv \omega/\omega_{p2}$ and $\underline{k} \equiv kU_1/\omega_{p2}$. The mapping of complex k as a function of $\omega = \omega_r - j\sigma$, σ varying from $\infty \rightarrow 0$ with ω_r held fixed, shown in Fig. P11.17.6a, is that characteristic of a convective instability (Fig. 11.12.8, for example).

(c) In the limit of counter-streaming beams $U_1 = U_2 \equiv U$, Eq. 8 becomes

$$\underline{k}^4 - (2\underline{\omega}^2 + r + 1)\underline{k}^2 + 2\underline{\omega}(1 - r)\underline{k} + \underline{\omega}^2[\underline{\omega}^2 - (r+1)] = 0 \tag{11}$$

where the normalization is as before. This time, the mapping is as illustrated by Fig. P11.17.6b, and it is clear that there is an absolute instability. (The loci are as typified by Fig. 11.13.3.)

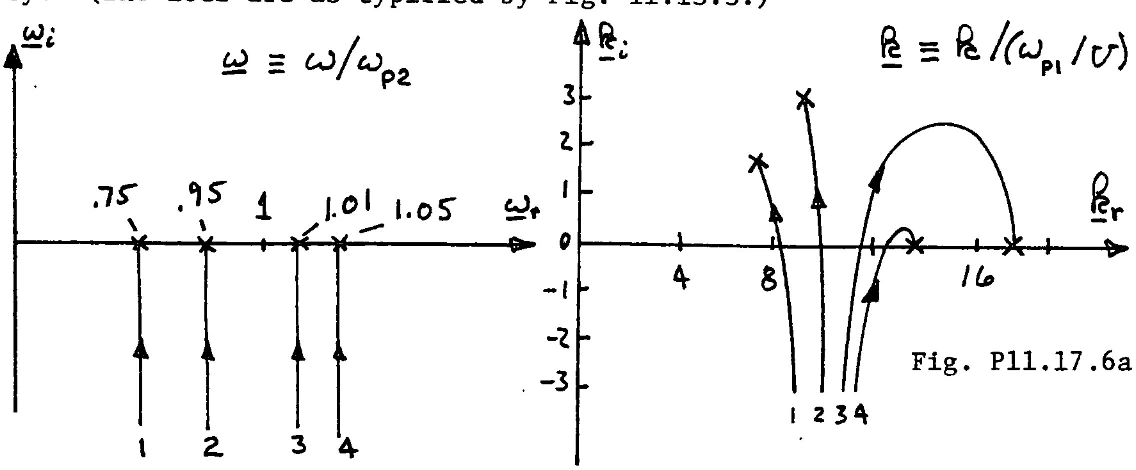

Fig. P11.17.6a

Prob. 11.17.6 (cont.)

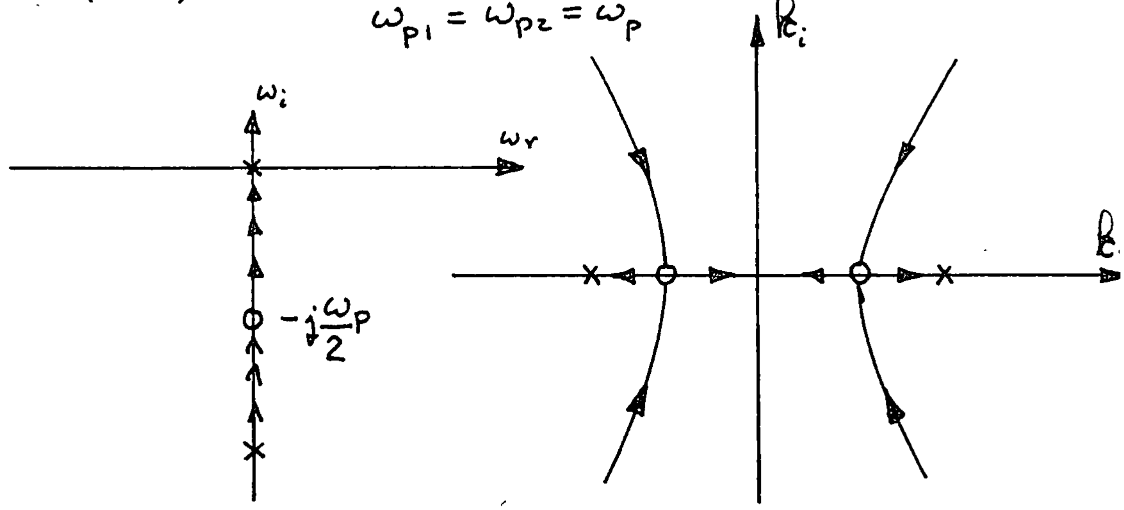

See, Briggs, R.J., Electron-Stream Interaction With Plasmas, M.I.T. Press (1964) pp 32-34 and 42-44.